CHARACTERIZATION OF THE TELOMERIC REPEAT BINDING FACTOR 2

CHARACTERIZATION

OF

THE TELOMERIC REPEAT BINDING FACTOR 2 (TRF2) IN THE UV-INDUCED DNA DAMAGE RESPONSE AND TELOMERE MAITENANCE

By

KIMBERLY GLENFIELD, B.Sc.

A Thesis

Submitted to the School of Graduate Studies

in Partial Fulfilment of the Requirements

For the Degree

Master of Science

McMaster University

MASTER OF SCIENCE (2008) McMaster University

(Biology) Hamilton, Ontario

TITLE:	Characterization of the telomeric repeat binding factor 2 (TRF2) in the UV-induced DNA damage response and telomere maintenance
AUTHOR:	Kimberly Glenfield, B.Sc. (University of Guelph)
SUPERVISOR:	Professor Xu-Dong Zhu
NUMBER OF PAGES:	xiv, 114

Abstract

TRF2 is an essential telomeric protein involved in preventing the telomere ends from being recognized as DNA breaks. I have shown that TRF2 does not appear to play a major role in the UV-induced DNA damage response in IMR90, Cockayne syndrome or XPC deficient cells. TRF2 binds telomeric DNA via its Myb domain and also contains an N-terminal basic domain. Expression of $TRF2^{\Delta B\Delta M}$ causes telomere fusions, whereas $TRF2^{\Delta B}$ causes rapid deletion of telomeric DNA, as both phenotypes result in senescence. These phenotypes are dependant upon recombination events. Thus, the basic domain of TRF2 may be essential to suppress recombination events at telomeres. However, it is not fully understood what amino acid residues in the basic domain of TRF2 are indispensable to maintain its function. By creating mutations in the arginine residues in the basic domain of TRF2, I have shown that the positive charge of the basic domain alone is not sufficient to maintain its protective function. By expressing these TRF2 mutants in the presence or absence of the Myb domain in HT1080 and BJ/hTERT cells, I have been able to recapitulate the $TRF2^{\Delta B}$ and $TRF2^{\Delta B\Delta M}$ decreased proliferation and senescence phenotypes. Furthermore, by analyzing anaphase and metaphase chromosomes and performing Southern blotting, I have shed light on the molecular mechanisms responsible for the deleterious phenotypes observed in the TRF2 mutants. Amino acid changes from arginines to lysines introduced into the basic domain of TRF2 results in a significant increase in telomere doublets. However, when these TRF2 mutants are expressed in the absence of the Myb domain, a significant increase in telomere fusions events occur. Collectively, my results indicate that more than one arginine residue in the basic domain

is essential to maintain the protective function of TRF2, as these arginine residues may act as substrates for protein arginine methyltransferases.

Acknowledgements

Firstly, I would like to thank my supervisor Dr. Xu-Dong Zhu for allowing me to complete my graduate studies under her supervision. Dr. Zhu has provided me with a strong technical and research background in the fields of molecular and cellular biology. She has taught me how to perform cutting edge independent research and how to critically evaluate other research in the field. Dr. Zhu is a very gifted and dedicated researcher. She has spent an enormous number of hours in the laboratory with me passing on her knowledge and skills. I have enjoyed the time spent working on my research project and the success of the project is owed in part to Dr. Zhu. She constantly challenged me throughout my studies to improve my abilities and enhance my knowledge and for that I am grateful.

I would also like to extend my appreciation to my committee members Dr. Rainbow and Dr. Bédard. Thank you very much for all of your time and critical comments. Both of you have enhanced my learning experience and have shown me how research is executed from different points of view. Dr. Rainbow and Dr. Bédard are both experienced and exceptional researchers. I feel that my thesis was strengthened because of having both of them on my committee.

Furthermore, I am also grateful to the past and present members of the Zhu laboratory. In particular, I would like to thank Taylor Mitchell and Megan McKerlie for being great co-workers and friends. My time in the lab was greatly enhanced by both of you and I will never forget some of the great times we had in the lab. Also, I am appreciative to other students in the department who I have had the opportunity to know.

Additionally, I would like to thank the other faculty and staff in the Biology Department who had taken the time to answer my questions and helped me when I was in need.

I am very grateful to my best friends Ashley Milmine, Stephanie Kendall, Jen Bader and Ashley Brown who have always been there for me. Lastly, I would like to thank my parent Glenda and Frank Glenfield and my siblings Michelle, Sean and Shane who have always been my biggest supporters. I also would like to express my gratitude to my partner Devin Staples who has always stuck by me with loving arms.

Table of Contents

List of Figures

Abbreviations

A	Alanine
ATM	Ataxia telangiectasia mutated
ATR	Ataxia telangiectasia RAD3-related
BCS	Bovine calf serum
BLM	Bloom's syndrome
βME	Beta-mercapto-ethanol
BSA	Bovine serum albumin
CDC	Cell division cycle
CDK	Cyclin-dependent kinase
CHK	Checkpoint
CS	Cockayne syndrome
DAPI	4', 6'-diamino-2-phenylindole
DMF	Dimethylformamide
DNA	Deoxyribonucleic acid
DNA-PK	DNA dependant protein kinase
DSB	Double-stranded break
DTT	Dithiothreitol
ECL	Enhanced chemiluminescence
EDTA	Ethylenediaminetetraacetic acid
ERCC	Excision repair cross complimenting
FBS	Fetal bovine serum
FISH	Fluorescent *in situ* hybridization
GAR	Glycine arginine rich
GGR	Global genomic repair
H2AX	Histone 2A variant
HEPES	4-(2-hydroxyethyl)-1-piperazineethanesulfonic acid
HJ	Holliday junction
HR	Homologous recombination
hRap1	Human transcriptional repressor/activator protein 1
hTERC	Human telomerase RNA component
hTERT	Human telomerase reverse transcriptase
IR	Ionizing radiation
K	Lysine
KDa	Kilodalton
MEF	Mouse embryonic fibroblast
MOPS	3-(N-morpholino)-propanesulfonic acid
MRE11	Meiotic recombination 11 homologue
NBS1	Nijmegen breakage syndrome
NER	Nucleotide excision repair
NHEJ	Non-homologous end joining
NT	Nucleotide
OB	Oligosaccharide/oligonucleotide binding

PAGE	Polyacrylamide gel electrophoresis
PARP	Poly(ADP-ribose) polymerase
PBS	Phosphate buffer saline
PCR	Polymerase chain reaction
PD	Population doubling
PI3-K	Phosphatidylinositol 3-kinase-related protein kinase
PMSF	Phenylmethylsulfonylfluoride
POT1	Protection of telomeres 1
pRb1	Retinoblastoma 1
PRMT	Protein arginine *N*-methyltransferase
PTM	Post-translational modification
R	Arginine
SDS	Sodium dodecyl sulphate
T-loop	Telomeric loop
TBE	Tris borate EDTA
TBS	Tris buffer saline
TCR	Transcription-coupled repair
TIF	Telomere dysfunctional-induced foci
TIN2	TRF1 interacting nuclear protein 2
TPP1	TINT1/PTOP/PIP1
TRF	Telomere repeat binding factor
TRF2$^{\Delta B}$	TRF2 delta-basic
TRF2$^{\Delta B\Delta M}$	TRF2 delta-basic-delta-Myb
TRF2$^{\Delta M}$	TRF2 delta-Myb
Tris	2-amino-2-hydroxymethyl-1,3-propanediol
UV	Ultraviolet light
WRN	Werner
WS	Werner syndrome
WT	Wild type
XP	Xeroderma pigmentosum
XRCC	X-ray repair cross complementing

Chapter 1 - Introduction

1.1 Telomeres

1.1.1 Telomere Structure, Length and Function

Telomeres are protein-DNA complexes found at the ends of linear eukaryotic chromosomes. Telomeres in humans consist of simple G-rich tandem 2 - 20 kb TTAGGG repeats, ending in a single-stranded 3' G overhang of 100 – 280 nt in length (Blackburn, 2001, Crabbe & Karlseder, 2005, Hahn, 2005, Huffman et al, 2000, Makarov et al, 1997, McElligott & Wellinger, 1997, Wright et al, 1997). The length of the telomeric repeats are variable depending on the organism, as the length of mouse telomeres are much longer than humans, reaching up to 150 kb in length (de Lange et al, 1990, Kipling & Cooke, 1990, Lejnine et al, 1995, Moyzis et al, 1988). Telomeres play an essential role in cell viability and the maintenance of genomic integrity (de Lange, 2002). Within cells, telomeres have two equally important functions, maintaining the length of telomeric DNA and protecting the DNA ends from being inappropriately processed by DNA repair proteins (Baird & Farr, 2006, de Lange, 2005).

A relationship exists between telomere integrity and cell survival. Cells expressing critically short telomeres enter senescence or apoptosis depending on the cell type (Crabbe & Karlseder, 2005, Hezel et al, 2005, Karlseder et al, 1999). One essential role of telomeres is to maintain the length of chromosomes, as with each cell division there is a continuous loss of ~70 – 200 bp of DNA from chromosome ends (Harley et al, 1990, Olovnikov, 1973, Watson, 1972). The loss of chromosome length occurs during lagging strand replication when the most distal RNA primer is removed. This

phenomenon is often referred to as the end replication problem (Crabbe & Karlseder, 2005, Makarov et al, 1997, McElligott & Wellinger, 1997, Olovnikov, 1973, Olovnikov, 1996, Watson, 1972, Wright et al, 1997). To help balance the progressive telomere loss, a reverse transcriptase ribonucleoprotein complex called telomerase recognizes an accessible 3' overhang and extends the telomeric repeats *de novo* to maintain telomeric DNA (Blackburn et al, 1989, Greider & Blackburn, 1985, Nugent & Lundblad, 1998). Telomerase is comprised of a catalytic subunit referred to as TERT and an RNA component referred to as TERC. Telomere shortening occurs in most human somatic tissues that do not have detectable telomerase activity. On the other hand, human germ line cells and some transformed human cancer cells express telomerase (Greider & Blackburn, 1985, Lingner et al, 1997, Nugent & Lundblad, 1998, Opitz, 2005). Human somatic cells proliferate for a predetermined number of population doublings (PDs), until the cells enter a state of permanent growth arrest, referred to as senescence (Hayflick & Moorehead, 1961). Immortalization can occur in cells by constitutive expression of the catalytic subunit of telomerase, hTERT (Counter et al, 1998, Shay & Bacchetti, 1997, Vaziri & Benchimol, 1998).

An additional function of telomeres is to protect the ends of chromosomes, a process which involves a complex of telomere specific binding proteins termed shelterin (de Lange, 2005). These shelterin proteins bind to telomeric DNA forming a telomeric protein cap that prevents the natural chromosome ends from being recognized as double-stranded breaks (DSBs) (Baird & Farr, 2006, de Lange, 2002, Palm & de Lange, 2008).

Thus, the shelterin complex is fundamentally essential to maintaining genomic stability and replicative lifespan in mammalian cells.

1.1.2 The Shelterin Complex

The shelterin complex is composed of six telomere-specific proteins, TRF1, TRF2, TPP1, TIN2, hRap1 and POT1 (Figure 1.1) (Bilaud et al, 1997, Broccoli et al, 1997, de Lange, 2005, Houghtaling et al, 2004, Kim et al, 1999, Li et al, 2000, Liu et al, 2004, Loayza & De Lange, 2003, Ye & de Lange, 2004, Zhong et al, 1992). The shelterin complex is associated with human telomeres throughout the entire cell cycle, as they function and accumulate at chromosome ends (de Lange, 2005). The proteins TRF1 and TRF2 are the only two components of the shelterin complex that bind directly to the double-stranded region of telomeric DNA as homodimers, anchoring the shelterin complex to mammalian telomeres (Bilaud et al, 1997, Broccoli et al, 1997, Chong et al, 1995). Human Rap1 acts as a negative regulator of telomerase and associates with telomeres through a direct protein-protein interaction with TRF2 (Li et al, 2000). POT1 and TPP1 are both positive and negative regulators of telomere length maintenance by regulating the access of telomerase to telomeric DNA (Xin et al, 2007). POT1 is the only shelterin protein that binds to the single-stranded 3' overhang via its DNA-binding OB fold (Baumann & Cech, 2001, de Lange, 2005, Loayza & De Lange, 2003). The shelterin complex is held together by TIN2, acting as a bridge between TPP1/POT1 to TRF1 and TRF2/Rap1 (de Lange, 2005).

Telomere length is suggested to be dependent on a homeostasis between proteins associated with telomeres and telomerase. Both TRF1 and TRF2 may regulate the

transition between an open and closed telomere state (Smogorzewska et al, 2000). Telomere shortening may occur in the protective closed state, in contrast to the open telomeric state, which would allow telomerase to access the telomeric ends resulting in telomere lengthening. TRF1 was the first shelterin protein to be identified due to its affinity for the telomeric repeats *in vitro*, as TRF2 was identified a few years later in 1997 based on a similar sequence homology to TRF1 (Bilaud et al, 1997, Broccoli et al, 1997, Chong et al, 1995, Zhong et al, 1992). TRF1 and TRF2 each contain a C-terminal Myb-like DNA-binding domain; a central domain, responsible for the formation of homodimers; and a N-terminal acidic domain in TRF1 or a basic domain in TRF2 (Bilaud et al, 1996, Bilaud et al, 1997, Broccoli et al, 1997, Chong et al, 1995, Zhong et al, 1992). Overexpression of either TRF1 or TRF2 in *vivo* leads to progressive telomere shortening over many PDs (Smogorzewska et al, 2000, van Steensel & de Lange, 1997). TRF2 and TRF1 cannot heterodimerize with each other and only interact through their common binding partner TIN2 (Broccoli et al, 1997, Kim et al, 1999). TRF1 is a negative regulator of telomere length (van Steensel & de Lange, 1997) and it has been suggested that TIN2 may act as a negative regulator as well, through a complex with TRF1 (Ye & de Lange, 2004, Ye et al, 2004). Overall, the shelterin complex plays an important role in the maintenance and protection of telomeres.

1.1.3 DNA Damage Response and Telomeres

Telomeres are associated with a number of DNA damage repair proteins such as Ku70/80, XPF/ERCC1, Apollo, RAD51D, PARP1, PARP2 and signalling proteins including ATM, Mre11 complex and 9-1-1 complex (de Laat et al, 1998, de Lange,

2005, Francia et al, 2006, Hoeijmakers, 2001, Hsu et al, 1999, Hsu et al, 2000, Karlseder et al, 2002, Karlseder et al, 2004, Lenain et al, 2006, Li et al, 2000, Machwe et al, 2004, Opresko et al, 2002, Opresko et al, 2003, Song et al, 2000, Stansel et al, 2001, Stavropoulos et al, 2002, Tarsounas et al, 2004, van Overbeek & de Lange, 2006, Winkler et al, 2001, Zhu et al, 2000, Zhu et al, 2003). Telomeres activate the DNA damage checkpoint pathway if the cell experiences critically shortened telomeres or unprotected telomeres via the p53 and ATM-dependent DNA damage response pathway resulting in G1/S cell cycle arrest (Figure 1.2A and B) (Celli & de Lange, 2005, Hezel et al, 2005, Karlseder et al, 1999). In the G2 phase of the cell cycle, activated NBS1, Mre11 and ATM are recruited to telomeres in telomerase-negative cells after replication, possibly to aid in the formation of the telomere end protection complex (Verdun et al, 2005) . Uncapped chromosomes form telomere dysfunctional-induced foci (TIFs), that contain multiple DNA damage response proteins accumulating at the telomeres including γH2AX, 53BP1, ATM or MRE11 (Crabbe & Karlseder, 2005, Takai et al, 2003).

DNA damage in mammals is detected by sensor proteins such as the MRN complex (MRE11/RAD50/NBS1), RAD17 and 911 complex (RAD9/RAD1/HUS1) (Figure 1.2A) (Lee & Paull, 2005, Lindsey-Boltz et al, 2001, Longhese et al, 1998, Melo & Toczyski, 2002, Paull & Lee, 2005, Paulovich et al, 1998, Zhou & Bartek, 2004). Initiation of the DNA damage response pathway leads to the activation of the two major transducer proteins ATR and ATM, which are members of the phosphatidylinositol 3-kinase-related protein (PI3-kinase) family (Abraham, 2001, Bakkenist & Kastan, 2003, Bao et al, 2001, Cimprich et al, 1996, Houtgraaf et al, 2006, Lee & Paull, 2005, Paull &

Lee, 2005). The DNA damage signal is amplified by ATM and ATR by phosphorylating their downstream effectors proteins such as CHK1, CHK2, p53 and CDC25 (Bartek & Lukas, 2001, Hirao et al, 2000, Matsuoka et al, 2000, McGowan, 2002, Rhind & Russell, 2000, Zhao & Piwnica-Worms, 2001). ATM becomes activated in response to DNA DSBs and associates with the MRN complex. ATR is activated by DNA damage such as bulky lesions or stalled DNA replication forks caused by ultraviolet (UV) light. Additionally, the p53 protein is activated in mammalian cells in response to cellular stresses and can initiate cell cycle arrest in G1 and G2, DNA repair or apoptosis (Prives & Hall, 1999, Vousden & Lu, 2002). p53 is an important tumor suppressor protein, as the *p53* gene is mutated in more than fifty-percent of all human cancers (Hainaut & Hollstein, 2000, Hollstein et al, 1991). Both ATM and ATR phosphorylate p53 on serine 15 in response to DNA damage (Banin et al, 1998, Canman et al, 1998, Lakin et al, 1999). The activated p53 protein regulates the transcription of p21, which is an inhibitor of several CDKs resulting in cell cycle arrest (el-Deiry et al, 1993). In mammals, DNA damage is repaired by one of four mechanisms; double-stranded break repair (DSBR), base excision repair (BER), mismatch repair (MMR) or nucleotide excision repair (NER), depending on the nature of the DNA damage (Hoeijmakers, 2001).

UV-induced DNA damage is repaired in mammalian cells by NER (Figure 1.2C) (Berdal et al, 1998, de Laat et al, 1999, Petit & Sancar, 1999, Saldivar et al, 2007, Wood, 1997). UVC radiation has a wavelength of 190-280 nm and is the highest energy component of UV light (Tyrrell, 1994). The short wavelengths of UVC are readily absorbed by the aromatic ring structures of the DNA bases, resulting in DNA damage (de

Gruijl et al, 2001, Ravanat et al, 2001). The proteins which are involved in NER are named after a photosensitive disorder deficient in NER called xeroderma pigmentosum (XP), and are referred to as XPA to XPG (Evans et al, 1997, Hanawalt, 2002, Mu et al, 1995, Mu et al, 1996). Two types of NER occur in cells, transcription coupled repair (TCR) and global genome repair (GGR) (Bohr et al, 1985, Hanawalt, 2002, Sugasawa et al, 1998). TCR occurs first in the cell and repairs the template strand of DNA in actively transcribing regions, where as GGR occurs later and repairs the non-transcribed regions. TCR also requires two other proteins, CS-A and CS-B, which are absent in the UV-induced hypersensitivity disorder Cockayne syndrome (CS) (Friedberg, 1996, Hanawalt, 2002, Venema et al, 1990). With the exception of the first initial recognition steps in NER, both GGR and TCR will utilize the same repair process. Cells deficient in the XPC protein are also deficient in GGR whereas CS cells are deficient in TCR, thus these cells provide a good model to study the effects of TRF2 in each pathway (Hwang et al, 1999, Venema et al, 1991). To date, research suggests that a relationship exists between DNA damage repair proteins and telomeres. However, the specific role of the shelterin proteins underlying the regulation of the DNA damage response are still being elucidated. At the time of my initial study, it was not known whether TRF2 played a role in the UV-induced DNA damage response.

1.2 TRF2

1.2.1 The Human TRF2 Protein

TRF2 is a small ubiquitously expressed protein that plays a large role in telomere end protection. TRF2 has an abundance of at least 100 copies per chromosome end (de

Lange, 2002). The human TRF2 protein has a high homology (82%) in comparison to the mouse TRF2 protein (Broccoli et al, 1997). The N-terminal basic domain of TRF2 spans amino acids 1 – 45, the central dimerization domain is located at positions 46 – 245 and the C-terminal Myb DNA binding domain at residues 446 - 500 (Figure 1.3A) (Bilaud et al, 1996, Bilaud et al, 1997, Broccoli et al, 1997, Chong et al, 1995, Court et al, 2005, de Lange, 2005, Fairall et al, 2001, Hanaoka et al, 2005, Nishikawa et al, 1998). The Myb domain consists of three alpha helices; as the second and third alpha helices form a helix-turn-helix motif. An unstructured long flexible linker region joins the dimerization domain and the Myb domain (Bianchi et al, 1999). TRF2 binds telomeric DNA preferentially at the junction between the double stranded and single stranded overhang *in vitro* (Bilaud et al, 1997, Stansel et al, 2001). The basic domain of TRF2 has a strong positive charge due to the presence of nine arginine (R) residues (Figure 1.3B). Additionally, the basic domain contains fourteen glycine (G) resides. The basic domain is very flexible and its structure has not yet been resolved. The function of the basic domain of TRF2 is still unclear, however it is thought to protect telomeres by suppressing recombination events at DNA ends (Bae & Baumann, 2007, Bailey et al, 2001, Smogorzewska et al, 2002, van Steensel et al, 1998, Wang et al, 2004).

1.2.2 The Role of TRF2 in Telomere Maintenance and Protection

Currently, it is thought TRF2 protects human chromosome ends by promoting the formation of a higher order structure at the ends of the telomeres, referred to as a telomeric loop (t-loop) structure (Griffith et al, 1999, Stansel et al, 2001). *In vitro*, it has been shown that TRF2 plays a role in remodeling artificial telomeric DNA into a t-loop

structure (Griffith et al, 1999, Stansel et al, 2001). The single-stranded 3' telomeric overhang invades the double-stranded telomeric tract, forming a large duplex loop structure at the ends of the chromosomes (Griffith et al, 1999, Hahn, 2005). Evidence to support the role of TRF2 in protecting the telomeric structure comes from overexpression studies performed in telomerase-negative primary lung fibroblast cells (Karlseder et al, 2002). Their studies reveal that the critical telomere length needed to induce senescence in the cells is decreased from 7 kb to 4 kb in length, when TRF2 is overexpressed. These data suggest that it may be the loss of the telomere state and not necessarily the loss of the telomere length that activates the DNA damage response in cells expressing critically shortened telomeres, leading to senescence (Crabbe & Karlseder, 2005, Karlseder et al, 2002). TRF2 may facilitate the t-loop structure in cells with critically shortened telomeric DNA or may recruit additional proteins essential for telomere end protection, thus delaying the entry into senescence (Crabbe & Karlseder, 2005, Karlseder et al, 2002, Stansel et al, 2001). When the t-loop structure becomes opened or the telomeres lose their G strand overhangs, the telomere ends are exposed, which can trigger the DNA damage checkpoint activation pathway.

Expression of a dominant negative *TRF2*$^{\Delta B \Delta M}$ allele which lacks the basic and Myb domains in cells, results in the formation of an inactive heterodimer with endogenous wild type TRF2. TRF2$^{\Delta B \Delta M}$ is unable to bind to DNA because the heterodimer contains only one functional Myb DNA binding domain, as opposed to two Myb domains in the wild type TRF2 homodimer (Smogorzewska et al, 2002, van Steensel et al, 1998). As a consequence of the *TRF2*$^{\Delta B \Delta M}$ allele expressed in cells, TRF2

and its interacting partners such as hRap1 do not accumulate at telomere ends (Li et al, 2000, Zhu et al, 2000). The stripping of TRF2 from the ends of chromosomes causes telomeric deprotection which results in catastrophic covalent end-to-end chromosome fusions (Smogorzewska et al, 2002, van Steensel et al, 1998). These fusion events occur between the G-stand of one telomere to the C-strand of another telomere, usually from two different chromosomes. Thus, these fusion events form a problematic DNA bridge during anaphase if the two centromeres are attached to opposite poles during segregation (Smogorzewska et al, 2002). In order for cell division to continue, the anaphase bridges must be broken or the microtubules must be disrupted. Subsequent progression of the broken fusion chromosomes through mitosis will lead to genomic instability (Verdun et al, 2005). These fusion events are thought to occur due to the inappropriate exposure of the telomere ends to the non-homologous end joining (NHEJ) DNA repair pathway (Figure 1.4A) (van Steensel et al, 1998). The formation of the dicentric chromosome fusions in $TRF2^{\Delta B\Delta M}$ cells require NHEJ factors such as DNA ligase IV and Ku70 (Celli & de Lange, 2005, Smogorzewska et al, 2002). In mouse embryonic fibroblasts expressing the $TRF2^{\Delta B\Delta M}$ allele, telomere fusions do not occur in the absence of DNA ligase IV (Smogorzewska et al, 2002). Additionally, removal of the 3' G-strand overhang by ERCC1/XPF endonuclease is a requirement for the fusion events (Zhu et al, 2003). The processing of dysfunctional telomeres by NHEJ may occur primarily in the G1 phase of the cell cycle, while the reestablishment of the protective telomeric state may occur throughout interphase (Konishi & de Lange, 2008). Dysfunctional telomeres refer to the telomeres which cannot maintain a protective telomeric state due to the loss of the G-

strand overhang. Furthermore, expression of a conditional knockout of TRF2 in mouse embryonic fibroblasts results in almost all of the telomeres engaged in end-to-end fusions (Celli & de Lange, 2005). An *in vitro* study suggests that it is a RAP1/TRF2 complex which is involved in capping short telomeric ends and preventing NHEJ mediated end-to-end fusions (Bae & Baumann, 2007). In contrast to the $TRF2^{\Delta B \Delta M}$ allele, expression of another TRF2 deletion mutant, $TRF2^{\Delta B}$, *in vivo* induces telomere shortening without telomere fusions (van Steensel et al, 1998, Wang et al, 2004).

Expression of $TRF2^{\Delta B}$ containing an N-terminal basic domain deletion does not affect the binding or localization of TRF2 to telomeres *in vivo* and does not inhibit the ability to form t-loops *in vitro* (Wang et al, 2004). Additionally, expression of $TRF2^{\Delta B}$ *in vivo* still has the ability to bind to Rap1 and does not diminish the presence of other telomeric proteins or interacting proteins at telomeres. Overexpression of $TRF2^{\Delta B}$ has been shown to lead to the generation of t-loop-sized telomeric circles. The formation of the telomeric circles is dependent on the homologous recombination (HR) proteins Nbs1 and XRCC3 (Figure 1.4B) (Wang et al, 2004). The t-loop structure resembles a Holliday junction (HJ) intermediate near the base of the t-loop. If this HJ is resolved, the loop segment could be deleted resulting in dramatically shorter telomeres and the formation of telomeric circles in $TRF2^{\Delta B}$ cells (de Lange & Petrini, 2000, Griffith et al, 1999). Furthermore, it has been demonstrated that the $TRF2^{\Delta B}$ telomere shortening and senescence phenotype also requires the helicase and exonuclease domain of WRN (Li et al, 2008). The amino terminus of TRF2 is found to interact with WRN. WRN is a member of the RecQ helicase family and is mutated in Werner syndrome (WS), a

premature ageing disease (Opresko et al, 2003, Yu et al, 1996). WRN plays a role in DNA recombination, replication and repair (Opresko et al, 2003, Suzuki et al, 1997, Watt et al, 1996). A number of findings link the genomic instability in WS cells to telomere dysfunction (Chang et al, 2004, Crabbe et al, 2004, Crabbe et al, 2007, Ouellette et al, 2000, Wyllie et al, 2000).

Interestingly, some of the phenotypes observed in $TRF2^{\Delta B}$ and $TRF2^{\Delta B\Delta M}$ cells are analogous (Figure 1.5A). Overexpression of $TRF2^{\Delta B}$ and $TRF2^{\Delta B\Delta M}$ in cells both leads to the formation of TIFs, growth arrest and characteristics of a senescence phenotype (van Steensel et al, 1998, Wang et al, 2004). Additionally, TRF2 plays a role in protecting the 3' G-rich tail, as expression of $TRF2^{\Delta B\Delta M}$ promotes the loss of 50% of the G-strand overhangs by the endonuclease ERCC1/XPF (van Steensel et al, 1998, Zhu et al, 2003). It is not clear which pathway HR versus NHEJ will be activated but it may depend on whether the 3' overhang is maintained as a result of the type of cellular stress experienced (Longhese, 2008). The 3' overhang is essential to strand invasion during HR, as the 3' overhang is maintained in the $TRF2^{\Delta B}$ cells (Wang et al, 2004). In $TRF2^{\Delta B\Delta M}$ cells, the 3' overhangs are degraded, leading to telomere end-end fusions that are dependant on NHEJ (van Steensel et al, 1998). One current model suggests that TRF2 interacts with proteins involved in NHEJ and HR pathways to help aid in the formation and resolving of the t-loop structure during telomere replication (van Steensel et al, 1998, Verdun et al, 2005, Verdun & Karlseder, 2006, Wang et al, 2004). Overall, there is much evidence to suggest that TRF2 plays a large role in telomere maintenance and protects functional telomeres

from HR and NHEJ pathways. The mechanisms by which TRF2 controls HR or NHEJ at telomeres is not fully understood.

1.2.3 The Role of TRF2 in the DNA Damage Response

It has been demonstrated that TRF2 has the ability to remodel telomeric DNA into t-loops *in vitro*, as it is suggested TRF2 may require the interaction with other DNA repair proteins to form the t-loop structure and protect the chromosome ends (de Lange, 2002, Griffith et al, 1999, Stansel et al, 2001). Previous studies have identified that TRF2 has interactions with proteins and enzymes involved in DNA repair, and may play a role in the DNA damage response. In particular, TRF2 has been shown to interact with DNA repair proteins Mre11, Rad50, NBS1, Ku70 and ATM and DNA processing enzymes WRN helicase, BLM helicase, ERCC1/XPF endonuclease and Apollo exonuclease (de Laat et al, 1998, Hoeijmakers, 2001, Karlseder et al, 2002, Karlseder et al, 2004, Lenain et al, 2006, Machwe et al, 2004, Opresko et al, 2002, Song et al, 2000, Stansel et al, 2001, Stavropoulos et al, 2002, van Overbeek & de Lange, 2006, Winkler et al, 2001, Zhu et al, 2000). Overexpression of TRF2 in human primary cells inhibited the autophosphorylation of ATM, and the phosphorylation of its downstream targets Nbs1 and p53. These results suggest TRF2 may block the DNA damage response at telomeres by inhibiting the autophosphorylation of ATM in response to ionizing irradiation (IR) (Karlseder et al, 2004). Additionally, it was observed that TRF2 associates with photo-induced DSBs in non-telomeric DNA in human fibroblast cells within 2 sec after irradiation (Bradshaw et al, 2005). It has been suggested that TRF2 may act as an early sensor of DSBs that occurs before ATM. Recently, it has been suggested TRF2 may play

a role in human disease and tumorigenesis. When TRF2 was overexpressed in mouse keratinocytes, the mice displayed severe phenotypes in the skin in response to UV light. These phenotypes include susceptibility to skin cancer, skin discolouration and hyperpigmentation; symptoms which are closely related to the human disease XP (Munoz et al, 2005). The skin cells of the mice had shortened telomeres, loss of G-overhangs and increased chromosome instability. In Addition, an increase in the levels of TRF2 in human skin carcinomas has also been reported (Munoz et al, 2005). TRF2 overexpression has also been observed in human cancers of the breast, lung, gastric system and lymphomas (Klapper et al, 2003, Miyachi et al, 2002, Nakanishi et al, 2003, Nijjar et al, 2005). TRF2 overexpression has also been shown to promote carcinogenesis in the absence of telomerase by inducing telomere dysfunction and chromatin instability (Blanco et al, 2007). Taken together, these findings suggest that TRF2 might play a negative role in the DNA damage response pathway. The objective of part one of my thesis was to determine whether TRF2 may play a role in modulating the ability of cells to sense and repair UV-induced DNA damage mediated through ATR.

1.3 TRF2 Mutants Utilized in Part Two of this Study

Although the phenotypes of TRF2 deletion mutant proteins $TRF2^{\Delta B}$ and $TRF2^{\Delta B\Delta M}$ have been previously characterized (van Steensel et al, 1998, Wang et al, 2004), the important residues in the basic domain of TRF2 have not been entirely elucidated. Preliminary mass spectrometric analysis of immuno-purified TRF2 revealed several methylated arginine residues in the basic domain of TRF2, including arginines at positions 13, 17 and 18 (Figure 1.3B) (T. Mitchell and X.-D. Zhu unpublished data). To

determine the critical amino acids that are indispensable to the function of TRF2 in protecting human telomeres, several mutations were introduced in the basic domain of TRF2 (Figure 1.5B). Arginine residues 13, 17, 18, 21, 25, 27, 28 and 30 in the basic domain of TRF2 were mutated to alanine (A) or lysine (K). These mutations were introduced into the full length wild type *TRF2* or *TRF2* lacking the Myb domain expressed in a retroviral pLPC vector. Analysis of these mutants constitutes the second part of my thesis. The objectives of my second research project are to identify the key arginine residues which are essential to the function of the basic domain of TRF2 and to determine the molecular mechanisms responsible for the observed detrimental phenotypes in TRF2 mutant cells.

Figure 1.1. Components of the shelterin complex. TRF1 and TRF2/Rap1 bind to the double-stranded telomeric DNA, which are joined by TIN2. TPP1 links the single-stranded telomeric binding protein POT1 to the rest of the shelterin complex. Illustration obtained from de Lange (2005).

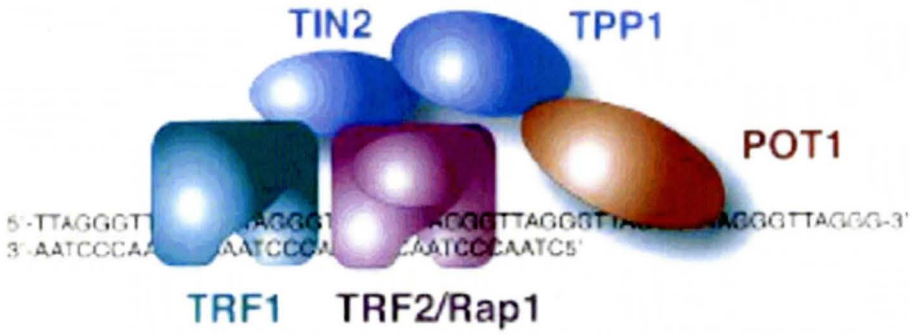
TIN2
TPP1
POT1
TRF1
TRF2/Rap1

Figure 1.2. DNA damage response in mammalian cells. A) The DNA damage response pathway is activated in response to different types of cellular stresses. ATM responds primarily to DNA DSBs throughout the cell cycle. ATR responds to disruptions in DNA replication induced by agents such as ultraviolet light or hydroxyurea. Activation of ATM or ATR results in an integrated signaling cascade as a result of the activation of effector proteins. Activation of the DNA damage response leads to apoptosis, DNA repair, cell-cycle arrest and chromatin remodeling. B) Deletion or inhibition of TRF2 leads to the activation of the DNA damage response mediated *via* ATM. The activation of the DNA damage signal leads to senescence or apoptosis *via* the p53/p21 pathway depending on the cell type. Deletion of POT1 leads to the activation of the DNA damage response *via* ATR. Illustrations in A and B were obtained from Palm and de Lange (2008). C) Illustration of nucleotide excision repair in mammals. The DNA damage recognition proteins are different in global genome repair and transcription coupled repair but the subsequent steps of repair are identical. The damaged DNA will be unwound, excised and a new DNA strand will be synthesized and ligated. Illustration obtained Saldivar *et al.* (2007).

A

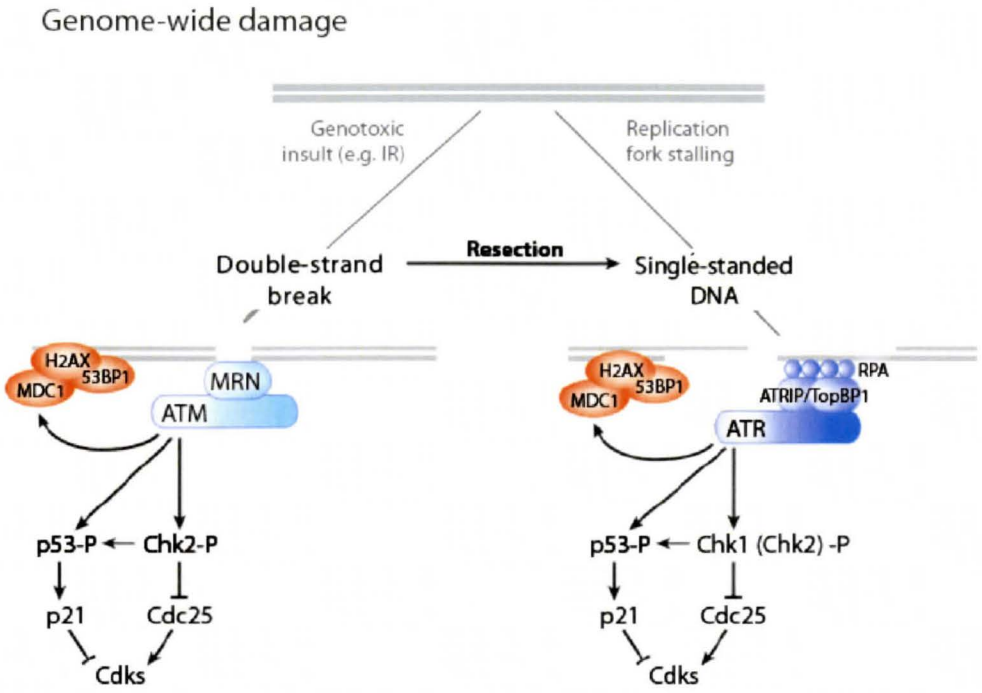
Genome-wide damage
Genotoxic insult (e.g. IR)
Replication fork stalling
Double-strand break
Resection
Single-standed DNA
H2AX
53BP1
MDC1
MRN
ATM
RPA
ATRIP/TopBP1
ATR
p53-P
Chk2-P
Chk1 (Chk2) -P
p21
Cdc25
Cdks

B

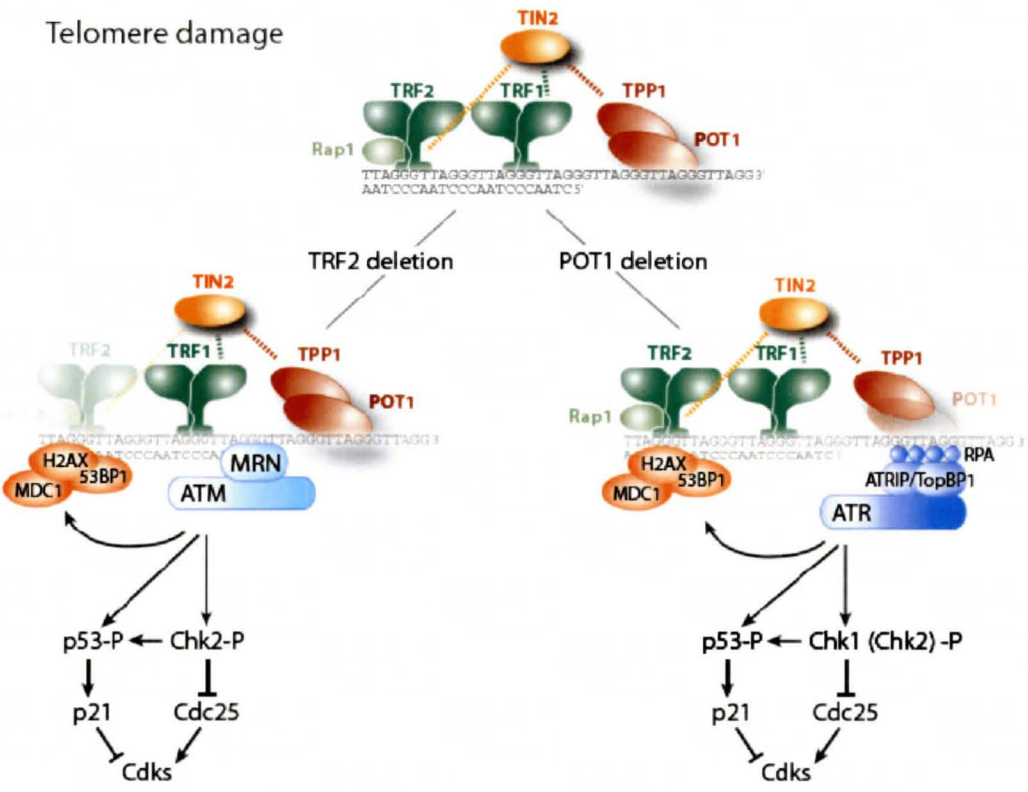
Telomere damage
TIN2
TRF2
TRF1
TPP1
POT1
Rap1
TRF2 deletion
POT1 deletion
H2AX
53BP1
MDC1
MRN
ATM
RPA
ATRIP/TopBP1
ATR
p53-P
Chk2-P
Chk1 (Chk2) -P
p21
Cdc25
Cdks

C

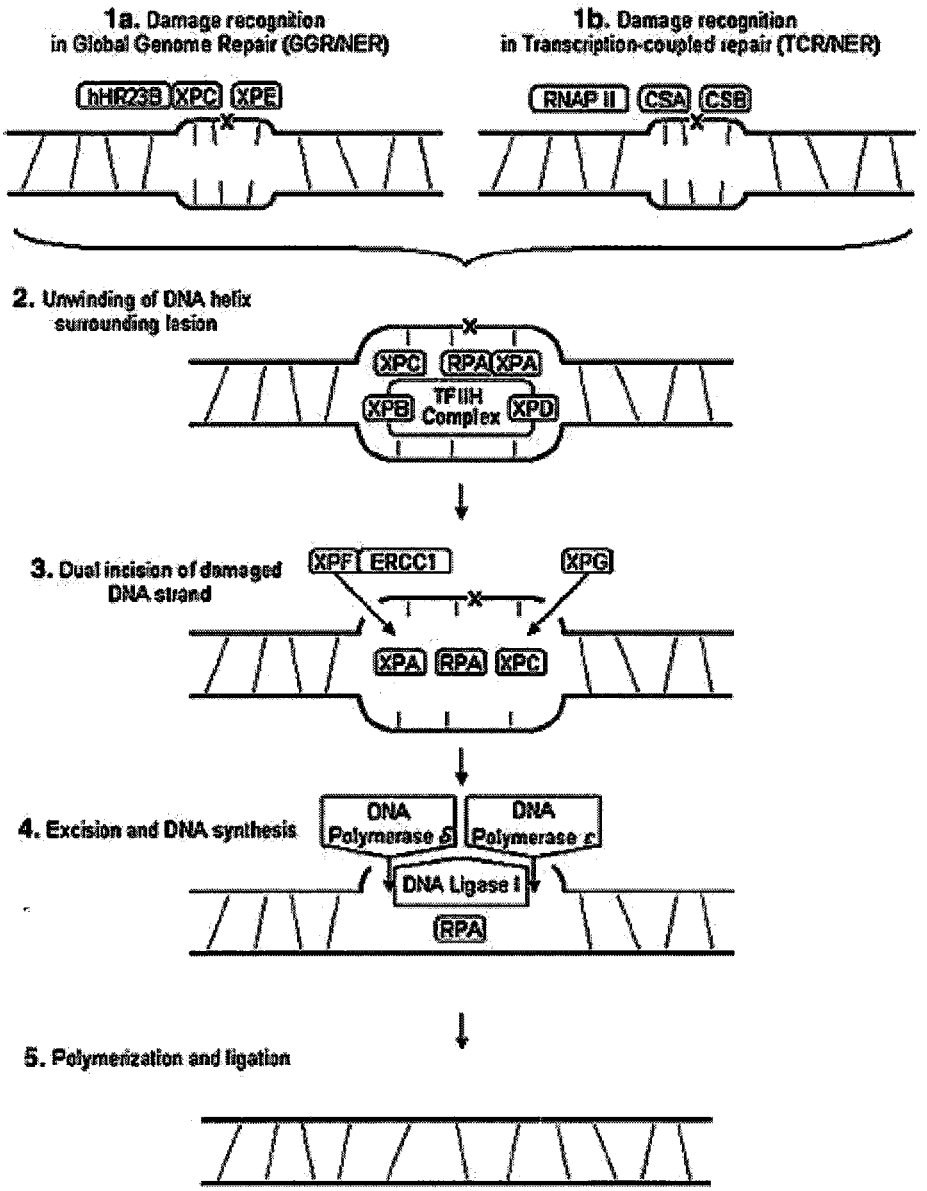
1a. Damage recognition in Global Genome Repair (GGR/NER)
1b. Damage recognition in Transcription-coupled repair (TCR/NER)
hHR23B
XPC
XPE
RNAP II
CSA
CSB
2. Unwinding of DNA helix surrounding lesion
XPC
RPA
XPA
XPB
TFIIH Complex
XPD
3. Dual incision of damaged DNA strand
XPF
ERCC1
XPG
XPA
RPA
XPC
4. Excision and DNA synthesis
DNA Polymerase δ
DNA Polymerase ε
DNA Ligase I
RPA
5. Polymerization and ligation

Figure 1.3. The human TRF2 protein. A) Illustration of the full-length human TRF2 and the deletion mutants used in this study TRF2$^{\Delta B}$, TRF2$^{\Delta M}$ and TRF2$^{\Delta B\Delta M}$. B) Illustration of the amino acids in the basic domain of human TRF2. Underlined residues are the arginine residues which are mutated in this study. Bold residues are the amino acids which were identified by mass spectrometry to be possibly modified by methylation. Modified from van Steensel *et al.* (1998).

A

B

MAGGGGSSDGSG**R**[13]AAG**R**[17]**R**[18]AS**R**[21]S
SG**R**[25]A**R**[27]**R**[28]G**R**[30]HEPGLGGPAERGAGE

Figure 1.4. Model of telomere deprotection induced by TRF2$^{\Delta B\Delta M}$ and TRF2$^{\Delta B}$. A) Expression of TRF2$^{\Delta B\Delta M}$ results in the inability to reform the t-loop structure after DNA replication. The exposed telomere ends activate the DNA damage response, resulting in the loss of the 3' overhang. The blunt-ended telomere may be processed by NHEJ resulting in a dicentric telomere fusion. The fusion events may be observed as anaphase bridges in anaphase cells or as chromosome, chromatid or sister telomere fusions in metaphase cells. B) Expression of TRF2$^{\Delta B}$ leads to an unprotected telomere. Branch migration of the C strand at the telomere loop resembles a Holliday junction. If the HJ is cleaved by XRCC3 (solid arrows) and nicked by a nuclease (open arrow) telomere shortening and telomere circles are formed. Modified from de Lange (2002), Smogorzewska *et al.* (2002) and Wang *et al.* (1998).

A

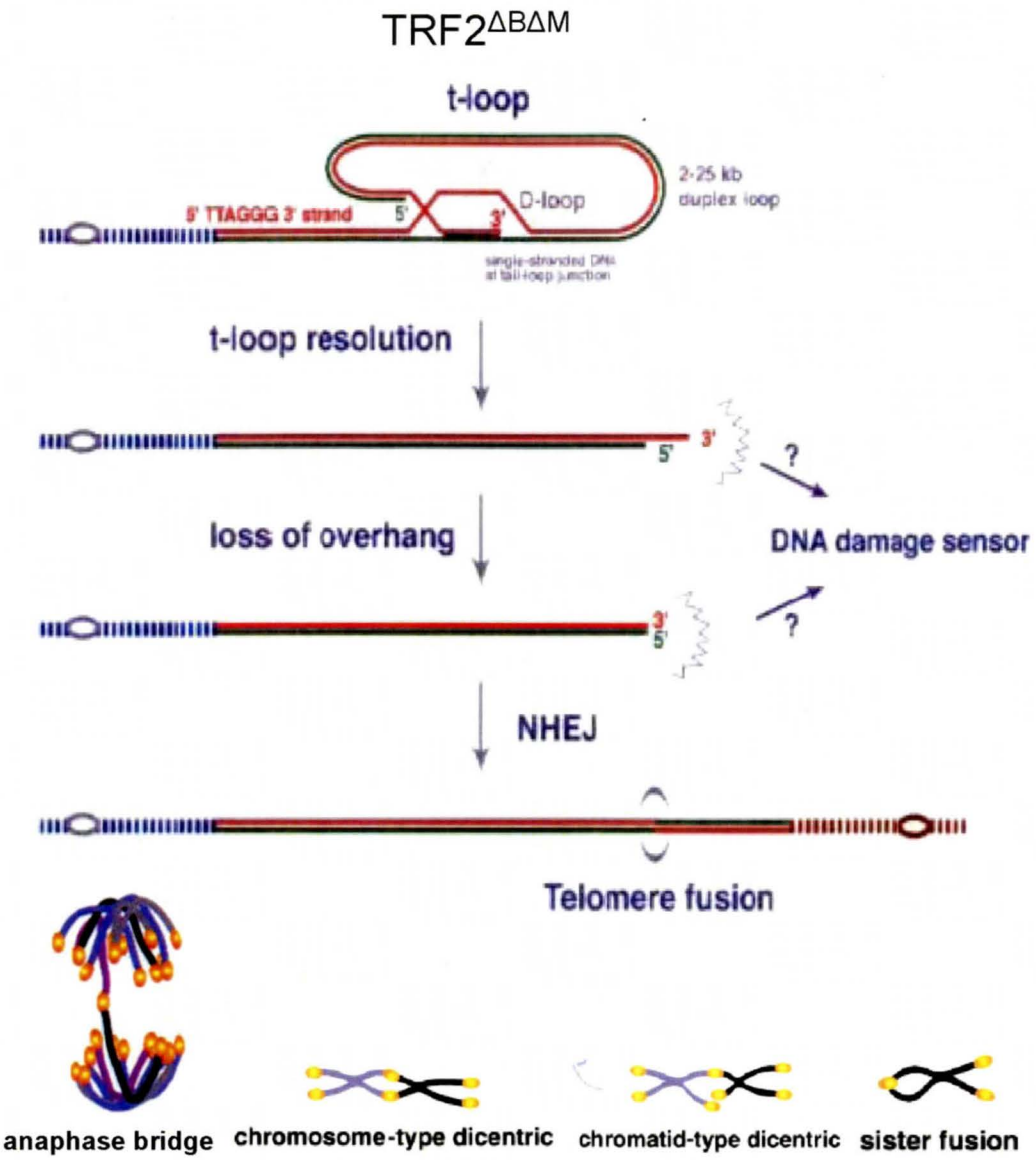
TRF2ΔBΔM
t-loop
2-25 kb
duplex loop
5' TTAGGG 3' strand
5'
3'
D-loop
single-stranded DNA
at tail-loop junction
t-loop resolution
3'
5'
?
DNA damage sensor
loss of overhang
3'
5'
?
NHEJ
Telomere fusion
anaphase bridge
chromosome-type dicentric
chromatid-type dicentric
sister fusion

B

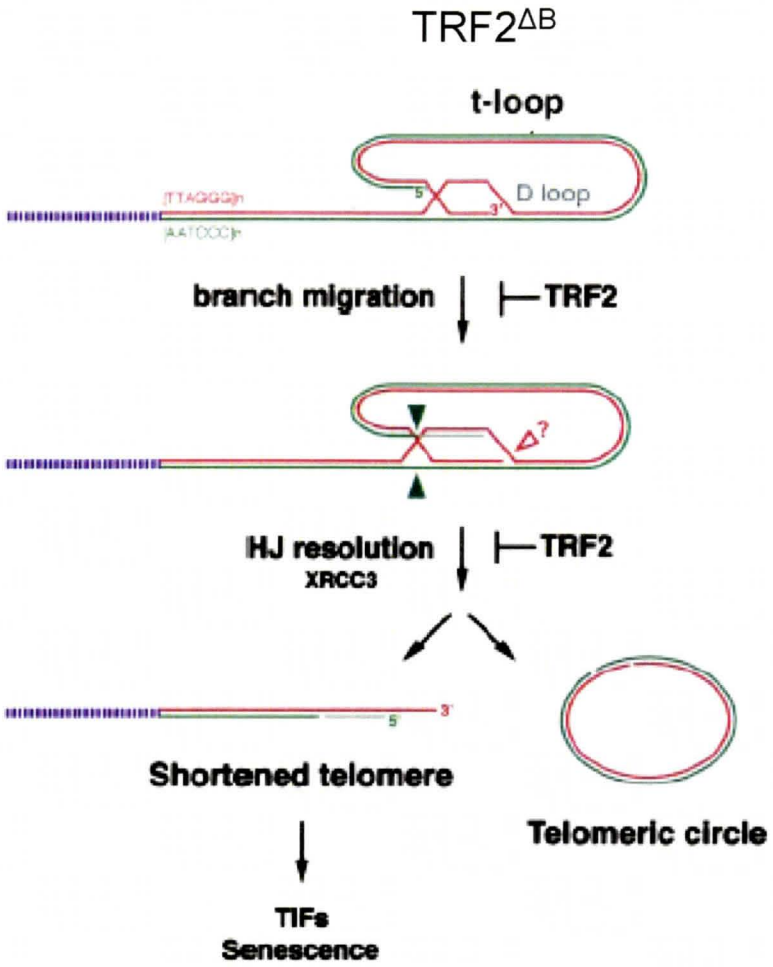
TRF2ΔB
t-loop
D loop
branch migration
TRF2
HJ resolution
XRCC3
TRF2
Shortened telomere
Telomeric circle
TIFs
Senescence

Figure 1.5. TRF2 mutations. A) Description of the TRF2$^{\Delta B}$ and TRF2$^{\Delta B \Delta M}$ dominant negative deletion mutant observed phenotypes. B) Abbreviation and description of the deletion mutations TRF2$^{\Delta B}$, TRF2$^{\Delta M}$ and TRF2$^{\Delta B \Delta M}$ and arginine mutations TRF2-RA, TRF2-RK, TRF2RK-1-4 and TRF2RK-5-8 used in this study.

A

$TRF2^{\Delta B}$	$TRF2^{\Delta B \Delta M}$
Able to bind telomeric DNA	Unable to bind telomeric DNA
Slow growth	Slow growth
Senescence characteristics	Senescence characteristics
Formation of TIFs	Formation of TIFs
Generation of t-looped sized telomeric circles	No telomeric circles
Telomere shortening	No telomere shortening
No anaphase bridges	Anaphase bridges
No telomere end-end fusions	Telomere end-end fusions
No loss of G-strand overhang	Loss of G-strand overhang

B

Abbreviation	Description of Mutation
$TRF2^{\Delta B}$	Deletion of the basic domain of TRF2
$TRF2^{\Delta M}$	Deletion of the Myb domain of TRF2
$TRF2^{\Delta B \Delta M}$	Deletion of both the basic and Myb domains of TRF2
TRF2-RA	Mutation of arginines (R) 13, 17, 18, 21, 25, 27, 28 and 30 in the basic domain of TRF2 to alanines (A)
TRF2-RK	Mutation of arginines (R) 13, 17, 18, 21, 25, 27, 28 and 30 in the basic domain of TRF2 to lysines (K)
TRF2-RK1-4	Mutation of arginines (R) 13, 17, 18 and 21 in the basic domain of TRF2 to lysines (K)
TRF2-RK5-8	Mutation of arginines (R) 25, 27, 28 and 30 in the basic domain of TRF2 to lysines (K)

Chapter 2 - Materials and Methods

2.1 Cloning of TRF2 Mutants

2.1.1 Cloning of pLPC-TRF2-RK1-4 and pLPC-TRF2$^{\Delta M}$-RK1-4

pLPC-TRF2-RK (plasmid #2018) was used as a template for PCR using the forward primer 5'GCGCAAGCTTCCAAGAGTAGCGGGCGGGCCCGGCGGGGGCG CCACGAGCCGGGGCTGGGGGGCCCG3' for both constructs, 5'GCGCCTCGAGT CAGTTCATGCCAAGTCTTTTC3' as reverse primer for TRF2-RK1-4 and 5'AGTCCT CGAGTCATTCTACAGTCCACTTCTGCTT3' as reverse primer for TRF2$^{\Delta M}$-RK1-4. The PCR products were digested with *HindIII* and *XhoI,* followed by GFX column purification. The purified DNA was ligated to digested *HindIII* and *Xhol* pKS plasmid (plasmid #2014). The resulting constructs numbered 2045 and 2046 were digested with *BamH1* and *Xho1.* The final linearized constructs were ligated into the pLPC vector (plasmid #2025) cut with *BamH1* and *Xho1.* Positive constructs pLPC-TRF2-RK1-4 (plasmid #2043) and pLPC-TRF2$^{\Delta M}$-RK1-4 (plasmid #2035) were verified for the correct mutations by sequencing analysis. All enzymes were purchased from New England BioLabs Inc.

2.1.2 Cloning of pLPC-Bg-TRF2-RK5-8

pLPC-TRF2 (plasmid #2033) was used as a template for PCR amplification using the forward primer 5'GCGCGGATCCAGCGGGAAGGCCAAGAAGGGGAAGCAC GAGCCGGGGCTGGGGGGCC3'and reverse primer 5'GCGCCTCGAGTCAGTTCAT GCCAAGTCTTTTC3'. The PCR product was digested with *BamHI* and *XhoI,* followed by GFX column purification. The purified DNA fragment was ligated into the pLPC-Bg

vector (plasmid #1001) cut with *BamHI* and *XhoI*. The resulting construct number 2050 was cut with *BamHI* and *EcoRI* and ligated with annealed oligos #125/126. The positive construct pLPC-Bg-TRF2-RK5-8 (plasmid #2044) was verified for the correct mutations by sequence analysis.

The retroviral constructs expressing TRF1, TRF2, TIN2, POT1, hRap1, TRF2$^{\Delta B}$, TRF2$^{\Delta M}$ and TRF2$^{\Delta B\Delta M}$ were generously provided by Titia de Lange. pLPC-TRF2-RA (#2024), TRF2-RK (#2018), TRF2$^{\Delta M}$-RA (#2027), TRF2$^{\Delta M}$-RK (#2028) and TRF2$^{\Delta M}$-RK5-8 (#2043) were constructed by Taylor Mitchell in the lab.

2.1.3 GFX™ Gel Band Purification

The correct size linearized DNA fragments were excised from a 1% agarose gel, mixed with the correct volume of capture buffer (containing acetate and chaotrope) and incubated at 60°C for 15 min. After the agarose was completely dissolved, the samples were incubated for 1 min in a MicroSpin™ column containing a glass fiber matrix and spun at 13,000 RPM for 1 min. A total of 500 µl of wash buffer (10mM Tris-HCL [pH 8.0], 1mM EDTA) was added to each column and spun at 13,000 RPM for 1 min. The DNA was eluted from the column using 50 µl of TE buffer (100 mM Tris, 10 mM EDTA [pH 8.0]). The GFX DNA Purification Kit was purchased from GE Healthcare.

2.1.4 Transformation

Plasmid DNA was incubated with Top10 competent *E.coli* cells on ice for 30 min. The samples were heat shocked at 42°C for 45 sec and placed back on ice for 2 min. The cells were incubated at 37°C shaking for 1 hr in 900 µl of LB media (1% Bacto™ tryptone (w/v), 0.5% Bacto™ yeast extract (w/v), 17.1 mM NaCl, 2.8 mM NaOH, 0.1

mg/ml ampicillin). The cells were spread on LB agar plates containing 0.1 mg/ml ampicillin (1% Bacto™ tryptone (w/v), 0.5% Bacto™ yeast extract (w/v), 17.1 mM NaCl, 2.8 mM NaOH, 1.5% agar (w/v)) and incubate for 12 – 16 hr at 37°C.

2.1.5 Alkaline Lysis Minipreparation of DNA

A single transformed bacterial colony was inoculated into 2 ml of LB media containing 100 µg/ml ampicillin and incubated with shaking for 12 – 16 hr at 37°C. The next day, 1.5 ml of the bacterial cultures were transferred to a microcentrifuge tube and spun at 13,000 RPM for 1 min at 4°C. The bacterial pellets were resuspended in 100 µl of ice-cold alkaline solution I (50 mM glucose, 25 mM Tris-HCL [pH 8.0], 10 mM EDTA [pH 8.0]) and vortexed vigorously. The bacteria cells were lysed in 200 µl of freshly made alkaline solution II (0.2 M NaOH, 1% SDS (v/v)), mixed rapidly and incubated at room temperature for 5 min. One-hundred and fifty microlitres of alkaline solution III (5 M potassium acetate, 11.5% glacial acetic acid (v/v)) was added to the samples, inverted to mix and incubated on ice for 5 min. The bacterial lysates were centrifuged for 5 min, 13,000 RPM at 4°C and the supernatants were transferred to a new tube. Equal volumes of phenol:chloroform were added to the supernatants and mixed by vortexing followed by centrifugation for 2 min 13,000 RPM at 4°C. The upper aqueous layers were carefully transferred to fresh tubes. The nucleic acids were precipitated by the addition of twice the volume of ice-cold 95% ethanol and spun at max speed for 5 min at 4°C. The DNA pellets were air-dryed and dissolved in TE buffer [pH 8.0] containing 20 µg/ml RNase A.

2.1.6 QIAGEN® Plasmid Purification Maxipreparation Kit

A single transformed bacterial colony was used to inoculate a starter culture of 3 ml of LB media containing 100 μg/ml ampicillin. The culture was incubated with shaking for 8 hrs at 37°C. The starter culture was then diluted 1:1000 in 200 ml of LB media containing 100 μg/ml ampicillin and incubated for 12 – 16 hrs, 225 RPM at 37°C. The next morning, the bacterial pellets were harvested by centrifugation at 4000 RPM, for 15 min at 4°C. The pellets were resuspended in buffer P1 containing 50 mM Tris-HCL [pH 8.0], 10 mM EDTA, and 100 μg/ml RNase A. The bacterial cells were lysed by the addition of 10 ml of buffer P2 (200 mM NaOH, 1% SDS (w/v)), mixed by inverting and incubated at room temperature. Following the 5 min incubation, 10 ml of ice-cold neutralization buffer P3 (3.0 M potassium acetate [pH 5.0]) was added to the samples, mixed quickly and incubated on ice for 20 min. The cell debris was separated from the supernatant by spinning at 12,500 RPM for 30 min and then 15 min at 4°C. The supernatant was loaded into a QIAGEN column equilibrated with buffer QBT (750 mM NaCl, 50 mM MOPS [pH 7.0], 15% isopropanol (v/v), 0.15% Triton® X-100 (v/v)) and allowed to drain by gravity. The columns were washed twice with 30 ml of buffer QC (1.0 M NaCl, 50 mM MOPS [pH 7.0], 15% isopropanol (v/v)) and the DNA was eluted into a glass pyrex tube with 15 ml buffer QF (1.25 M NaCl, 50 mM Tris-HCL [pH 8.5], 15% isopropanol (v/v)). The plasmid DNA was precipitated with 10.5 ml isopropanol and centrifuged for 30 min, 12,500 RPM at 4°C. The DNA pellet was washed with 7 ml of 70% ethanol and spun again for 10 min, 12,500 RPM at 4°C. The DNA pellets were air-dried and resuspended in TE [pH 8.0].

2.2 Cell Culture

2.2.1 Cell Lines

IMR90, Cockayne syndrome GM739, XPC deficient GM677 and BJ-hTERT cells were grown in DMEM media with 15% FBS (v/v), HT1080 cells were grown in 10% BCS (v/v) and Phoenix cells were grown in media containing 10% FBS (v/v), supplemented with 1% non-essential amino acids (v/v), L-glutamine, penicillin (100 U/ml) and streptomycin (0.1mg/ml). All cell lines stably expressing pLPC or pLPC-Bg were grown in the presence of 2μg/ml puromycin at 37°C with 5% CO_2 and 100% humidity. Cockayne syndrome GM739 and XPC deficient cells GM677 lines were obtained from Dr. Andrew Rainbow.

2.2.2 Retroviral Transfection and Infection

Phoenix amphotropic retroviral packing cells were transfected with the vector control alone or the vector containing the gene inserts. For each cell line, 3.5 x 10^6 Phoenix cells were seeded 24 hr prior to transfection onto 10 cm culture plates. A total of 30 μg of DNA was ethanol-precipitated for each plate to be transfected. The plasmid DNA was mixed with 438 μl sterilized ddH_2O and 62 μl of 2 M $CaCl_2$. While bubbling the mix, 500 μl of 2 X HBS [pH 7.05] (50 mM HEPES, 10 mM KCL, 12 mM dextrose, 280 mM NaCl, 1.5 mM Na_2PO_4) was added slowly, drop by drop. A total of 1 ml of mix was carefully dropped onto the plate of Phoenix cells. The media was changed with 9 ml of fresh media 12 hr post-transfection and again changed with 4 ml of media 24 hr post-transfection. The virus-containing media was collected 8 – 12 hr later. The media was mixed with 100 μg/ml polybrene, 4 ml of FBS and filtered through a 0.45 μm filter. The

recipient cells were infected with the virus-containing media seven times over a period of 72 hr post-transfection. HT1080 cells were seeded at a density of 2.5 x 10^5 cells, while all other cells lines were seeded 1.0 x 10^6 cells, 24 hr prior to the first infection. The recipient cells received 9 ml of fresh media 12 hr after the last infection. The cells were selected in 9 ml of 2μg/ml puromycin containing media 24 hr after the last infection.

2.2.3 UV Irradiation

IMR90, Cockayne syndrome GM739 and XPC-A deficient GM677 cells were exposed to 15 J/m^2 or 30 J/m^2 UVC radiation in 1X PBS using an UV Stratalinker® 1800. The cells were incubated in 15% FBS and were harvested at 0, 6, 12, 24 and 48 hrs post-UVC treatment.

2.3 Protein Analysis

2.3.1 Whole Cell Extract

Cells grown on 6 or 10 cm plates were harvested by trypsinization and washed with the appropriate medium. The cells were collected by centrifugation at 1000 RPM, for 5 min at 4°C. The cell pellets were washed twice with ice-cold 1 X PBS [pH 7.4], spun at 3000 RPM for 2 min at 4°C. The final cell pellets were resuspended in the correct volume of buffer C (20 mM Hepes-KOH [pH 7.9], 0.42 M KCl, 25% glycerol, 0.1 mM EDTA, 5 mM $MgCl_2$, 0.2% NP40, 1 mM DTT, 0.5 mM PMSF, 1 μg/ml leupeptin, 1 μg/ml aprotinin, 1 μg/ml pepstatin, 10 mM NaF, 1mM $NaVO_4$, 20 mM Na-β-glycerol phosphate), to obtain a total cell concentration of 2.0 x 10^4 or 4.0 x 10^4 cells/μl. The samples were incubated on ice for 30 min. The cells were spun at 13,000 RPM for 10 min at 4°C and the supernatant was transferred to a new tube. The supernatants were mixed

with equal volumes of 2X laemmli buffer (100 mM Tris-HCL [pH 6.8], 20% glycerol (v/v), 2% SDS (v/v), 0.02% bromophenol blue (w/v), 0.04% beta-ME) and stored at -20°C.

2.3.2 Western Immunoblotting

Supernatant protein samples were heated for 5 min at 85°C and loaded onto a 8% or 15% SDS polyacrylamide gel. The SDS-PAGE gels were run in running buffer (25 mM Tris, 192 mM glycine, 0.1% SDS (w/v)) for 1.5 – 2 hr at 100 V. The proteins were electrophoretically transferred to a nitrocellulose membrane at 90 V for 1 – 1.5 hrs in blotting buffer (25 mM Tris, 125 mM glycine, 20% methanol, 0.02% SDS). The membranes were blocked in 10% non-fat milk, 0.5% Tween-20 in 1X PBS or 1X TBS for 1 hr at room temperature with shaking. Subsequently, the membranes were washed in 1X PBS or 1X TBS plus 0.1% milk and 0.1% Tween-20 three times for 5 min. The membranes were incubated with TRF2, p53, phospho-serine15 p53, p21 or γ-tubulin antibody for 2 hr at room temperature or over night at 4°C. The primary antibodies were washed as above. Each membrane was incubated in the appropriate HRP-conjugated secondary anti-mouse or anti-rabbit antibodies diluted 1:20,000 for 1hr shaking at room temperature and washed as above. The membranes were exposed using ECL reagent (GE Healthcare). Indicated membranes were stripped in 2 M Glycine [pH 2.2] for 1 hr. To quantify the band intensities, an AlphaImager-2200 was used with spot densitometry software version 5.5.

2.3.3 Antibodies

Primary antibody TRF2 (#647) is a polyclonal rabbit antibody and was a generous gift from Titia de Lange. Affinity purified TRF2 was used at a dilution of 1:500 in incubation buffer (1X PBS, 0.1% non-fat milk, 0.1% Tween-20). Phospho-p53 (Ser 15) polyclonal rabbit antibody (Cell Signaling #9284) was used at a concentration of 1:150 diluted in incubation buffer (1X TBS, 0.1% non-fat milk, 0.1% Tween-20). Mouse monoclonal p53 (diluted 1:250) and p21 (diluted 1:500) primary antibodies were purchased from Santa Cruz Biotechnology. Mouse monoclonal anti-γ-tubulin antibody (Sigma #T 6557) was used as a loading control at a concentration of 1:10,000. Both anti-mouse and anti-rabbit IgG peroxidase-linked secondary antibodies were purchased from Amersham Biosciences.

2.4 Proliferation Analysis

2.4.1 Proliferation Assay

HT1080 cells were seeded 250,000 in duplicate on day 3 of selection into 10 cm plates. Every two days the HT1080 cells were counted using a Beckman Z1 Coulter® Particle Counter, split appropriately and reseeded onto 10 cm plates. BJ/hTERT cells were seeded 20,000 cells per well into a 12-well plate in duplicate on day 3 of selection. The cells were counted on subsequent days and fresh media was replaced every four days.

2.4.2 Senescence Associated β-Galactosidase Staining Assay

HT1080 and BJ/hTERT cells were seeded into 3.5 cm plates at least one day prior to the experiment. The cells were washed with 2 ml of 1X PBS and fixed in 1 ml of

fixing solution (2% formaldehyde, 0.2% glutaraldehyde, 1X PBS) for 15 min. The fixing solution was washed twice with 2 ml of 1X PBS. The cells were incubated for 8 – 12 hr at 37°C, with low CO_2 in 1 ml of staining solution (1 mg/ml X-gal diluted in DMF, 40 mM NaHPO4 [pH 6.0], 150 mM NaCl, 2 mM $MgCl_2$, 5 mM $K_3Fe(CN)_6$, 5 mM $K_4Fe(CN)_6$). After the incubation, the cells were washed twice with ddH_2O, dried and stored at room temperature. Images of the stained cells were obtained from a phase contrast microscope (Nikon Eclipse TE2000-S) and a Nikon digital camera (DXM1200F). The senescent β-galactosidase staining kit was purchased from Cell Signaling Technology #9860.

2.5 Chromosome Analysis

2.5.1 Chromosome Analysis in Anaphase Cells

HT1080 cells were seeded and grown on coverslips in 6 cm plates. The cells were rinsed with 4 ml of 1X PBS and fixed in 2 ml of 3% paraformaldehyde and 2% sucrose in 1X PBS for 10 min. Subsequently, the cells were washed twice in 4 ml of 1X PBS, 5 min each. The fixed cells were permeabilized in 2 ml of 0.5% Triton-X 100 in 1X PBS for 10 min and washed twice in 1X PBS for 5 min each. The cells were stained with DAPI diluted in 1X PBS for 10 min and washed as above. The coverslips were mounted onto microscope slides in embedding media containing p-phenylene diamine and glycerol in PBS. The coverslips were sealed to the slides with nail polish. Fixed cells were stored in 1X PBS containing 0.02% sodium azide at 4°C and hybridized slides were stored at – 20°C. DAPI staining was analyzed using a Zeiss Axioplan 2 microscope with Openlab software (Improvision) connected to a Hamamatsu C4742-95 camera.

2.5.2 Telomere FISH Analysis of Metaphase Chromosomes

BJ/hTERT cells were incubated in 0.1 mg/ml colcemid in 15% FBS for 4 hr in 6 cm plates. The cells were harvested by trypsinization, collected in 15 ml Falcon tubes and spun for 5 min at 1000 RPM. The cell pellets were resuspended in 5 ml of prewarmed 0.075 M KCL and incubated at 37°C for 7 min. After incubation, the cells were centrifuged for 5 min at 1000 RPM and the supernatant was decanted. The cell pellet was resuspended by tapping. Drop by drop, 1 ml of fixing solution (3:1 methanol:glacial acetic acid) was added with tapping between each drop and then brought to a final volume of 10 ml. The fixed cells were stored at 4°C for at least one night. Prior to spreading the cells, the cells were spun at 1000 RPM for 3 min. The cells were resuspended in an appropriate amount of fixing solution, depending on the pellet size. Twenty microliters of cells were dropped onto water-wetted microscope slides, rinsed with fixing solution and incubated on a 70°C heating block for 1 min. The slides were dried in a fume hood over night. The next day, the slides were rehydrated in 1X PBS [pH 7.4] for 5 min. The cells were fixed in 4% formaldehyde in 1X PBS for 2 min and washed 3 x 5 min in 1X PBS. The slides were incubated in 1 mg/ml prewarmed pepsin in acidified ddH_2O [pH 2.0] for 10 min at 37°C. The treated slides were washed in 1X PBS 2 x 2 min each, fixed again in 4% formaldehyde for 2 min with subsequent washes 3 x 5 min each in 1X PBS. The slides were dehydrated in 70%, 95%, and 100% ethanol for 5 min each and air-dried. Each metaphase spread was incubated with 20 µl of hybridization mix (10 mM Tris-HCL [pH 7.4], 70% formamide, 0.5% blocking solution, 0.2 µg/ml FITC C_3TAA PNA probe) for 2 hr and denatured at 80°C for 3 min prior to hybridization.

The cells were washed twice for 15 min each in 70% formamide, 10 mM Tris-HCL [pH 7.4] and 0.1% BSA diluted in ddH_20. Next, the cells were washed in 0.1 M Tris-HCL [pH 7.4], 0.15 M NaCl and 0.08% Tween-20 three times, 5 min each. To the second wash, DAPI (diluted 1:1000) was added and incubated was extended 10 min. The cells were dehydrated as above in ethanol and air-dried. Coverslips were mounted onto the slides with embedding media and sealed with nail polish. Slides were stored at –20°C.

2.6 Genomic DNA Analysis

2.6.1 Isolation of Genomic DNA

Genomic DNA was isolated from BJ/hTERT cells by trypsinization, washed with 1X PBS and stored at -80°C. The genomic DNA pellets were quickly thawed at room temperature and resuspended in 1 ml of 1X TNE (10 mM Tris-HCL [pH 7.4], 100 mM NaCl, 10 mM EDTA). The DNA was squirted into a 15 ml phase lock tube containing 1 ml of fresh TENS buffer (1X TNE, 1% SDS, 100 µg/ml proteinase K) . The tubes were mixed gently and incubated overnight at 37°C. The next day, 2 ml of phenol:chloroform was added to the tubes, inverted until the phases are completely mixed and centrifuged for 10 min, 3000 RPM at 4°C. The top layer was transferred to a new phase lock tube containing 2 ml of phenol:chloroform. The tubes were mixed until one phase and spun at 3000 RPM, 10 min at 4°C. After spinning, the top layer was transferred to a 15 ml falcon tube containing 2 ml of iso-propanol and 220 µl of 2 M NaAc [pH 5.5]. The tubes were inverted until the DNA precipitates and the DNA was transferred to an eppendorf tube containing 300 µl of TNE plus 100 µg/ml RNase A. The DNA was incubated for 30 min at 37°C, resuspended and incubated for another 2 hr. Three-hundred microliters of TENS

plus 100 µg/ml proteinase K was added, mixed and incubated for 1 hr at 37°C. The DNA was then mixed with 600 µl of phenol:chloroform until one phase and spun for 10 min, 4°C at 13,000 RPM. The upper phase was transferred to a new eppendorf tube containing 600 µl of iso-propanol plus 66 µl of 2 M NaAc [pH 5.5]. The DNA was fished out and resuspended in 100 µl of $T_{10}E_{0.1}$ (10 mM Tris-HCL [pH 8.0], 0.1 mM EDTA). The genomic DNA was incubated at 37°C until the DNA was dissolved and stored at -20°C.

2.6.2 Digestion of Genomic DNA for Telomere Blots

A total of 30 µl of genomic DNA was mixed with either 2.5 µl *HinfI* and 2.5 µl *RsaI* or 2 µl of *AluI* and 4 µl *MboI*, 10 µl of 10X NEB buffer 2, ddH_2O and 0.02 µl RNase A (10 mg/ml). The samples were incubated over night at 37°C. The DNA concentrations were determined by fluorimetry using a calf thymus DNA standard in Hoechst dye.

2.6.3 Southern Blotting

A total of 3 or 4 µg of digested genomic DNA was loaded onto a 0.7% agarose gel in 0.5 X TBE and ran until at least the 1 kb marker was at the bottom of the gel. The gels were dried using a gel dryer (BIO RAD model #583) for 2 hr at 50°C. The gels were denatured when indicated for 30 min in 1.5 M NaCl and 0.5 M NaOH with shaking. The gels were neutralized in 3 M NaCl and 0.5 M Tris-HCL [pH 7.0] two times for 15 min each with shaking and rinsed with ddH_2O. The gels were subsequently prehybridized with 20 ml of churchmix (0.5 M NaPi [pH 7.2], 1 mM EDTA [pH 8.0], 7% SDS (w/v), 1% BSA (w/v)) for 1 hr at 55°C. Each gel was then hybridized with a radioactive γ-^{32}P telomere probe (Tel C) in 20 ml of churchmix and incubated over night at 55°C. The next day, the gels were washed three times, 20 min each in 4X SSC (0.6 M NaCl, 60 mM

sodium citrate) with shaking at room temperature. Then the gels were washed in pre-warmed 4X SSC plus 0.1% SDS, twice for 30 min each at 55°C with shaking. Each gel was exposed using a PhosphoImage screen (Amersham Biosciences) and scanned using a PhosphoImager (Storm 820, Amersham Pharmacia Biotech). Quantification of the telomere blots was performed by using ImageQuant software version 5.2.

Chapter 3 - Results and Discussion

Characterization of TRF2 in the UV-Induced DNA Damage Response

TRF2 interacts with DNA repair proteins and DNA processing enzymes (de Laat et al, 1998, Hoeijmakers, 2001, Karlseder et al, 2002, Karlseder et al, 2004, Lenain et al, 2006, Machwe et al, 2004, Opresko et al, 2002, Song et al, 2000, Stansel et al, 2001, Stavropoulos et al, 2002, van Overbeek & de Lange, 2006, Winkler et al, 2001, Zhu et al, 2000). TRF2 may protect telomeres by preventing the chromosome ends from being recognized as DNA breaks (Baird & Farr, 2006, de Lange, 2002, Palm & de Lange, 2008). The precise mechanisms underlying the function of TRF2 in the regulation of the UV-induced DNA damage response was not fully elucidated at the time of this study. Past findings suggest that TRF2 may play a role in the UV-induced DNA damage response. In particular, one study reported an increase in the levels of TRF2 in human skin carcinomas (Munoz et al, 2005). Additionally, mouse Keratinocytes which overexpress TRF2 are hypersensitive to UV irradiation (Munoz et al, 2005). Furthermore, TRF2 has been shown to play a role in the DNA DSB repair pathway. Overexpression of TRF2 in human primary cells inhibits the autophosphorylation ATM after ionizing irradiation (Karlseder et al, 2004). As well, it was suggested TRF2 may act as an early DNA DSB sensor, as TRF2 was observed to associate with non-telomeric DNA before ATM association in response to photo-induced DSBs (Bradshaw et al, 2005). In general, these findings help support the hypothesis that TRF2 may negatively regulate the UV-induced DNA damage response.

3.1 Overexpression of TRF2 Does Not Appear to Have Any Significant Impact on the UV-Induced DNA Damage Response in IMR90 Cells

In order to determine whether TRF2 influences the UV-induced DNA damage response pathway, I examined p53 induction in response to UVC treatment in IMR90 cells. IMR90 cells were retrovirally infected with the vector alone or the vector containing the wild type TRF2 construct. IMR90 cells were treated with 15 J/m^2 or 30 J/m^2 UVC. Protein extracts were harvested at 6, 12, 24 and 48 hr post-UVC treatment in the presence or absence of phosphatase inhibitors. Immunoblotting for p53 and p53 phosphorylated on serine 15 was performed for five independent experiments. Figure 3.1A is a representative blot demonstrating no attenuation of the p53 protein in TRF2 overexpression cells in response to UVC treatment as compared to the vector control. Figures 3.1 B and C are quantification results obtained from using spot-densitometry to evaluate the levels of p53 and phosphorylated-p53 from four independent experiments. The quantified values were determined based on the quantity of protein loaded and normalized to the untreated vector control. Results of the quantification for all four experiments demonstrate a high variability between each experiment. The p53 and phosphorylated-p53 values quantified show no significant difference between the vector and TRF2 at 12, 24 and 48 hrs. Based on my findings under these experimental conditions, TRF2 does not appear to play a major role in negatively regulating the DNA damage signaling pathway in response to UVC treatment in IMR90 cells.

The results of my experiments are not consistent with the publication of TRF2 levels being correlated with hypersensitivity to UV irradiation in a transgenic mouse line

or the increase of TRF2 expression being associated with human skin carcinogenesis (Munoz et al, 2005). However, one cannot rule out the possibility that TRF2 may still have a role in the UV-induced DNA damage response pathway in an alternate cell line or under different experimental conditions. My experiments were performed in a human primary lung fibroblast cell line. The hypothesis of TRF2 negatively regulating the DNA damage response pathway may still hold true for another human skin cell line but further investigation will be needed. Additionally, the results of my TRF2 overexpression experiments were observed only over a short period of time. It is possible TRF2 may only have a negative impact on the long-term survival of the cells. On the other hand, my results are consistent with a report which demonstrates that inhibition of the ATR pathway is mediated by POT1 and not TRF2 (Denchi & de Lange, 2007). ATR is the main transducer protein which is activated in response to stalled DNA replication forks or bulky lesions caused by UV irradiation (Palm & de Lange, 2008). In conclusion, there is not enough positive evidence based on my results to conclude that TRF2 plays a major inhibitory role in the UV-induced DNA damage response in IMR90 cells.

3.2 Overexpression of TRF2 Does Not Appear to Have Any Significant Affect on the Repair Ability of Cockayne Syndrome or XPC Deficient Cells

Overexpression of TRF2 in IMR90 cells failed to demonstrate a major role of TRF2 in the UV-induced DNA damage response. However, it may be possible that IMR90 cells may be masking the effect of TRF2 on the nucleotide excision repair pathway as both transcription coupled repair and global genome repair pathways are functional in this cell line. In order to determine if TRF2 overexpression had an impact

on either TCR or GGR, Cockayne syndrome GM739 and XPC-A deficient GM677 cell lines were utilized. Cells deficient in XPC are deficient in GGR, which allows one to compare the effect of TRF2 on the TCR pathway, whereas CS cells are deficient in TCR, which allows one to study the effect of TRF2 on the GGR pathway (Hwang et al, 1999, Venema et al, 1991). It has been suggested that p53 plays a role in the direct transcription of NER genes, specifically the proteins involved in GGR but not TCR (Bohr et al, 1985, Ford & Hanawalt, 1997, Mellon et al, 1987). In order to establish whether GGR or TCR was affected by TRF2 overexpression in response to UVC treatment, CS and XPC deficient cell lines were retrovirally infected with the vector alone or the vector containing wild type TRF2. The two deficient cell lines were treated with or without 30 J/m^2 UVC radiation and harvested at 6, 12, 24 and 48 hrs post-UVC treatment. The protein samples were immunoblotted for p53 and phosphorylated-p53 at position serine 15. Figure 3.2A represents the results of immunoblotting of p53 and phosphorylated-p53 in Cockayne syndrome cells. The p53 protein level in both the control and TRF2 overexpression cells shows a gradual induction of p53. Additionally, there is no large difference observed in the control versus TRF2 overexpression cells in the immunoblot for phosphorylated-p53. Figure 3.2B represents the results of immunoblotting of p53 and phosphorylated-p53 in XPC deficient cells. The levels of p53 in the vector peaks at 24 and 48 hr as compared to TRF2 overexpression cells which peak at 12 and 24 hrs. The levels of phosphorylated-p53 were low for both the vector and TRF2 overexpression cells. In general, based on my observations, overexpression of TRF2 does not appear to have a substantial impact on the global genome repair or transcription coupled repair of

Cockayne syndrome or XPC deficient cells respectively in response to UVC treatment. Taken together, overexpression of TRF2 does not appear to have a significant impact on the UV-induced DNA damage response in IMR90 cells, Cockayne syndrome cells and XPC deficient cells. However further investigation is needed to determine whether this conclusion is exclusive to these cell lines and experimental conditions.

Figure 3.1. Overexpression of TRF2 does not appear to attenuate the p53 DNA damage response after UVC treatment. IMR90 cells were retrovirally infected with the pLPC vector alone or the vector containing the *TRF2* gene insert and selected in puromycin containing medium for eight days. IMR90 cells were treated with or without UVC radiation in 1 X PBS using a Stratagene UV cross-linker and incubated in 15% FBS. A) Representative blot of IMR90 cells PD-34 were harvested at 0, 6, 12, 24 and 48 hrs post-UVC treatment by scraping the cells in cold 1 X PBS and a buffer-C whole cell extract protocol was performed. The supernatant fractions were collected and stored in 4 X laemmli buffer. Protein samples were loaded on to a 15% SDS polyacrylamide gel at a concentration of 25 μg/μl. The nitrocellulose membrane was immunoblotted with p53 primary antibody, subsequently stripped and re-incubated with γ-tubulin antibody. The proteins were visualized on hyperfilm using enhanced chemiluminescence. B) Quantification of p53 using spot densitometry normalized to the untreated vector control. C) Quantification of phosphorylated-p53 serine 15 using spot densitometry normalized to the untreated vector control. Quantifications were performed on four independent experiments. Error bars represent the standard deviation of the mean.

A

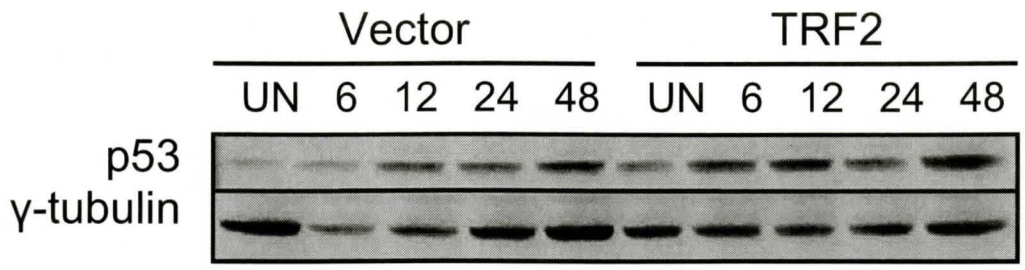
Vector
TRF2
UN 6 12 24 48 UN 6 12 24 48
p53
γ-tubulin

B

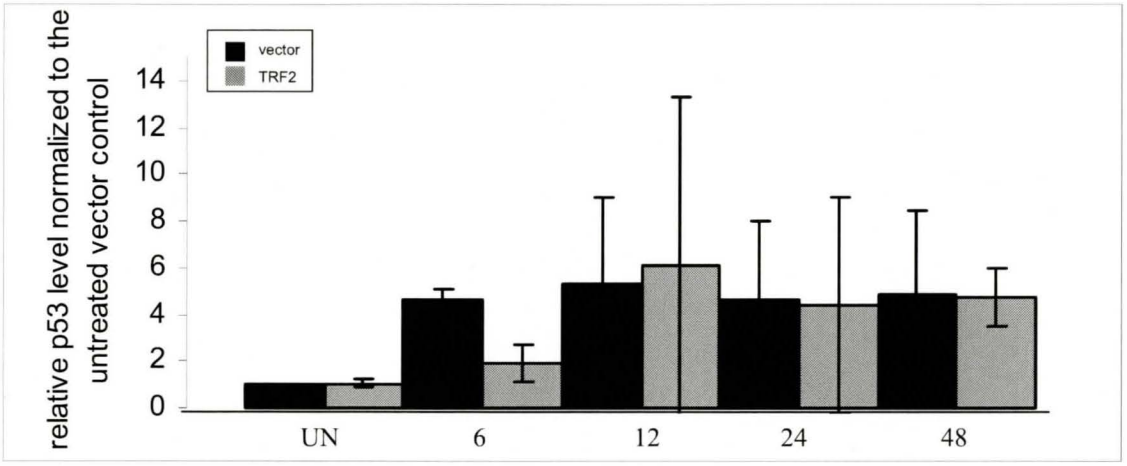
relative p53 level normalized to the untreated vector control
vector
TRF2
0 2 4 6 8 10 12 14
UN 6 12 24 48

C

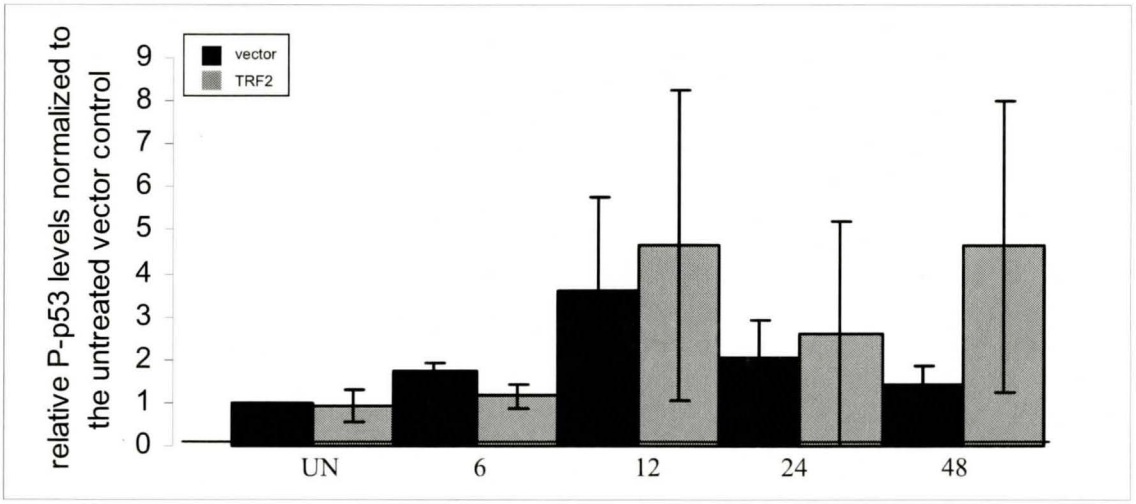
relative P-p53 levels normalized to the untreated vector control
vector
TRF2
0 1 2 3 4 5 6 7 8 9
UN 6 12 24 48

Figure 3.2. Overexpression of TRF2 does not have a substantial impact on nucleotide excision repair in response to UVC treatment. A) Cockayne syndrome cells were treated with or without 30 J/m^2 UVC radiation. Protein samples were harvested at 6, 12, 24 and 48 hrs post-UVC treatment. Protein samples were immunoblotted for p53, phosphorylated-p53 serine 15 and γ-tubulin. Blots were stripped between primary antibody incubations. B) XPC deficient cells treated with or without 30 J/m^2 UVC radiation. Protein samples were harvested at 6, 12, 24 and 48 hrs post-UVC treatment. Protein samples were immunoblotted for p53, phosphorylated-p53 serine 15, and γ-tubulin. Blots were stripped between primary antibody incubations.

A

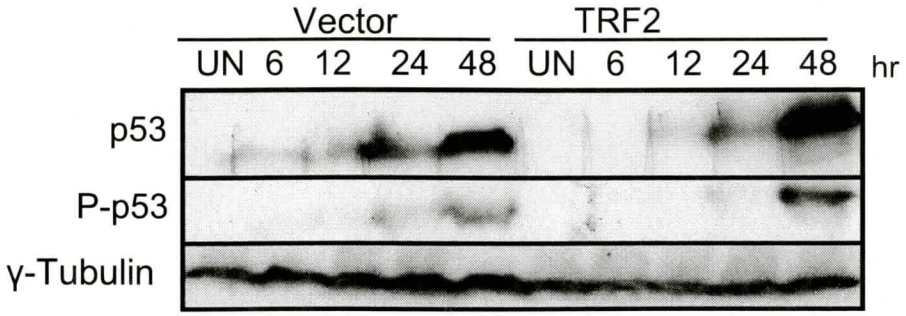
Vector
TRF2
UN 6 12 24 48 UN 6 12 24 48 hr
p53
P-p53
γ-Tubulin

B

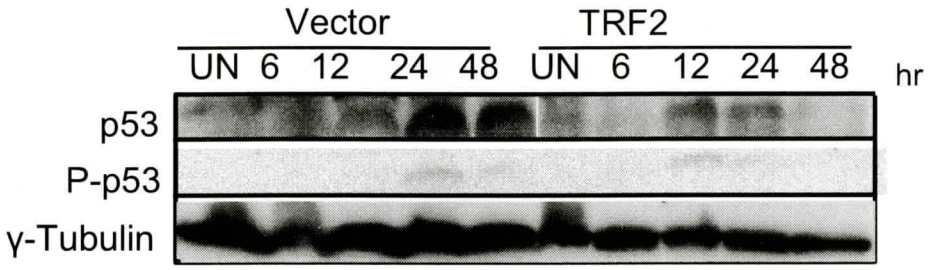
Vector
TRF2
UN 6 12 24 48 UN 6 12 24 48 hr
p53
P-p53
γ-Tubulin

Chapter 4 - Results

Characterization of TRF2 in Telomere Maintenance

TRF2 protects the telomeres from being illegitimately processed by the DNA DSB repair pathways, as it is thought to facilitate the formation of the t-loop structure (Griffith et al, 1999, Stansel et al, 2001). The t-loop model hides the ends of the chromosomes and protects the telomeres from the homologous recombination and non-homologous end joining pathways. The t-loop structure resembles a HJ intermediate and is processed by homologous recombination when the basic domain of TRF2 is deleted (Wang et al, 2004). Additionally, in the absence of the basic and Myb domains of TRF2, TRF2 cannot bind to the telomeric repeats and thus the chromosome ends are processed by the non-homologous end joining pathway (van Steensel et al, 1998). However, it is not fully understood what amino acid residues in the basic domain of TRF2 are indispensable to suppress these recombination events.

4.1 Analysis of TRF2 Mutants in HT1080 Cells

4.1.1 Overexpression of TRF2 Carrying Amino Acid Changes from Arginines to Alanines in the Basic Domain Induces Decreased Proliferation and Senescence in HT1080 Cells

Lack of the basic domain of TRF2 causes a decreased proliferation rate and senescence (Wang et al, 2004). To determine whether the charge alone in the basic domain of TRF2 is sufficient for its protective function, eight positively charged arginine residues were mutated to eight neutral alanine residues. To study the effects of the alanine mutant on the function of the basic domain of TRF2, proliferation assays and a

senescence assay was completed to observe whether this TRF2 mutant will show a similar phenotype to the lack of the basic domain of TRF2. The proliferation assay performed in HT1080 cells expressing the TRF2 mutant containing the amino acid changes from arginines to alanines in the basic domain demonstrated to have a decreased proliferation phenotype as compared to the vector control (Figure 4.1A). Overexpression of the vector and wild type TRF2 in HT1080 cells does not result in reduced proliferation, as at day 13 both cell lines had the same cumulative cell number. At day 13 TRF2-RA had a significantly decreased proliferation rate as compared to the controls. TRF2-RA had a proliferation rate of almost a four fold decrease as compared to the vector and TRF2 at day 13. To confirm that overexpression of the TRF2 mutants were maintained throughout the experiment, western blotting was performed (Figure 4.1B). Western blotting indicates that all of the TRF2 mutant overexpression constructs in HT180 cells were being expressed at similar levels to the wild type TRF2 at day 3 and day 15.

Expression of TRF2 lacking both the basic and Myb domains leads to a decreased proliferation rate and senescence (van Steensel et al, 1998). To further investigate whether the charge of the basic domain is essential to the function of the domain, I additionally examined a TRF2 mutant carrying amino acid substitutions from arginines to alanines in the basic domain in combination with the absence of the Myb domain. A second proliferation assay was constructed in HT1080 cells which expressed this TRF2 mutant (Figure 4.2A). Both the vector control and TRF2 proliferated at a similar rate however, TRF2$^{\Delta M}$-RA had about a 3.5 fold decreased proliferation rate at day 15 as

compared to the controls. Immunoblotting revealed overexpression of the TRF2 mutant constructs were maintained at similar levels to TRF2 at days 3, 12 and 15 (Figure 4.2B).

To test if the decreased replicative potential phenotype in TRF2$^{\Delta M}$-RA expressing HT1080 cells leads to permanent growth arrest, as observed in TRF2$^{\Delta B\Delta M}$ cells (van Steensel et al, 1998), a senescence assay was performed. The marker used for senescence is the expression of senescence-associated β-galactosidase in the cells, as represented by the blue coloured staining (Dimri et al, 1995). In addition to the expression of β-galactosidase, most of the HT1080 cells were flat, enlarged and were multi-nucleated (Figure 4.3A). The number of senescence cells was scored by counting at least 500 total cells per cell line. The number of senescence cells in the vector and TRF2 cell lines had a scoring of 4%. Analysis of TRF2$^{\Delta M}$-RA in HT1080 cells revealed an increase in the number of senescence cells totalling about 50% (Figure 4.3B). Overall, these results suggest that arginines in the basic domain are essential for TRF2 function.

4.1.2 Overexpression of TRF2 Carrying Amino Acid Changes from Arginines to Lysines in the Basic Domain Induces Decreased Proliferation and Senescence in HT1080 Cells

Formally, it is possible that the positive charges of arginines instead of the arginines themselves are important for TRF2 function. To test this hypothesis, eight arginine residues in the basic domain of TRF2 were mutated to positively charged lysine residues. However, one may argue that mutating eight arginine residues in the basic domain may disrupt the protein folding even if the positive charge is maintained. In order to address this concern, two sets of four TRF2 mutants containing amino acid changes

from arginines to lysines in the basic domain were constructed and referred to as TRF2-RK1-4 and TRF2-RK5-8. Additionally, by creating these two mutants which contain only four changed residues as opposed to eight mutated residues may help identify whether one arginine residue is more essential to the function of the basic domain. However, it may be unlikely that one arginine in the basic domain of TRF2 is indispensable but a stretch of arginine residues may be necessary to maintain the function of the domain.

To investigate whether the arginine residues in the basic domain are essential to the function of the domain, proliferation assays and a senescence assay was performed. HT1080 cells were retrovirally infected with the vector alone, or the vector containing TRF2, TRF2-RK, TRF2-RK1-4, TRF2-RK5-8, $TRF2^{\Delta M}$ or $TRF2^{\Delta B}$. Overexpression of TRF2-RK had a 4 fold decreased in proliferation rate as compared to the vector control and wild type TRF2 at day 15 (Figure 4.1A). Expression of TRF2-RK5-8 and TRF2-RK1-4 similarly had about a 4 fold decreased in proliferation rates as compared to the vector. Additionally, all the TRF2 mutants had a proliferation rate similar to $TRF2^{\Delta B}$ at day 13.

To gain further evidence that the arginine residues are essential to the function of the basic domain, arginine to lysine mutations were introduced into the basic domain of TRF2 in the absence of the Myb domain. A similar pattern of a decreased proliferation rate was also observed in $TRF2^{\Delta M}$-RK HT1080 cells as compared to the vector control (Figure 4.2A). The vector had a cumulative cell number of about 6.5×10^8 cells as compared to $TRF2^{\Delta M}$-RK which had a cumulative cell number of about 1.5×10^8 cells at day 15. Wild type TRF2 overexpression showed a similar proliferation rate to the vector

control. Both TRF2$^{\Delta M}$-RK1-4 and TRF2$^{\Delta M}$-RK5-8 had the same proliferation rate of about 2.5 x 10^8 cells at day 15. TRF2$^{\Delta B\Delta M}$ demonstrated to have the slowest replicative potential.

Microscopic analysis of HT1080 cells overexpressing TRF2 mutants carrying amino acid changes from arginines to lysines in the basic domain and in the absence of the Myb domain at day 7 revealed a senescence like phenotype (Figure 4.3A). This phenotype was further confirmed by senescence associated β-galactosidase staining. The total numbers of senescence cells observed in the various TRF2 mutants were scored by counting over 500 cells per cell line (Figure 4.3B). The vector and TRF2 had a total scoring of 4% senescence cells as compared to TRF2$^{\Delta M}$-RK which had a total of 53% senescence cells. Additionally, TRF2$^{\Delta M}$-RK1-4 and TRF2$^{\Delta M}$-RK5-8 had a similar number of senescence cells 48.1% and 48.5% respectively. Overexpression of TRF2$^{\Delta B\Delta M}$ lead to the induction of senescence in over 60% of cells, consistent with previous findings (van Steensel et al, 1998). Taken together, these results suggest that the arginine residues play a large role in maintaining the protective function of TRF2. Similarly, the positive charge alone in the basic domain is insufficient for maintaining TRF2 function.

4.1.3 Amino Acid Changes from Arginines to Lysines Introduced in the Basic Domain of TRF2 in Combination with the Deletion of the Myb Domain Induces the Formation of Anaphase Bridges in HT1080 Cells

To further compare whether the TRF2$^{\Delta B\Delta M}$ chromosome end-end fusion phenotype can be recapitulated when arginine to lysine mutations are introduced into the basic domain of TRF2 in combination with the deletion of the Myb domain, the ability of

these mutations to cause anaphase bridges were analyzed. An increase of chromosome fusions during anaphase were observed in HT1080 cells as compared to the vector control when these TRF2 mutants were overexpressed at day 6 of selection (Figure 4.4A). The cells were grown on cover slips, fixed, stained with DAPI and analyzed using a fluorescent microscope. A total of over 200 anaphase cells were counted per cell line for each time point and the number of anaphase bridges and lagging chromosomes were scored in day 6 and day 7 HT1080 cells (Figure 4.4B). At day 6, TRF2$^{\Delta M}$-RK had 60% anaphase bridges, similar to TRF2$^{\Delta B\Delta M}$ which had 65% anaphase bridges, both of which were dramatically different from the vector control (5%). Overexpression of TRF2$^{\Delta M}$-RK5-8, TRF2$^{\Delta M}$-RK1-4 and TRF2$^{\Delta M}$-RA also revealed a 10 fold increase in anaphase bridges at day 6 as compared to the vector and wild type TRF2. In day 7 cells, the number of anaphase bridges dropped slightly to 61% in the TRF2$^{\Delta B\Delta M}$ construct and the number of anaphase bridges in TRF2$^{\Delta M}$-RK5-8 increased to 75% as compared to day 6 counts of 65%. The mutant constructs TRF2$^{\Delta M}$-RA, TRF2$^{\Delta M}$-RK and TRF2$^{\Delta M}$-RK1-4 had similar scoring in their number of anaphase bridges of 68%, 66% and 64% respectively at day 7. The number of lagging chromosomes in all of the TRF2 constructs showed slight variation among day 6 and day 7 counts. Overall, there was a significant increase in the number of anaphase bridges observed in HT1080 cells overexpressing TRF2 mutants containing arginine to lysine substitutions in the basic domain and in the absence of the Myb domain, which is consistent with the phenotype of TRF2$^{\Delta B\Delta M}$ (van Steensel et al, 1998). These results further suggest the importance of these arginine residues in maintaining the function of TRF2.

4.1.4 Amino Acid Changes from Arginines to Lysines Introduced into the Basic Domain of TRF2 and in the Presence of the Myb Domain Does Not Induce Anaphase Bridges in HT1080 Cells

On the contrary, when TRF2 mutants containing arginine to lysine amino acid changes in the basic domain and in the presence of the Myb domain are expressed in HT1080 cells at day 9, no significant increase in chromosome fusions were observed (Figure 4.4C). Over 300 anaphase cells were counted per cell line and the number of lagging chromosomes and anaphase bridges were scored. Expression of TRF2-RK, TRF2-RK1-4 and TRF2-RK5-8 had less than 10% anaphase bridges which were similar to the vector which had about 4% anaphase bridges and wild type TRF2 scored about 8% anaphase bridges. $TRF2^{\Delta B}$ and $TRF2^{\Delta M}$ had an anaphase bridge scoring of 18.5% and 26.1% respectively. The number of lagging chromosomes was similar between all cell lines ranging from 9% to 13%. Thus, these data suggests that the arginine to lysine amino acid changes in the basic domain of TRF2 in the presence of the Myb domain have a similar low fusion phenotype to $TRF2^{\Delta B}$. In general, analysis of the anaphase bridge results also reiterates the importance of the arginine residues in the basic domain of TRF2.

4.2 Analysis of the Overexpression of TRF2 Mutants in BJ/hTERT Cells Carrying Amino Acid Substitutions from Arginines to Lysines in the Basic Domain

4.2.1 Overexpression of TRF2 Mutants Carrying Amino Acid Changes from Arginines to Lysines in the Basic Domain Induces Decreased Proliferation and Senescence in BJ/hTERT Cells

To establish that the decreased proliferation potential and senescence phenotype was reproducible and not limited to a transformed cell line, similar proliferation assays and β-galactosidase expression experiments were performed in a human primary immortalized cell line BJ/hTERT. Additionally, BJ/hTERT cells have long telomeres about 15 kb in length, which allows one to study telomere abnormalities through fluorescence *in situ* hybridization (FISH) analysis. Compared to the vector alone, overexpression of TRF2-RK, TRF2-RK1-4 and TRF2-RK5-8 resulted in a significant reduction in the rate of proliferation in BJhTERT cells (Figure 4.5A). No significant decrease in the proliferation rate was observed for cells expressing TRF2. However, overexpression of wild type TRF2 grew slightly slower than the vector control at later time points, consistent with previous findings (Li et al, 2008, Smogorzewska & de Lange, 2002, Wang et al, 2004). TRF2-RK5-8 repeatedly had grown twice as fast as TRF2-RK1-4 by day 15 but overall the arginine mutants still had a decreased replicative potential as compared to the vector and wild type TRF2. Interestingly, TRF2-RK grew almost at the same rate as $TRF2^{\Delta B}$ throughout the entire proliferation assay. Western blot analysis indicated that all TRF2 mutant constructs were expressed at a comparable level to wild type TRF2 at day 15, for three independent experiments (Figure 4.5B).

Furthermore, senescence was induced in the mutant TRF2 BJ/hTERT cells containing amino acid substitutions from arginines to lysines in the basic domain (Figure 4.6A). Staining of β-galactosidase was also observed in BJ/hTERT cells, as well as the phenotypic characteristics associated with senescence in human cells. Quantification of the average number of senescence cells obtained from counting over a total of 1500 cells

per cell line at day 13 was performed for three independent experiments (Figure 4.6B). The vector control (5.5%) and full length TRF2 (11.1%) had a low number of senescence cells. TRF2-RK had 76.8% senescence cells as compared to 70% in TRF2-RK1-4, 67.8% in TRF2-RK5-8 and $TRF2^{\Delta B}$ had 84.1% senescence cells. Results of the proliferation assay and senescence assay demonstrate the ability of the arginine to lysine mutations introduced into the basic domain of TRF2 to mimic the decreased proliferation and senescence phenotype similar to $TRF2^{\Delta B}$ (Wang et al, 2004).

4.2.2 Increase in Telomere Doublets and No Significant Telomere Loss Observed in BJ/hTERT Cells Expressing TRF2 Mutants Carrying Amino Acid Changes from Arginines to Lysines in the Basic Domain

To determine whether the molecular mechanisms responsible for the known $TRF2^{\Delta B}$ telomere loss phenotype are the same mechanism utilized by the TRF2 mutants containing amino acid substitutions from arginines to lysines in the basic domain, telomere FISH was performed. FISH was carried out using a telomere specific probe on metaphase spreads in BJ/hTERT cells expressing the vector, TRF2, TRF2-RK, TRF2-RK1-4, TRF2-RK5-8 and $TRF2^{\Delta B}$ (Figure 4.7A). Telomere dysfunction phenotypes were quantified including calculating the average of ≥2 telomere signals at each chromatid end, the average sister telomere loss per chromatid end and the average of terminal deletions per chromosome (Figure 4.7B). The average number of ≥2 telomere signals (telomere doublets) at each chromatid end in TRF2-RK (7.05%), TRF2-RK1-4 (5.69%) and TRF2-RK5-8 (6.13%) were significantly different from the vector (1.76%), TRF2 (2.91%) and $TRF2^{\Delta B}$ (2.40%) (Figure 4.7C). Interestingly, the TRF2 mutants TRF2-RK, TRF2-RK1-4

and TRF2-RK5-8 showed no significant difference from the vector in comparison of the amount of sister telomere loss and terminal deletions (Figure 4.7 D and E). However, the amount of sister telomere loss and terminal deletions in TRF2$^{\Delta B}$ cells was significantly different from the vector and the TRF2 mutants. Altogether, the TRF2 mutants TRF2-RK, TRF2-RK1-4 and TRF2-RK5-8 do not display a similar telomere loss phenotype as compared to the previously published phenotype of TRF2$^{\Delta B}$ (Wang et al, 2004). However, the TRF2 mutants display a significant increase in telomere doublets, which is not observed in TRF2$^{\Delta B}$.

4.2.3 Overexpression of TRF2 Mutants Carrying Amino Acid Changes from Arginines to Lysines in the Basic Domain Do Not Appear to Lead to Telomere Shortening

Analysis of a denaturing telomere blot was performed to further characterize the mechanisms involved in the formation of the phenotypes observed in the TRF2 mutants containing amino acid substitutions from arginines to lysines in the basic domain. Analysis of the telomere restriction fragments indicates no substantial telomere shortening in the TRF2 mutants obtained from BJ/hTERT genomic DNA at day 9, as compared to the vector (Figure 4.8). Quantification of the relative telomere signal in the vector was normalized to 1.0, where as wildtype TRF2, TRF2-RK, TRF2-RK1-4 and TRF2-RK5-8 show slight telomere degradation with telomere signals of 0.90, 0.83, 0.85 and 0.82 respectively. Relative telomere signals were calculated by quantifying the total telomere restriction fragments in each lane and standardized to the quantification of the intrachromsomal telomeric repeats to account for differences in the loading of the

genomic DNA. Although the relative telomere signal in TRF2$^{\Delta B}$ could not be accurately quantified, it has been previously observed that TRF2$^{\Delta B}$ induces rapid telomere deletion of the duplex telomeric DNA (Wang et al, 2004). Analysis of the telomere blot shows evidence of telomere deletion as represented by the smear of telomeric DNA at the lower molecular weight markers, as compared to the vector. These finding reveal different telomere aberrations may be responsible for the decreased proliferation rate and senescence observed in the TRF2 mutants. Overall, expression of TRF2-RK, TRF2-RK1-4 and TRF2-RK5-8 results in the increase of telomere doublets with no significant loss of telomere DNA, whereas TRF2$^{\Delta B}$ shows no evidence of an increase in telomere doublets but a significant increase in telomere loss.

4.3 Analysis of the Overexpression of TRF2 Mutants Carrying Amino Acid Substitutions from Arginines to Lysines in the Basic Domain in Combination with the Deletion of the Myb Domain in BJ/hTERT Cells

4.3.1 Overexpression of TRF2 Mutants Carrying Amino Acid Changes from Arginines to Lysines in the Basic Domain in Combination with the Deletion of the Myb Domain Induces Decreased Proliferation and Senescence in BJ/hTERT Cells

In agreement with the previous results, a decreased proliferation phenotype was observed in BJ/hTERT cells expressing TRF2 mutants containing amino acid substitutions from arginines to lysines in the basic domain in combination with the deletion of the Myb domain (Figure 4.9A). The vector control had about a 10 fold increase in replicative potential as compared to TRF2$^{\Delta M}$-RK and about a 9 fold increase in replicative potential as compared to TRF2$^{\Delta M}$-RK1-4 at day 15. TRF2$^{\Delta M}$-RK grew very

similar to the control TRF2$^{\Delta B\Delta M}$ at day 15. The deletion mutant TRF2$^{\Delta M}$ had the most replicative potential next to the vector and wild type TRF2 cells. Immunoblotting was performed on day 15 BJ/hTERT cells, demonstrating an increase of expression levels of TRF2, TRF2$^{\Delta M}$-RK, TRF2$^{\Delta M}$-RK1-4, TRF2$^{\Delta M}$-RK5-8, TRF2$^{\Delta M}$ and TRF2$^{\Delta B\Delta M}$ as compared to the vector (Figure 4.9B). These data demonstrate that the arginine residues are important to maintain the function of the basic domain of TRF2, as the mutated arginine to lysine residues caused a decreased replicative potential in both HT1080 and BJ/hTERT cells.

Consistent with the previous experiments, expression of the TRF2 mutants in BJ/hTERT cells carrying amino acid changes from arginines to lysines in the basic domain and in the absence of the Myb domain also results in a senescence phenotype (Figure 4.10A). The average number of senescence cells was plotted from counting over 1500 cells per cell line at day 13 for three independent experiments (Figure 4.10B). Both the vector and TRF2 control cell lines had the least amount of senescence cells of 5.5% and 11.1% respectively. TRF2$^{\Delta M}$-RK had 83.4% senescence cells followed by 81.8% in TRF2$^{\Delta B\Delta M}$. Expression of TRF2$^{\Delta M}$-RK1-4 had a senescence scoring of roughly 10% more senescence cells than TRF2$^{\Delta M}$-RK5-8 (66.5%), followed by 30% senescence cells in TRF2$^{\Delta M}$. Collectively, the senescence assay results performed both in HT1080 and BJ/hTERT cells demonstrate that the arginine residues are important to maintain the protective telomeric function of the basic domain of TRF2.

4.3.2 Overexpression of TRF2 Mutants Containing Amino Acid Substitutions from Arginines to Lysines in the Basic Domain in Combination with the Deletion of the Myb Domain Causes Telomere Fusions in BJ/hTERT Metaphase Cells

FISH was performed to determine whether the molecular mechanisms involved in the formation of the TRF2$^{\Delta B\Delta M}$ fusion phenotype is the same mechanisms utilized by the TRF2 mutants lacking the Myb domain and containing amino acid substitutions from arginines to lysines in the basic domain. A telomere specific probe was used on metaphase spreads in BJ/hTERT cells expressing the vector, TRF2, TRF2$^{\Delta M}$-RK, TRF2$^{\Delta M}$-RK1-4, TRF2$^{\Delta M}$-RK5-8, TRF2$^{\Delta M}$, TRF2$^{\Delta B}$ or TRF2$^{\Delta B\Delta M}$ (Figure 4.11A). The metaphase spreads were quantified and the number of telomere doublets, sister telomere loss, number of fusion events and fraction of fusion events were scored for three independent experiments in a blinded fashion (Figure 4.11B). The total number of fusion events in each cell line was counted, which includes telomere end-end fusions, chromatid fusions and sister chromatid fusions. Overexpression of the vector, wild type TRF2, TRF2$^{\Delta M}$ and TRF2$^{\Delta B\Delta M}$ had a comparable phenotype to TRF2$^{\Delta M}$-RK, TRF2$^{\Delta M}$-RK1-4 and TRF2$^{\Delta M}$-RK5-8 when the average number of chromatid ends with telomere doublets and sister telomere loss was calculated. However, the TRF2$^{\Delta M}$-RK, TRF2$^{\Delta M}$-RK1-4 and TRF2$^{\Delta M}$-RK5-8 had a distinct telomere fusion phenotype as compared to the vector and wild type TRF2 (Figure 4.11C and D). The average number of fusion events in the vector (0.04) and TRF2 (0.04) were low as compared to the TRF2 mutants. The average fusion events per metaphase cell was 1.78 for TRF2$^{\Delta M}$-RK, 1.20 for TRF2$^{\Delta M}$-RK1-4 and 1.87 TRF2$^{\Delta M}$-RK5-8, which were comparable values to TRF2$^{\Delta B\Delta M}$ of 1.82. The average fusion

events per cell in the cell lines TRF2$^{\Delta M}$-RK, TRF2$^{\Delta M}$-RK1-4 and TRF2$^{\Delta M}$-RK5-8 were found to be significantly different from both the vector and TRF2$^{\Delta M}$. Additionally, the fraction of metaphase cells with fusion events in the vector (4.4%) and TRF2 (4.4%) was low as compared to the TRF2 mutants. The fraction of metaphase cells with ≥1 fusion event on average was 84.2% for TRF2$^{\Delta M}$-RK, 70.5% for TRF2$^{\Delta M}$-RK1-4 and 70.9% for TRF2$^{\Delta M}$-RK5-8. Again, these values were similar to TRF2$^{\Delta B\Delta M}$ that had 72.2% fraction of metaphase cells with fusions. The cell lines TRF2$^{\Delta M}$-RK, TRF2$^{\Delta M}$-RK1-4 and TRF2$^{\Delta M}$-RK5-8 were also found to be significantly different from the vector and TRF2$^{\Delta M}$ when comparing the fraction of cells with ≥1 fusion event. Overall, TRF2$^{\Delta M}$-RK, TRF2$^{\Delta M}$-RK1-4 and TRF2$^{\Delta M}$-RK5-8 do not show a significant amount of telomere loss but do have significant increase in telomere fusions, which is similar to the published phenotype of TRF2$^{\Delta B\Delta M}$ (van Steensel et al, 1998).

To further examine whether NHEJ was occurring at telomeres in the various TRF2 mutants, telomeric DNA was analyzed for the loss of the 3'G-rich overhangs and the formation of telomere fusions. Genomic DNA was isolated from day 10 BJ/hTERT cells expressing the vector, wildtype TRF2, TRF2$^{\Delta M}$-RK, TRF2$^{\Delta M}$-RK1-4, TRF2$^{\Delta M}$-RK5-8, TRF2$^{\Delta M}$ and TRF2$^{\Delta B\Delta M}$ and the telomere restriction fragments were analyzed on the same native and then subsequently denatured telomere blot (Figure 4.12). A native telomere blot allows for the analysis of the loss of the 3'G-rich overhangs, which occurs as a result of the inability of TRF2 to protect the telomere ends. Quantification of the overhang signal in the native gel reveals a loss of overhangs as compared to the vector (1.0) in the various TRF2 mutants TRF2$^{\Delta M}$ (0.86), TRF2$^{\Delta M}$-RK (0.88), TRF2$^{\Delta M}$-RK1-4

(0.80), TRF2$^{\Delta M}$-RK5-8 (0.72), and TRF2$^{\Delta B\Delta M}$ (0.65) (Figure 4.12A). The overhang signal was obtained by the quantification of the telomere restriction fragments in the native gel normalized to the total telomeric DNA signal obtained after the same gel was denatured. Additionally, analysis of the denatured telomere blot reveals the appearance of high-molecular weight telomere-fusion fragments predominantly in the BJ/hTERT cells expressing TRF2$^{\Delta B\Delta M}$ and TRF2$^{\Delta M}$-RK (Figure 4.12B). Unfortunately, the precise amount of telomere fusions in the denatured gel cannot be quantified as there are no intrachromosomal telomeric repeats to account for differences in the amount of DNA loaded per lane. Overall, results of the native and denatured telomere blots suggest that the TRF2 mutants lacking the Myb domain and containing arginine to lysine changes in the basic domain lose their 3'G-rich overhangs and are processed by NHEJ resulting in telomere fusions.

Figure 4.1. Growth arrest induced in HT1080 cells overexpressing TRF2 mutants containing amino acid substitutions in the basic domain. A) Proliferation assay of HT1080 cells retrovirally infected with the pLPC vector alone or the vector expressing TRF2, TRF2-RA, TRF2-RK, TRF2-RK1-4, TRF2-RK5-8, $TRF2^{\Delta M}$ or $TRF2^{\Delta B}$. The cells were seeded 250,000 in 10 cm plates after three days of selection and counted every two days performed in duplicate. The cells were split appropriately when required. B) HT1080 cells from panel A were harvested at day 3 and day 15 of selection. The whole cell pellets were resuspended in buffer-C to obtain a total cell number of 2.0×10^4 cells/μl. The supernatant fractions were collected and stored in 2 X laemmli buffer. A total of 10 μl of protein samples were loaded on to a 8% SDS polyacrylamide gel. The nitrocellulose membranes were immunoblotted with TRF2 primary antibody and exposed on hyperfilm using ECL. The membranes were subsequently stripped and re-incubated with γ-tubulin antibody as a loading control.

A

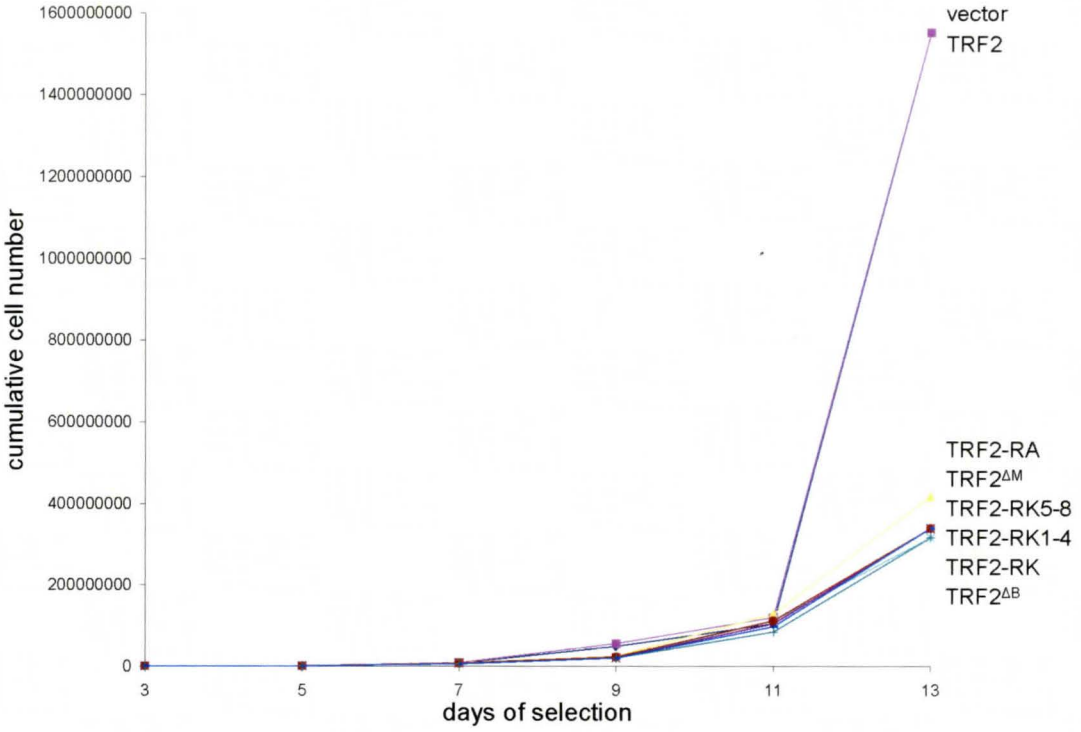
1600000000
1400000000
1200000000
1000000000
800000000
600000000
400000000
200000000
0
cumulative cell number
3
5
7
9
11
13
days of selection
vector
TRF2
TRF2-RA
TRF2ΔM
TRF2-RK5-8
TRF2-RK1-4
TRF2-RK
TRF2ΔB

B

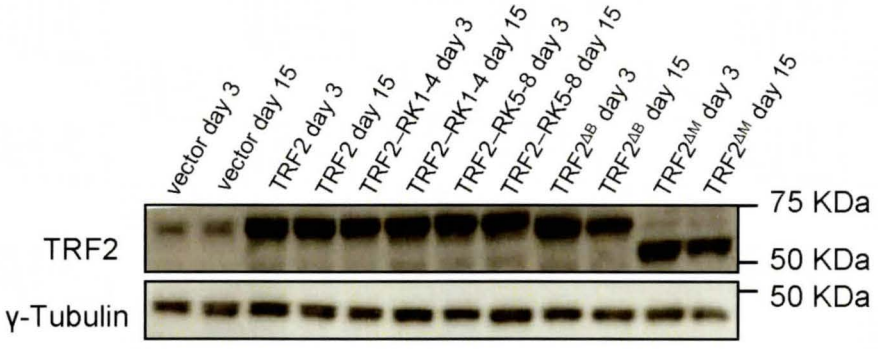
vector day 3
vector day 15
TRF2 day 3
TRF2 day 15
TRF2–RK1-4 day 3
TRF2–RK1-4 day 15
TRF2–RK5-8 day 3
TRF2–RK5-8 day 15
TRF2ΔB day 3
TRF2ΔB day 15
TRF2ΔM day 3
TRF2ΔM day 15
TRF2
γ-Tubulin
75 KDa
50 KDa
50 KDa

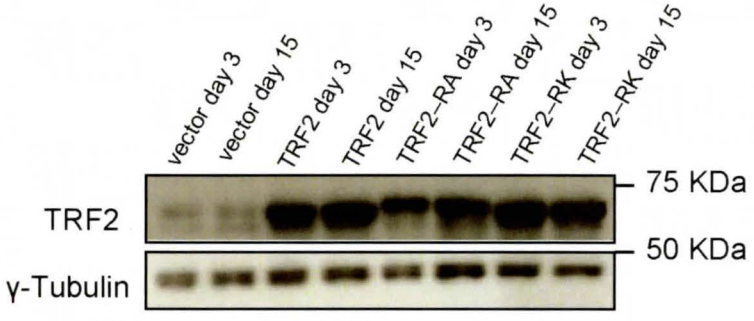
vector day 3
vector day 15
TRF2 day 3
TRF2 day 15
TRF2–RA day 3
TRF2–RA day 15
TRF2–RK day 3
TRF2–RK day 15
TRF2
γ-Tubulin
75 KDa
50 KDa

Figure 4.2. Growth arrest induced in HT1080 overexpressing TRF2 mutants containing amino acid changes in the basic domain in combination with the deletion of the Myb domain. A) Proliferation assay of HT1080 cells retrovirally infected with the pLPC vector alone or the vector expressing TRF2, TRF2$^{\Delta M}$-RA, TRF2$^{\Delta M}$-RK, TRF2$^{\Delta M}$-RK1-4, TRF2$^{\Delta M}$-RK5-8 or TRF2$^{\Delta B\Delta M}$. The cells were seeded 250,000 into 10 cm plates after three days of selection and counted every two days performed in duplicate. The cells were split appropriately when required. B) HT1080 cells from panel A were harvested at day 3, 12 and 15 of selection. The whole cell pellets were resuspended in buffer-C to obtain a total cell number of 2.0 x 10^4 cells/µl. The supernatant fractions were collected and stored in 2 X laemmli buffer. A total of 10 µl of protein samples were loaded on to a 8% SDS polyacrylamide gel. The nitrocellulose membranes were immunoblotted with TRF2 primary antibody and exposed on hyperfilm using ECL. The membranes were subsequently stripped and re-incubated with γ-tubulin antibody as a loading control.

A

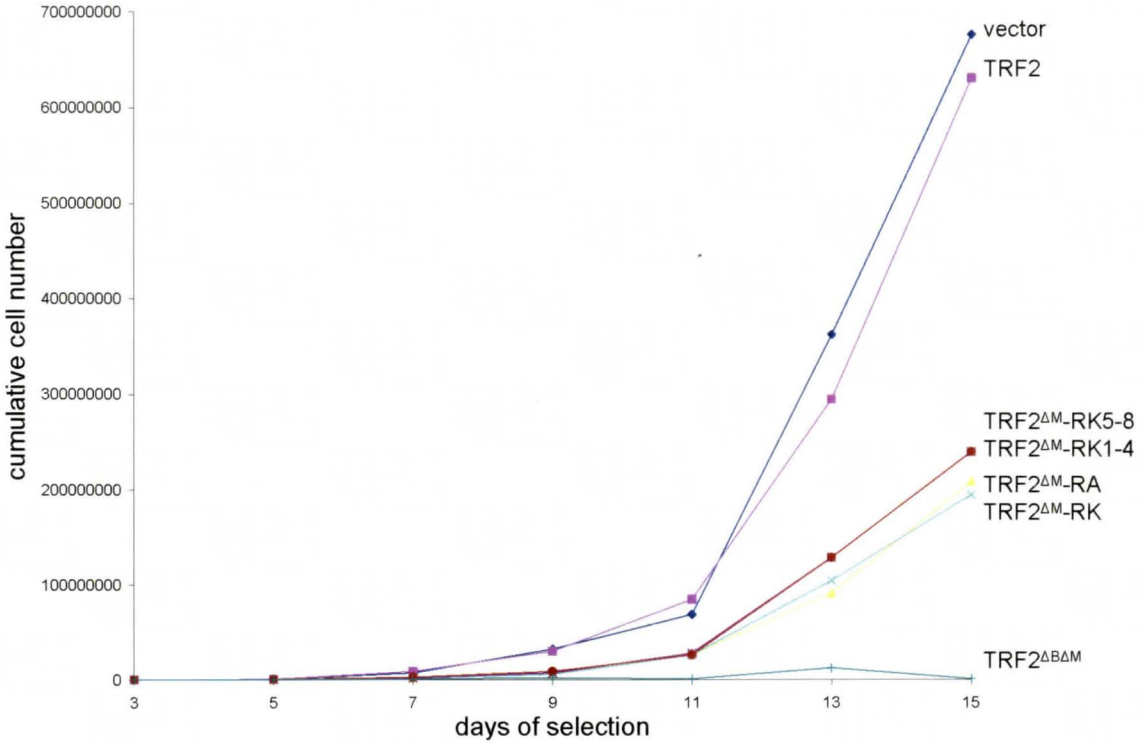
700000000
600000000
500000000
400000000
300000000
200000000
100000000
0
cumulative cell number
3
5
7
9
11
13
15
days of selection
vector
TRF2
TRF2ΔM-RK5-8
TRF2ΔM-RK1-4
TRF2ΔM-RA
TRF2ΔM-RK
TRF2ΔBΔM

B

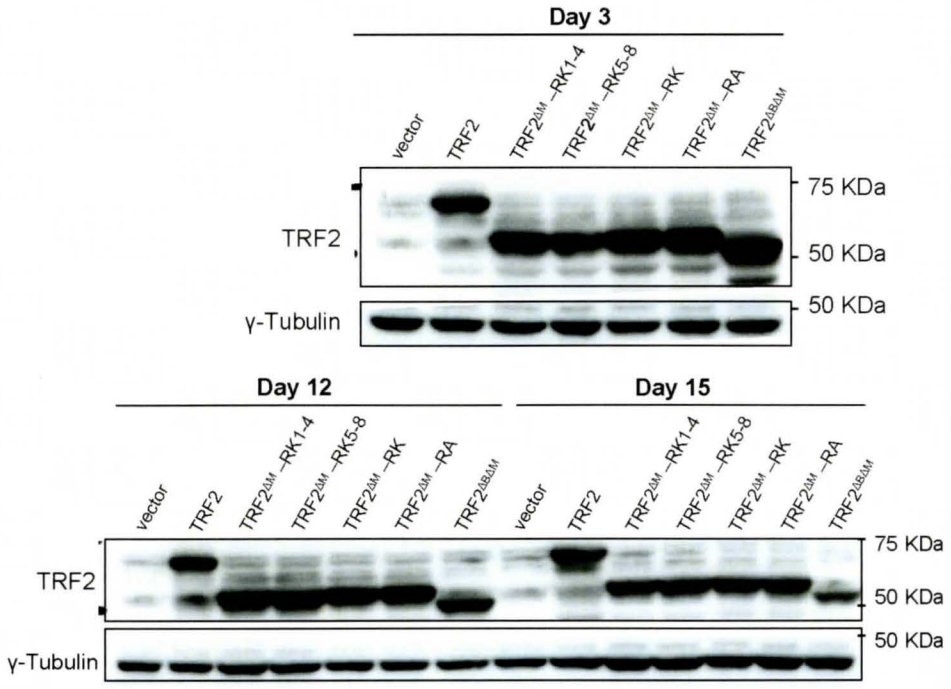
Day 3
vector
TRF2
TRF2ΔM-RK1-4
TRF2ΔM-RK5-8
TRF2ΔM-RK
TRF2ΔM-RA
TRF2ΔBΔM
TRF2
γ-Tubulin
75 KDa
50 KDa
50 KDa
Day 12
Day 15
vector
TRF2
TRF2ΔM-RK1-4
TRF2ΔM-RK5-8
TRF2ΔM-RK
TRF2ΔM-RA
TRF2ΔBΔM
vector
TRF2
TRF2ΔM-RK1-4
TRF2ΔM-RK5-8
TRF2ΔM-RK
TRF2ΔM-RA
TRF2ΔBΔM
TRF2
γ-Tubulin
75 KDa
50 KDa
50 KDa

Figure 4.3. Senescence induced in HT1080 cells overexpressing TRF2 mutants carrying amino acid substitutions in the basic domain in combination with the deletion of the Myb domain. A) HT1080 cells were retrovirally infected with the vector pLPC alone or the vector containing TRF2, TRF2$^{\Delta M}$-RA, TRF2$^{\Delta M}$-RK, TRF2$^{\Delta M}$-RK1-4, TRF2$^{\Delta M}$-RK5-8 or TRF2$^{\Delta B\Delta M}$. The cells were fixed at day seven of selection and incubated in staining solution containing X-gal at pH 6.0. The cells were visualized using a microscope for the senescence associated marker β-galactosidase. B) Quantification of the total number of positively stained β-galactosidase HT1080 cells among at least 500 cells were counted.

A

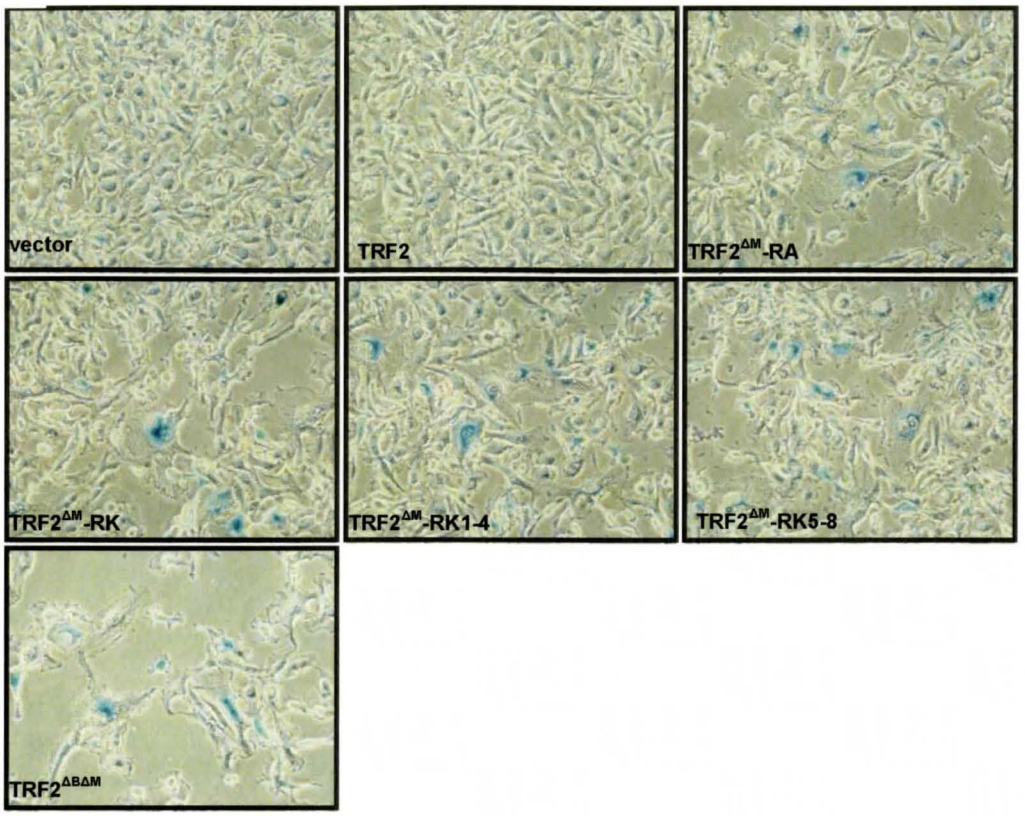
vector
TRF2
TRF2ΔM-RA
TRF2ΔM-RK
TRF2ΔM-RK1-4
TRF2ΔM-RK5-8
TRF2ΔBΔM

B

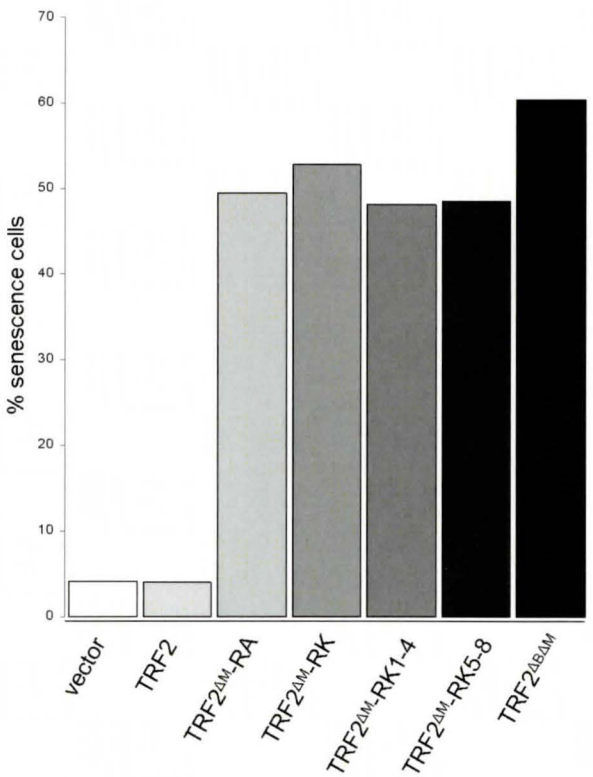
% senescence cells
0
10
20
30
40
50
60
70
vector
TRF2
TRF2ΔM-RA
TRF2ΔM-RK
TRF2ΔM-RK1-4
TRF2ΔM-RK5-8
TRF2ΔBΔM

Figure 4.4. A combination of the deletion of the Myb domain and amino acid changes from arginines to lysines in the basic domain of TRF2 induce anaphase bridges in HT1080 cells. A) HT1080 anaphase cells expressing the vector alone or TRF2, TRF2-RA$^{\Delta M}$, TRF2-RK$^{\Delta M}$, TRF2-RK1-4$^{\Delta M}$, TRF2-RK5-8$^{\Delta M}$ or TRF2$^{\Delta B\Delta M}$ after six days of selection. Cells were fixed on cover slips and stained with DAPI. B) Quantification of the total number anaphase bridges and lagging chromosomes scored in at least 200 anaphase HT1080 cells from panel A, at days six and seven of selection. Quantification of day seven was performed in a blinded fashion. C) Quantification of the total number anaphase bridges and lagging chromosomes scored in at least 300 anaphase HT1080 cells expressing TRF2, TRF2-RA, TRF2-RK, TRF2-RK1-4, TRF2-RK5-8, TRF2$^{\Delta B}$ and TRF2$^{\Delta M}$ at day nine of selection, performed in a blinded fashion.

A

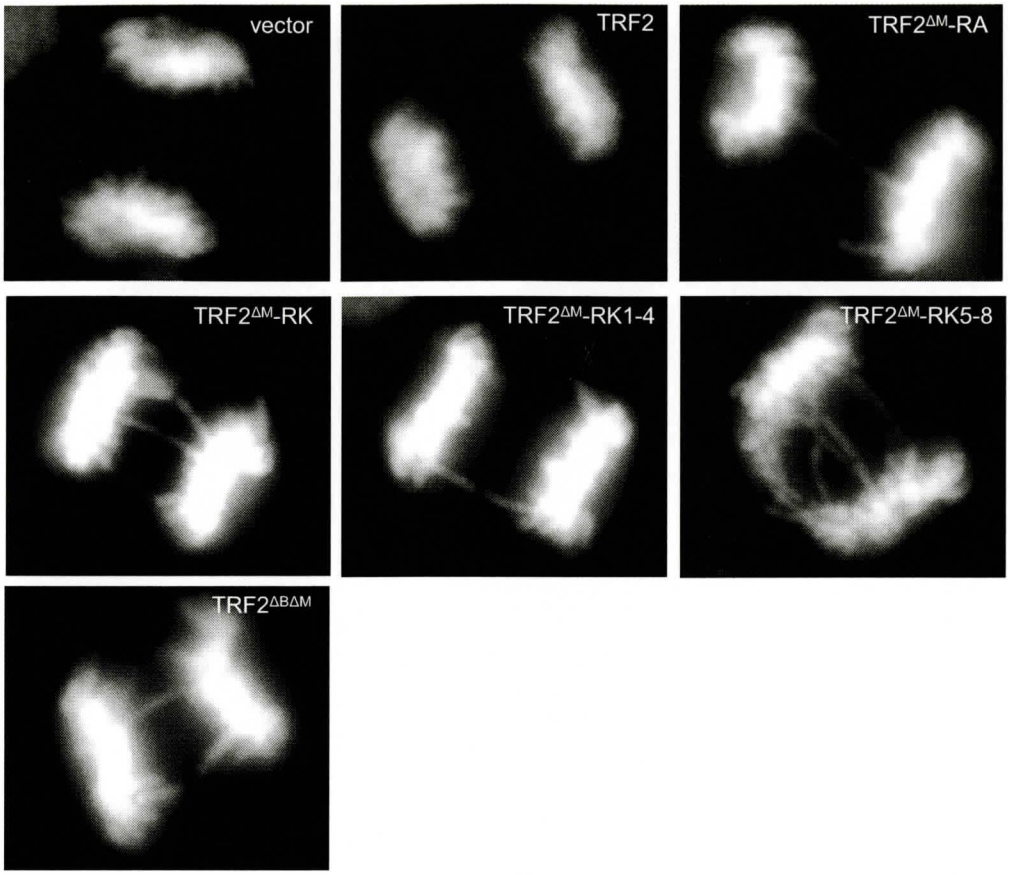
vector
TRF2
TRF2ΔM-RA
TRF2ΔM-RK
TRF2ΔM-RK1-4
TRF2ΔM-RK5-8
TRF2ΔBΔM

B

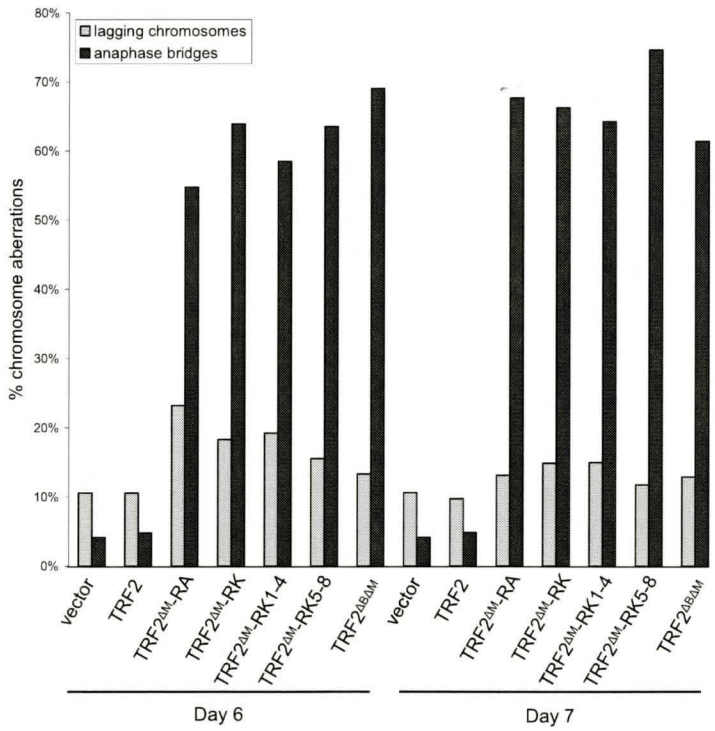
lagging chromosomes
anaphase bridges
% chromosome aberrations
80%
70%
60%
50%
40%
30%
20%
10%
0%
vector
TRF2
TRF2ΔM-RA
TRF2ΔM-RK
TRF2ΔM-RK1-4
TRF2ΔM-RK5-8
TRF2ΔBΔM
Day 6
Day 7

C

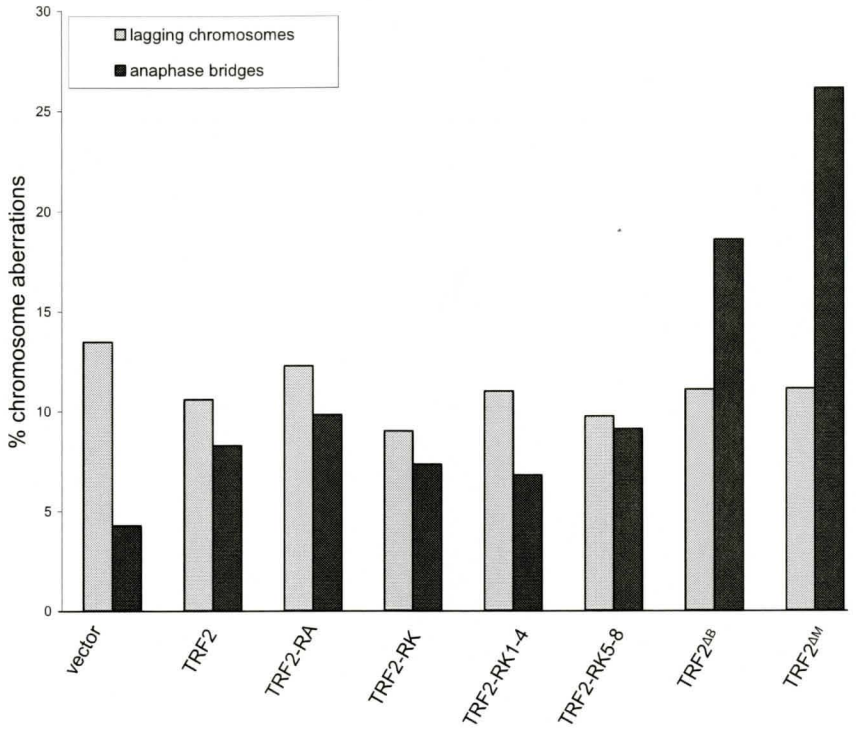
lagging chromosomes
anaphase bridges
% chromosome aberrations
30
25
20
15
10
5
0
vector
TRF2
TRF2-RA
TRF2-RK
TRF2-RK1-4
TRF2-RK5-8
TRF2ΔB
TRF2ΔM

Figure 4.5. Growth arrest induced in BJ/hTERT cells overexpressing TRF2 mutants containing amino acid changes from arginines to lysines in the basic domain. A) Proliferation assay of BJ/hTERT cells retrovirally infected with the pLPC vector alone or TRF2, TRF2-RK, TRF2-RK1-4, TRF2-RK5-8 or $TRF2^{\Delta B}$. The cells were seeded 20,000 in duplicate into 12-well plates after three days of selection and counted every two days. Error bars represent the standard deviation of the mean for three independent experiments. B) BJ/hTERT cells from panel A were harvested at day 15 of selection. The whole cell extracts were made in buffer-C to obtain a total cell number of 2.0 x 10^4 cells/µl. The supernatant fractions were collected and stored in 2 X laemmli buffer. A total of 10 µl of protein samples were loaded on to a 8% SDS polyacrylamide gel. The nitrocellulose membranes were immunoblotted with TRF2 primary antibody and exposed on hyperfilm using ECL. The membranes were subsequently stripped and re-incubated with γ-tubulin antibody as a loading control.

A

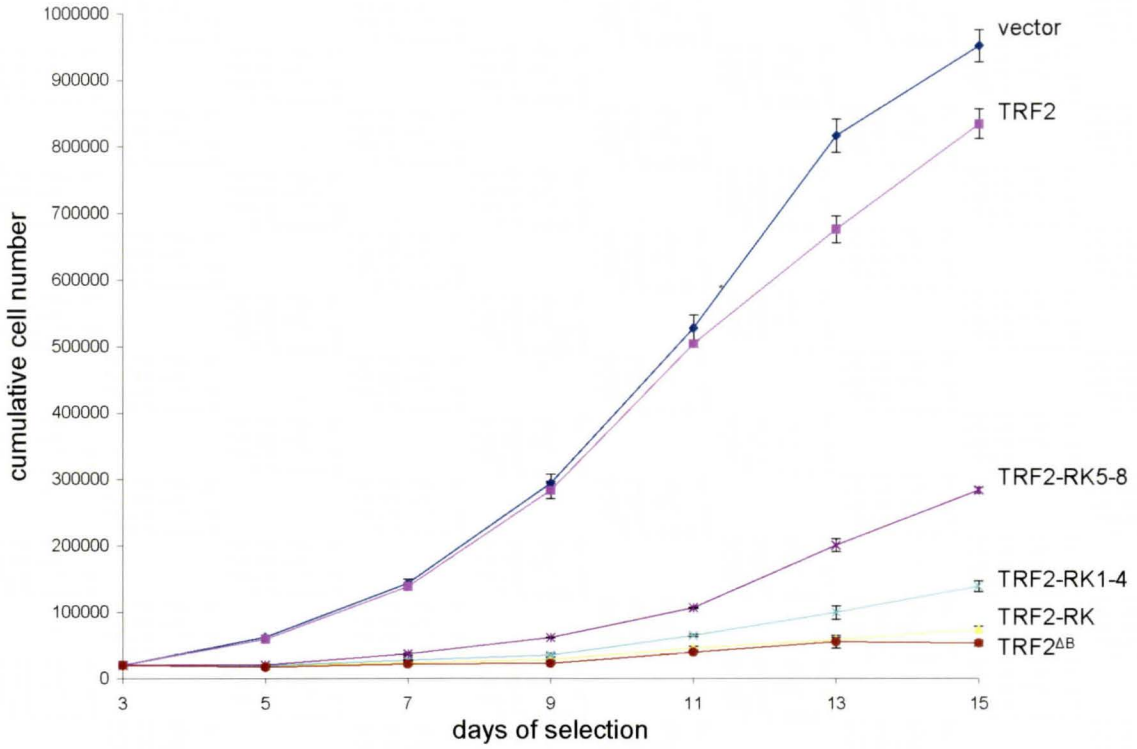
1000000
900000
800000
700000
600000
500000
400000
300000
200000
100000
0
cumulative cell number
3
5
7
9
11
13
15
days of selection
vector
TRF2
TRF2-RK5-8
TRF2-RK1-4
TRF2-RK
TRF2ΔB

B

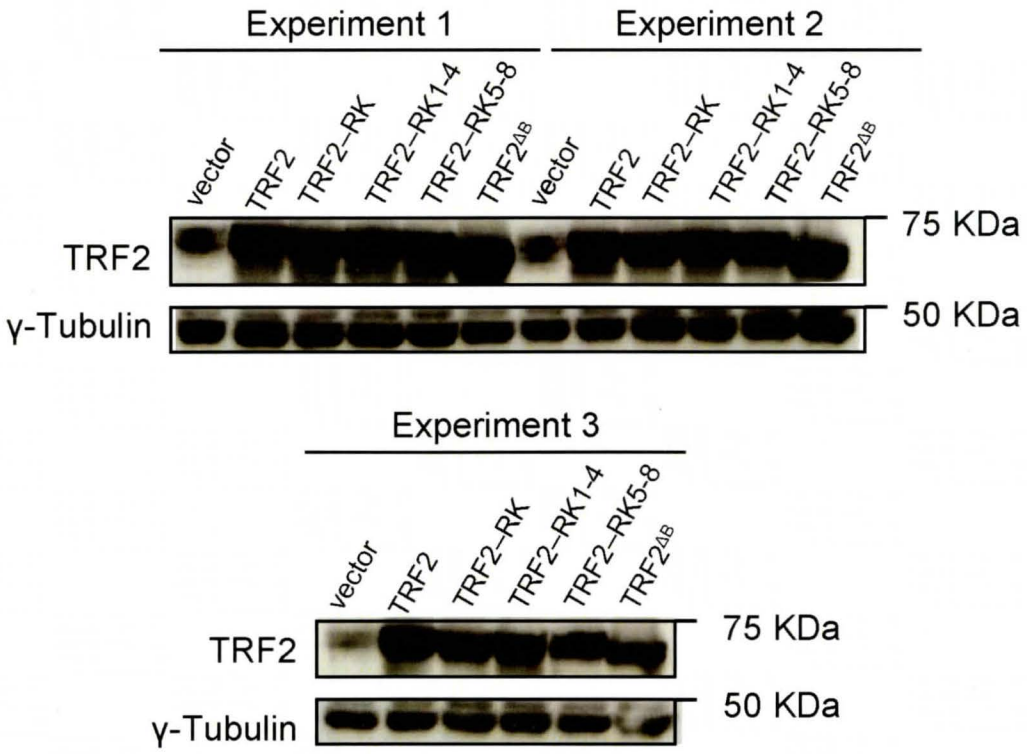
Experiment 1
Experiment 2
vector
TRF2
TRF2-RK
TRF2-RK1-4
TRF2-RK5-8
TRF2ΔB
TRF2
γ-Tubulin
75 KDa
50 KDa
Experiment 3
vector
TRF2
TRF2-RK
TRF2-RK1-4
TRF2-RK5-8
TRF2ΔB
TRF2
γ-Tubulin
75 KDa
50 KDa

Figure 4.6. Senescence induced in BJ/hTERT cells overexpressing TRF2 mutants containing amino acid substitutions from arginines to lysines in the basic domain. A) BJ/hTERT cells were retrovirally infected with the vector pLPC alone or the vector containing TRF2, TRF2-RK, TRF2-RK1-4, TRF2-RK5-8 or $TRF2^{\Delta B}$. The cells were fixed at day thirteen of selection and incubated in staining solution containing X-gal at pH 6.0. The cells were visualized using a microscope for the senescence associated marker β-galactosidase. B) Quantification of the total number of positively stained β-galactosidase BJ/hTERT cells among at least 1500 cells were counted. The error bars represent the standard deviation of the mean for thee independent experiments.

A

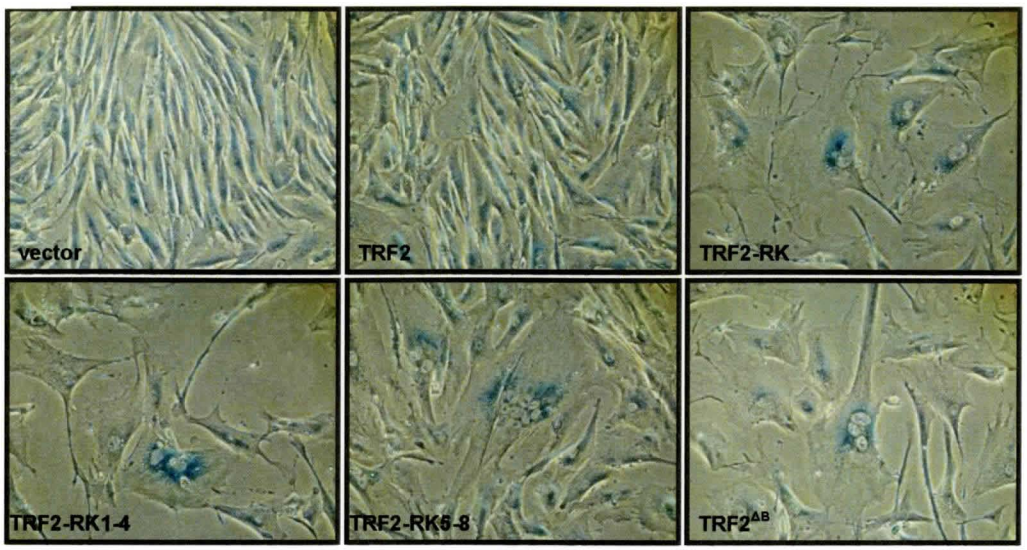
vector
TRF2
TRF2-RK
TRF2-RK1-4
TRF2-RK5-8
TRF2ΔB

B

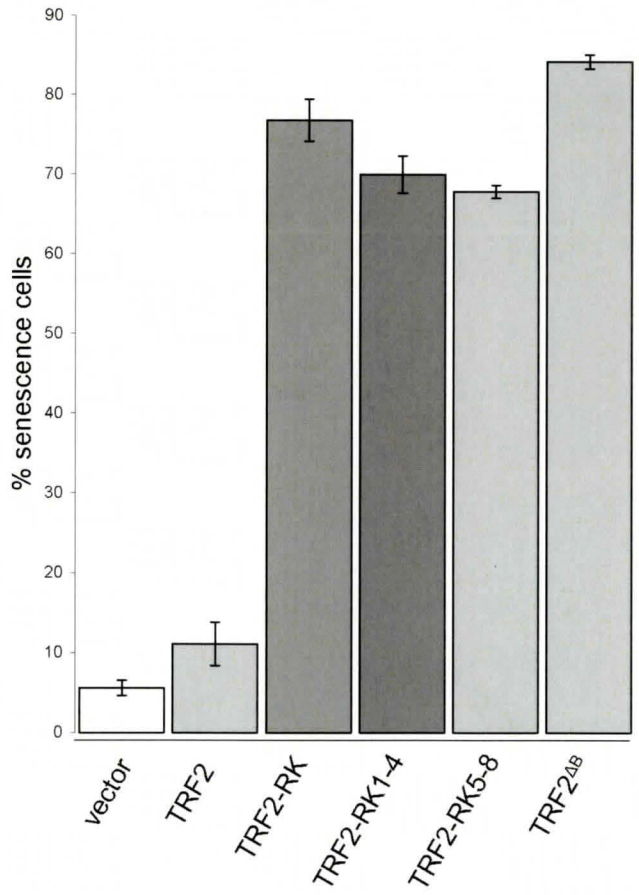
% senescence cells
0
10
20
30
40
50
60
70
80
90
vector
TRF2
TRF2-RK
TRF2-RK1-4
TRF2-RK5-8
TRF2ΔB

Figure 4.7. Telomere doublets and little telomere loss observed in BJ/hTERT metaphase cells expressing TRF2 mutants carrying amino acid changes from arginines to lysines in the basic domain. A) BJ/hTERT metaphase cells expressing the vector alone or TRF2, TRF2-RK, TRF2-RK1-4, TRF2-RK5-8 or $TRF2^{\Delta B}$ at day nine of selection. Cells were arrested with colcemid for 4 hr, incubated with a G-strand specific fluorescent PNA telomeric probe and stained with DAPI. Arrows indicate telomere doublets. Asterisk indicates telomere loss. B) Quantification of metaphase telomere dysfunction in BJ/hTERT cells analyzed by telomeric FISH at day nine of selection. Quantification was performed for three independent experiments in a blinded fashion. Values in brackets represent the *P*-value determined by a two-tailed Student's *t*-test as compared to the vector control. C) Quantification of the percentage of chromatid ends with ≥2 telomere signals. D) Percentage of chromatid ends with sister telomere loss. E) percentage of terminal deletions per chromosome. Error bars represent the standard deviation of the mean, from three independent experiments.

A

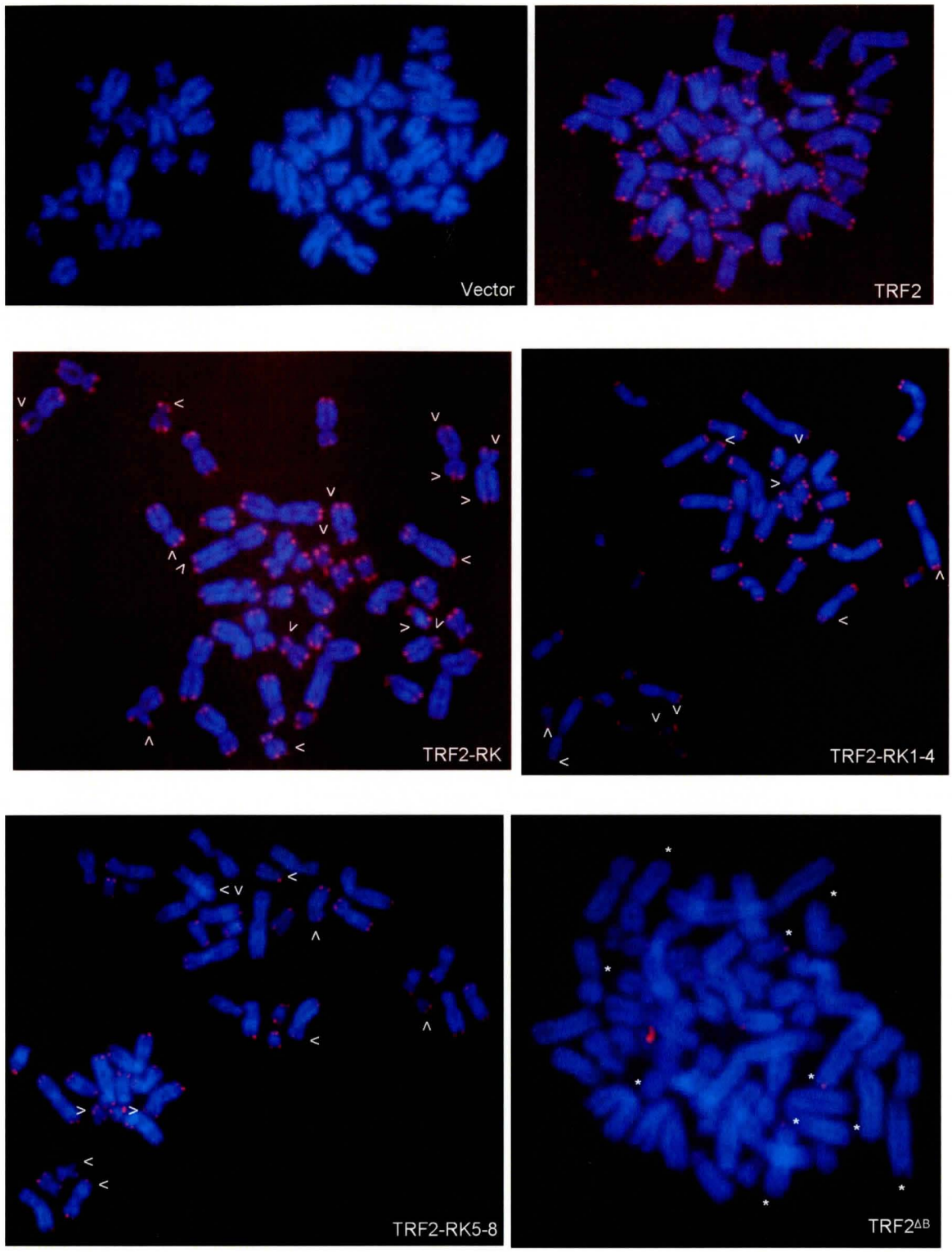

I

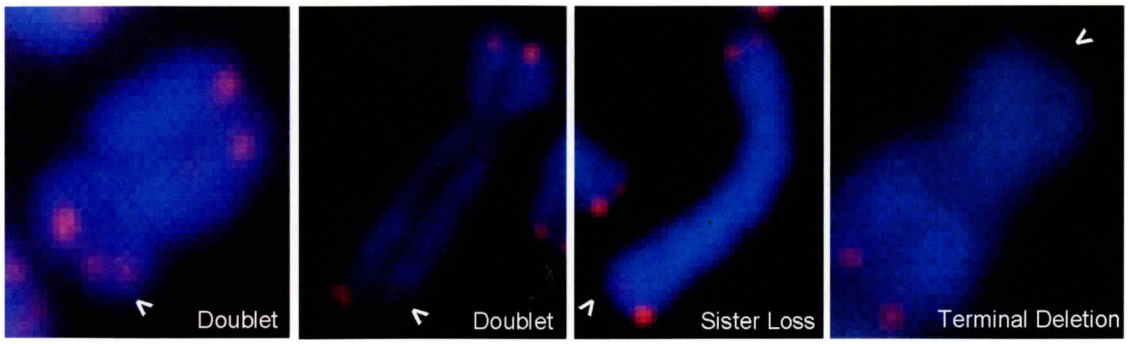

Cell Line	Total Metaphase Cells	Total Metaphase Chromosomes	Average of ≥2 Telomere Signals at Each Chromatid End (%), (P-Value)	Average of Sister Telomere Loss at Each Chromatid End (%), (P-Value)	Average of Terminal Deletions Per Chromosome (%), (P-Value)
Vector	45	1856	1.76, (1.000)	0.42, (1.000)	0.37, (1.000)
TRF2	45	1774	2.91, (0.007)	0.74, (0.282)	1.13, (0.069)
TRF2-RK	45	1786	7.05, (0.005)	1.07, (0.060)	0.54, (0.310)
TRF2-RK1-4	43	1600	5.69, (0.003)	0.69, (0.412)	0.47, (0.348)
TRF2-RK5-8	42	1636	6.13, (0.002)	0.92, (0.096)	1.10, (0.118)
$TRF2^{\Delta B}$	43	1631	2.40, (0.236)	3.27, (0.002)	9.83, (0.003)

C

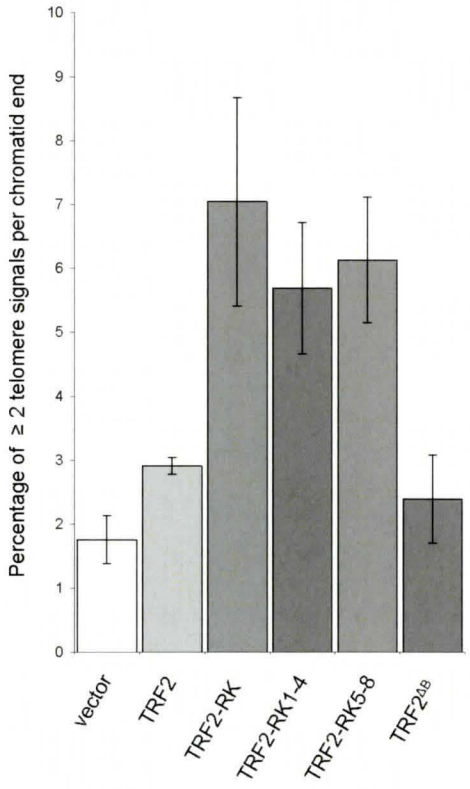

D

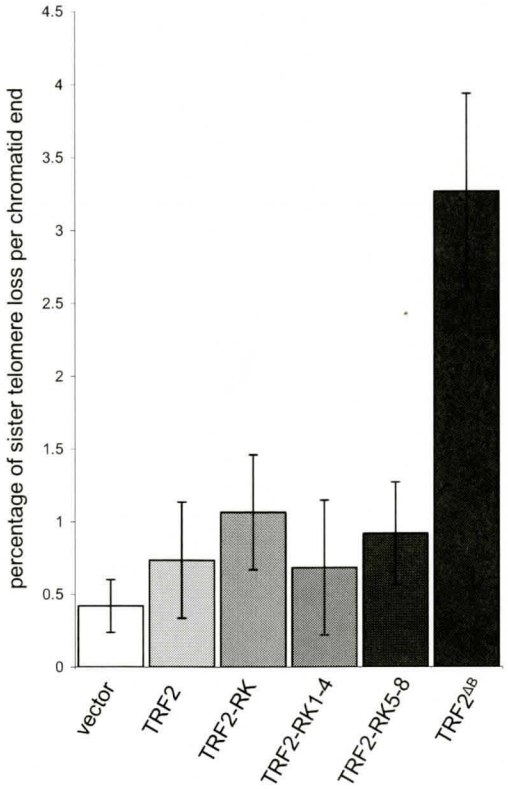
percentage of sister telomere loss per chromatid end
4.5
4
3.5
3
2.5
2
1.5
1
0.5
0
vector
TRF2
TRF2-RK
TRF2-RK1-4
TRF2-RK5-8
TRF2ΔB

E

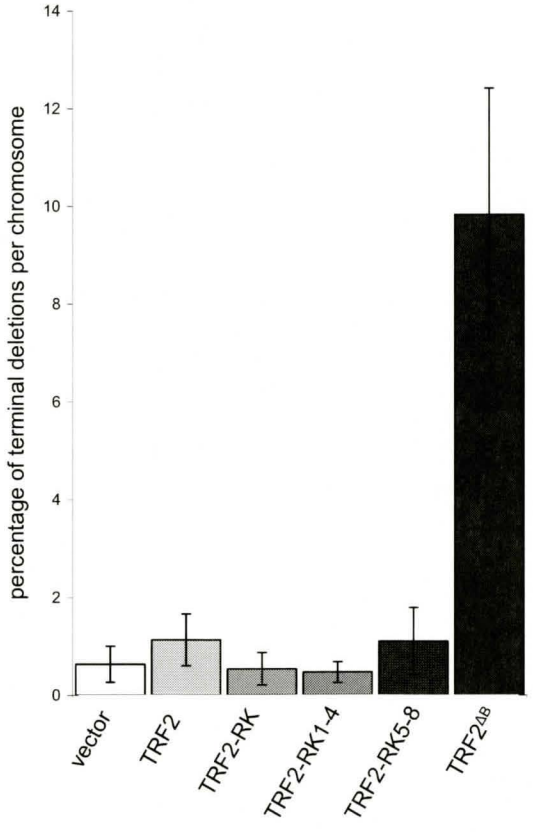
percentage of terminal deletions per chromosome
14
12
10
8
6
4
2
0
vector
TRF2
TRF2-RK
TRF2-RK1-4
TRF2-RK5-8
TRF2ΔB

Figure 4.8. No substantial telomere loss observed on a genomic blot in BJ/hTERT cells expressing TRF2 mutants carrying amino acid substitutions from arginines to lysines in the basic domain. Telomere genomic blot of BJ/hTERT cells expressing the vector alone or TRF2, TRF2-RK, TRF2-RK1-4, TRF2-RK5-8, or TRF2$^{\Delta B}$ after nine days of selection. The genomic DNA was phenol-chloroform extracted and digested with *HinfI* and *RsaI*. A total of 3μg of DNA was loaded onto a 0.7% agarose gel, run until the 1 kb molecular marker was at the bottom of the gel and dried. The gel was denatured and hybridized with a radioactive telomere G-strand probe. The telomere blot was exposed on a PhosphoImager screen overnight and scanned with a PhosphoImager. The relative telomere signal was determined by quantifying the total telomere restriction fragments in each lane and standardized to the intrachromosomal telomeric signal. The standard deviation of the relative telomere signal was obtained from one experiment performed in triplicate.

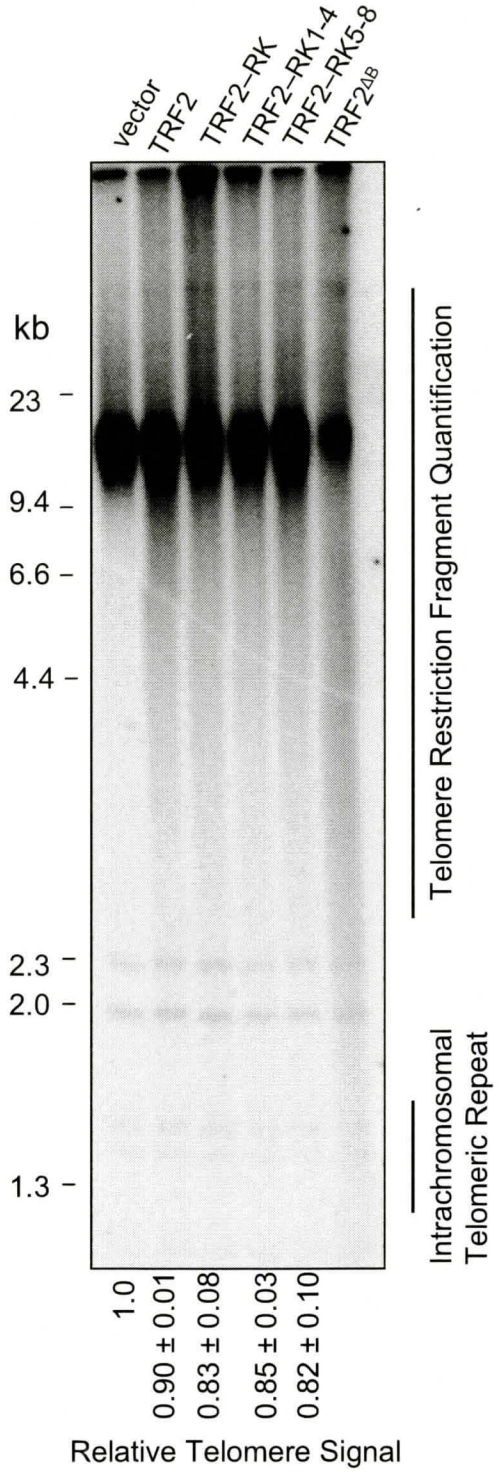
vector
TRF2
TRF2–RK
TRF2–RK1-4
TRF2–RK5-8
TRF2ΔB
kb
23
9.4
6.6
4.4
2.3
2.0
1.3
Telomere Restriction Fragment Quantification
Intrachromosomal Telomeric Repeat
1.0
0.90 ± 0.01
0.83 ± 0.08
0.85 ± 0.03
0.82 ± 0.10
Relative Telomere Signal

Figure 4.9. Growth arrest induced in BJ/hTERT cells overexpressing TRF2 mutants carrying a deletion of the Myb domain and amino acid changes from arginine to lysine in the basic domain. A) Proliferation assay of BJ/hTERT cells retrovirally infected with the pLPC vector alone or TRF2, TRF2$^{\Delta M}$-RK, TRF2$^{\Delta M}$-RK1-4, TRF2$^{\Delta M}$-RK5-8, TRF2$^{\Delta M}$ or TRF2$^{\Delta B \Delta M}$. The cells were seeded 20,000 in duplicate into 12-well plates after three days of selection and counted every two days. Error bars represent the standard deviation of the mean for three independent experiments. B) BJ/hTERT cells from panel A were harvested at day 15 of selection. The whole cell extracts were made in buffer-C to obtain a total cell number of 2.0 x 10^4 cells/μl. The supernatant fractions were collected and stored in 2 X laemmli buffer. A total of 10 μl of protein samples were loaded on to a 8% SDS polyacrylamide gel. The nitrocellulose membranes were immunoblotted with TRF2 primary antibody and exposed on hyperfilm using ECL. The membranes were subsequently stripped and re-incubated with γ-tubulin antibody as a loading control.

A

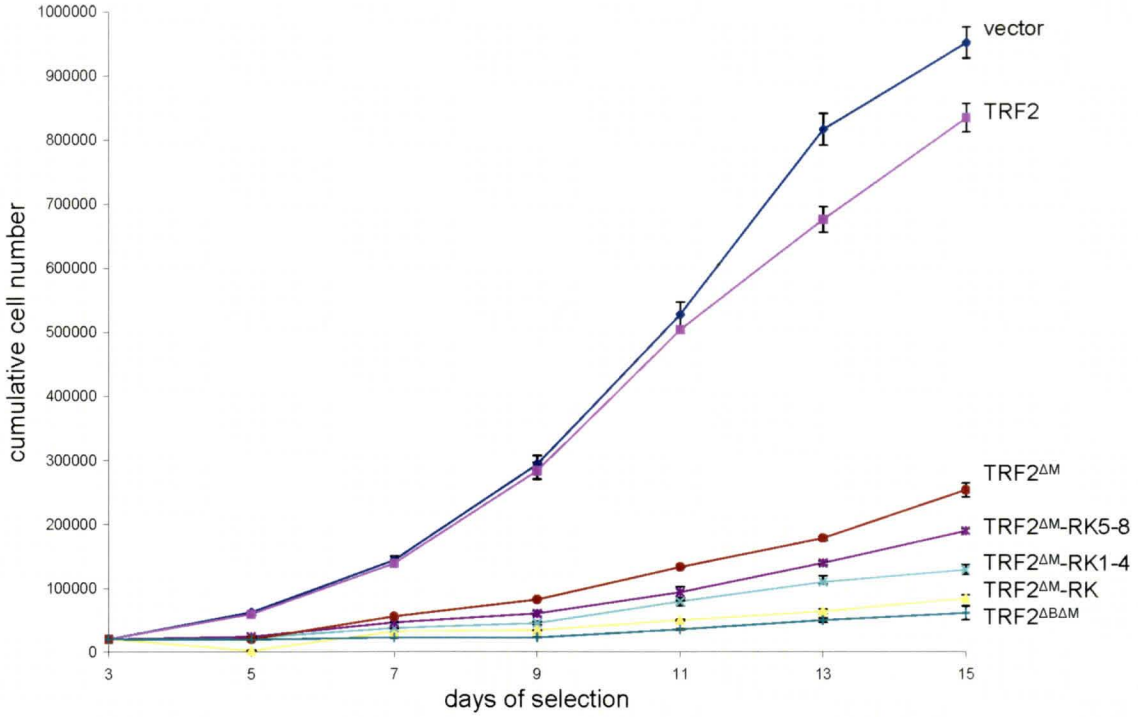
1000000
900000
800000
700000
600000
500000
400000
300000
200000
100000
0
cumulative cell number
3
5
7
9
11
13
15
days of selection
vector
TRF2
TRF2ΔM
TRF2ΔM-RK5-8
TRF2ΔM-RK1-4
TRF2ΔM-RK
TRF2ΔBΔM

B

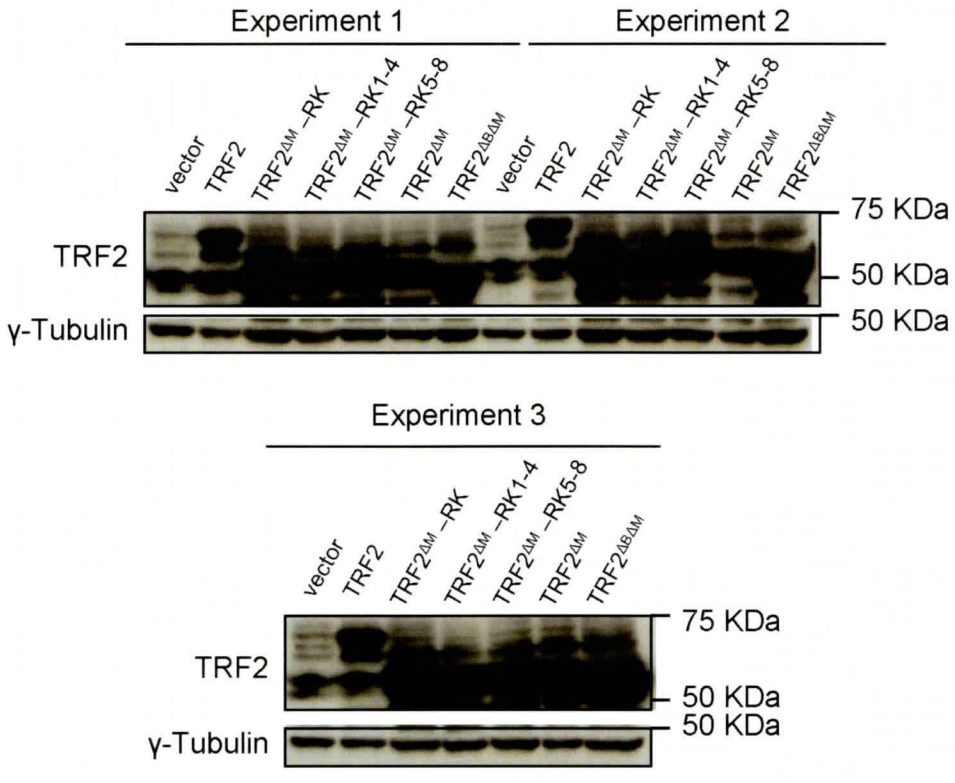
Experiment 1
Experiment 2
vector
TRF2
TRF2ΔM-RK
TRF2ΔM-RK1-4
TRF2ΔM-RK5-8
TRF2ΔM
TRF2ΔBΔM
TRF2
γ-Tubulin
75 KDa
50 KDa
50 KDa
Experiment 3
vector
TRF2
TRF2ΔM-RK
TRF2ΔM-RK1-4
TRF2ΔM-RK5-8
TRF2ΔM
TRF2ΔBΔM
TRF2
γ-Tubulin
75 KDa
50 KDa
50 KDa

Figure 4.10. Senescence induced in BJ/hTERT cells overexpressing TRF2 mutants containing amino acid changes from arginines to lysines in the basic domain of TRF2 in combination with the deletion of the Myb domain. A) BJ/hTERT cells were retrovirally infected with the vector pLPC alone or the vector containing TRF2, TRF2-RK$^{\Delta M}$, TRF2-RK1-4$^{\Delta M}$, TRF2-RK5-8$^{\Delta M}$, TRF2$^{\Delta M}$ or TRF2$^{\Delta B \Delta M}$. The cells were fixed at day thirteen of selection and incubated in staining solution containing X-gal at pH 6.0. The cells were visualized using a microscope for the senescence associated marker β-galactosidase. B) Quantification of the total number of positively stained β-galactosidase BJ/hTERT cells among at least 1500 cells were counted. The error bars represent the standard deviation of the mean for three independent experiments.

A

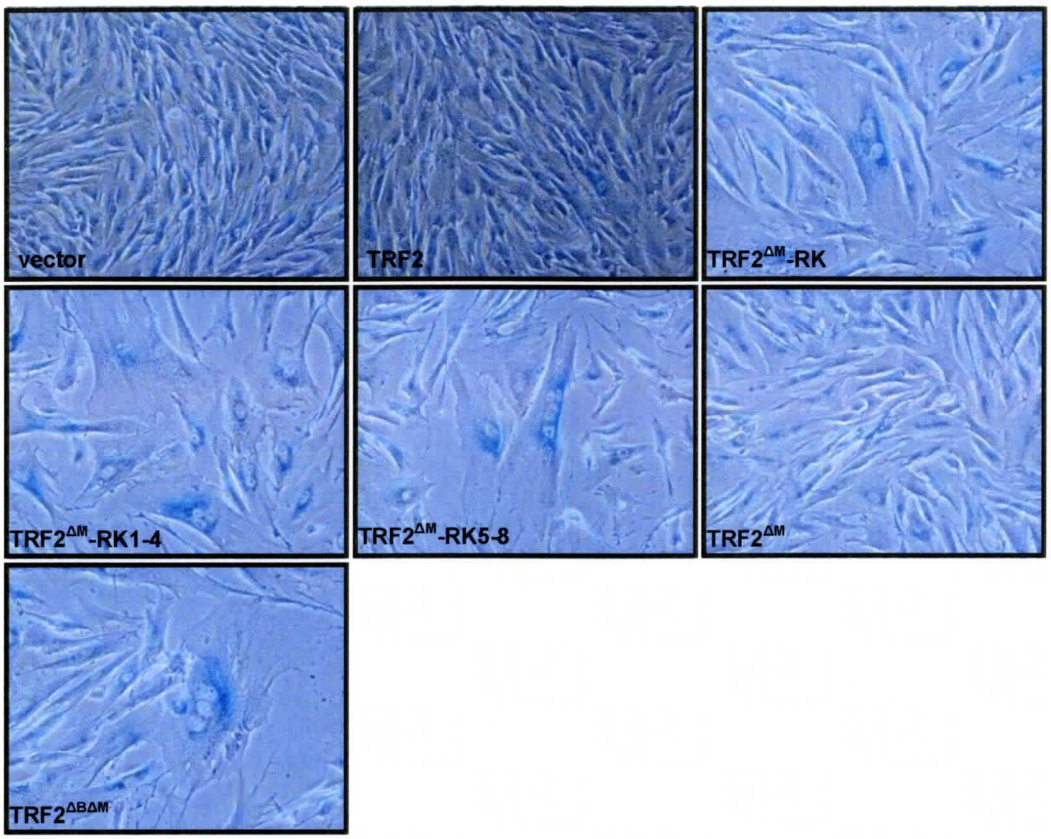
vector
TRF2
TRF2ΔM-RK
TRF2ΔM-RK1-4
TRF2ΔM-RK5-8
TRF2ΔM
TRF2ΔBΔM

B

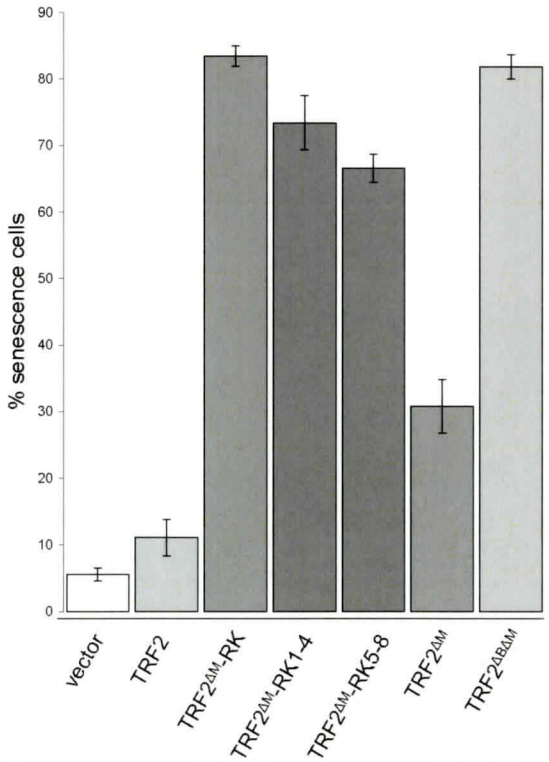
% senescence cells
0
10
20
30
40
50
60
70
80
90
vector
TRF2
TRF2ΔM-RK
TRF2ΔM-RK1-4
TRF2ΔM-RK5-8
TRF2ΔM
TRF2ΔBΔM

Figure 4.11. Telomere fusions observed at a high rate in BJ/hTERT metaphase cells expressing TRF2 mutants carrying a combination of the deletion of the Myb domain and amino acid substitutions from arginine to lysine in the basic domain. A) BJ/hTERT metaphase cells expressing the vector alone or TRF2, TRF2$^{\Delta M}$-RK, TRF2$^{\Delta M}$-RK1-4, TRF2$^{\Delta M}$-RK5-8, TRF2$^{\Delta M}$ or TRF2$^{\Delta B \Delta M}$ at day ten of selection. Cells were arrested with colcemid for 4 hr, incubated with a G-strand specific fluorescent PNA telomeric probe and stained with DAPI. Arrows indicate telomere fusion events. B) Quantification of metaphase telomere dysfunction in BJ/hTERT cells analyzed by telomeric FISH at day ten of selection. Quantification was performed for three independent experiments in a blinded fashion. Values in brackets represent the standard deviation of the mean or the *P*-value where indicated. *P*-value was determined by a two-tailed Student's *t*-test as compared to the vector control. C) Quantification of the number of telomere fusion events per metaphase cell. D) The fraction of metaphase cells with fusions. Error bars represent the standard deviation of the mean for three independent experiments.

A

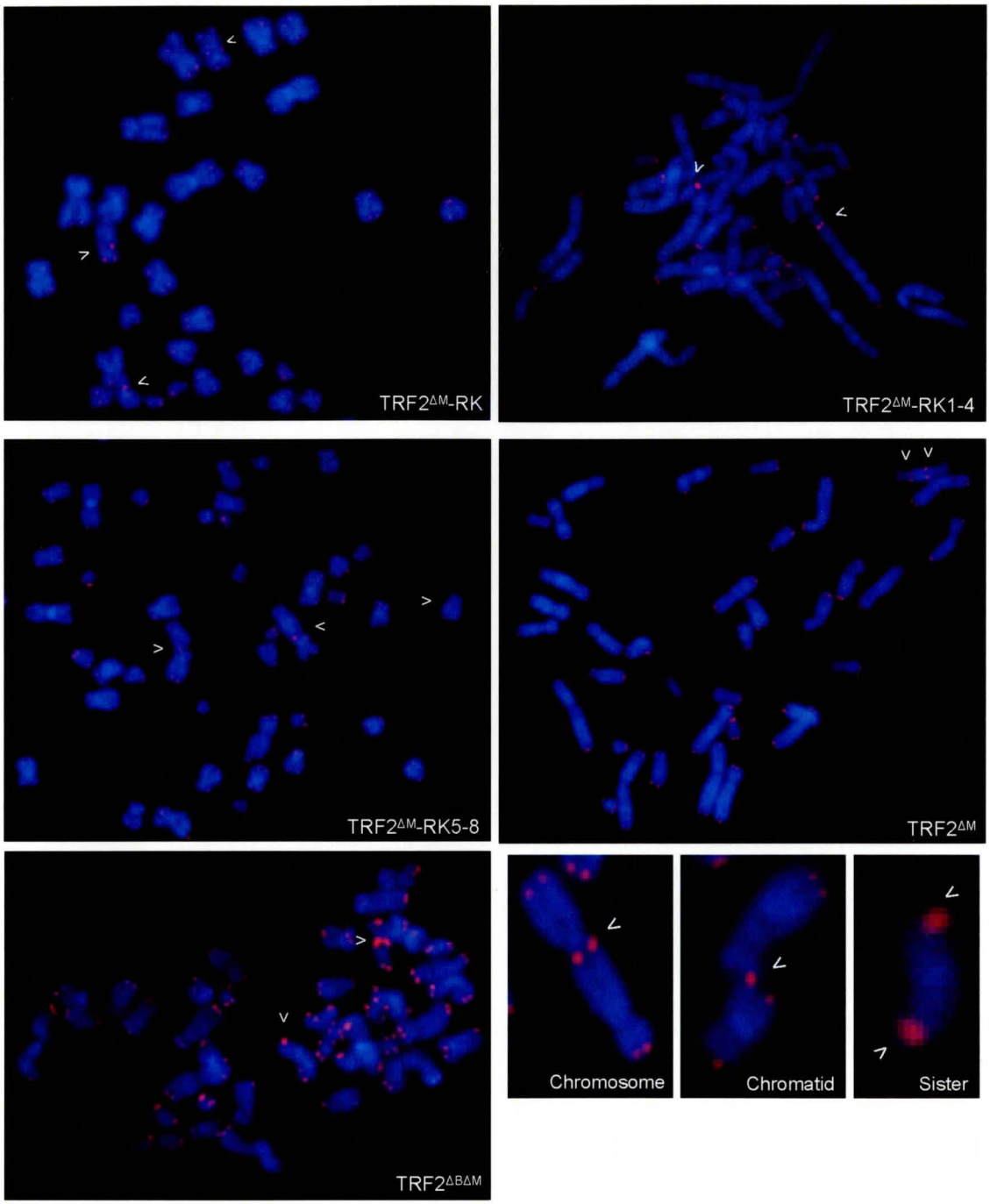
TRF2ΔM-RK
TRF2ΔM-RK1-4
TRF2ΔM-RK5-8
TRF2ΔM
TRF2ΔBΔM
Chromosome
Chromatid
Sister

B

Cell Line	Total Metaphase Cells	Total Metaphase Chromosomes	Average Telomere Doublets at Each Chromatid End (%), (+/- S.D)	Average Sister Telomere Loss at Each Chromatid End (%), (+/- S.D)	Average Fusion Events Per Metaphase Cell, (P-Value)	Fraction of Metaphase Cells With ≥ 1 Fusion Event (%), (P-Value)
Vector	45	1856	1.8, (0.37)	0.42, (0.18)	0.04, (1.000)	4.44, (1.00)
TRF2	45	1774	3.5, (0.82)	0.74, (0.40)	0.04, (0.999)	4.44, (0.999)
$TRF2^{\Delta M}$-RK	46	1758	1.5, (0.05)	0.54, (0.09)	1.78, (0.002)	84.2, (<0.001)
$TRF2^{\Delta M}$-RK1-4	38	1399	1.4, (0.12)	0.69, (0.42)	1.20, (<0.001)	70.5, (<0.001)
$TRF2^{\Delta M}$-RK5-8	38	1491	1.0, (0.16)	0.69, (0.16)	1.87, (0.001)	70.9, (<0.001)
$TRF2^{\Delta M}$	38	1435	1.6, (0.29)	1.00, (0.22)	0.60, (0.003)	47.2, (0.003)
$TRF2^{\Delta B}$	43	1636	2.4, (0.70)	3.3, (0.67)	0.02, (0.561)	2.40, (0.561)
$TRF2^{\Delta B\Delta M}$	32	1163	1.8, (0.46)	0.64, (0.13)	1.82, (0.003)	72.2, (<0.001)

C

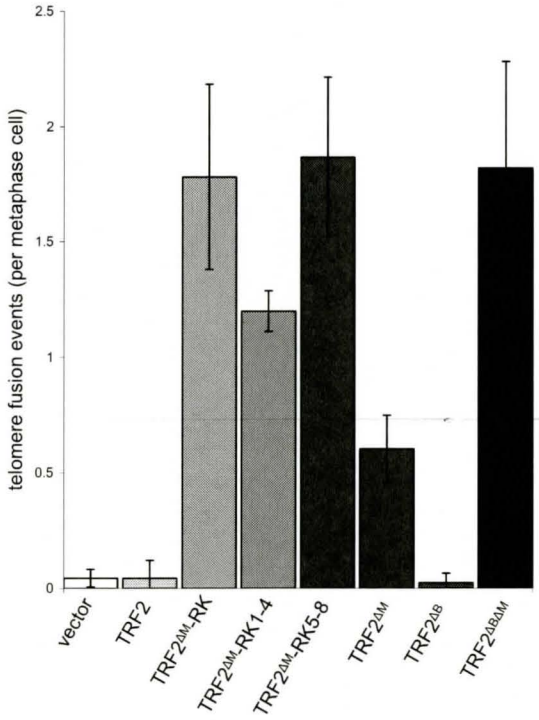

D

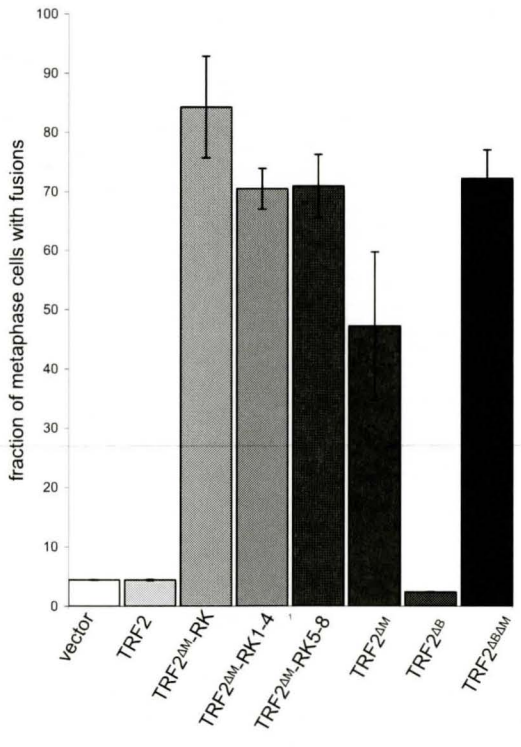

Figure 4.12. Loss of G-strand overhang and telomere fusions observed on genomic blots in BJ/hTERT cells expressing TRF2 mutants containing arginine to lysine amino acid substitutions in the basic domain. Telomere genomic blots of BJ/hTERT cells expressing the vector alone or TRF2, $TRF2^{\Delta M}$-RK, $TRF2^{\Delta M}$-RK1-4, $TRF2^{\Delta M}$-RK5-8, $TRF2^{\Delta M}$ or $TRF2^{\Delta B\Delta M}$ after ten days of selection. A) Native telomere blot demonstrating the loss of overhang signal. B) Denatured telomere blot representing larger molecular weight telomere fusions. The genomic DNA was phenol-chloroform extracted and digested with *AluI* and *MboI*. A total of 4μg of DNA was loaded onto a 0.7% agarose gel, run until the 1.3 kb molecular marker was at the bottom of the gel and dried. The native gel was hybridized with a radioactive telomere G-strand probe and exposed on a PhosphoImager screen overnight. The same gel was subsequently denatured in NaOH. The denatured gel was hybridized with a radioactive telomere G-strand probe and exposed on a PhosphoImager screen overnight. The overhang signal was determined by quantifying the total telomere restriction fragments in the native gel normalized to the total telomeric signal obtained from the denatured gel.

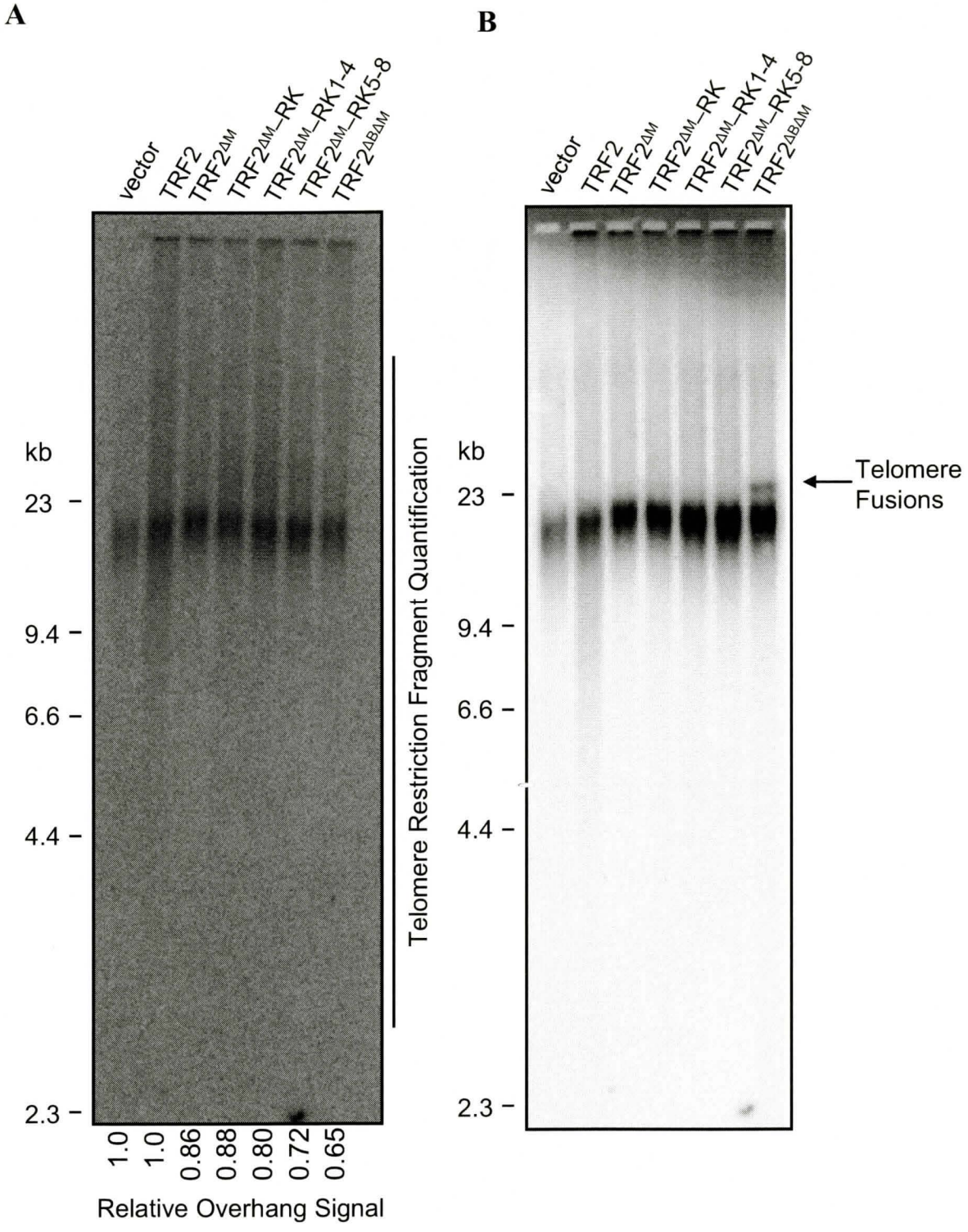
A
B
vector
TRF2
TRF2ΔM
TRF2ΔM–RK
TRF2ΔM–RK1-4
TRF2ΔM–RK5-8
TRF2ΔBΔM
kb
23
9.4
6.6
4.4
2.3
Telomere Restriction Fragment Quantification
1.0
1.0
0.86
0.88
0.80
0.72
0.65
Relative Overhang Signal
Telomere Fusions

Chapter 5 - Discussion

Characterization of TRF2 in Telomere Maintenance

I have demonstrated that the charge in the basic domain alone is not sufficient to maintain the protective function of TRF2. My results suggest that more than one arginine residue is essential to maintain the protective telomeric function of the basic domain of TRF2. Overexpression of TRF2-RK and TRF2$^{\Delta M}$-RK mutants in both HT1080 and BJ/hTERT cells have shown to virtually recapitulate the TRF2$^{\Delta B}$ and TRF2$^{\Delta B\Delta M}$ decreased proliferation and senescence phenotypes respectively. My results also indicate the possible molecular mechanisms responsible for the decreased proliferation rate and senescence phenotypes observed in the TRF2 mutants. Overexpression of TRF2-RK, TRF2-RK1-4 and TRF2-RK5-8 causes an increase in telomere doublets, this increase may be the trigger leading to cellular senescence. However, the telomere doublet phenotype is not observed in TRF2$^{\Delta B}$ cells (Wang et al, 2004). Overexpression of TRF2$^{\Delta M}$-RK, TRF2$^{\Delta M}$-RK1-4 and TRF2$^{\Delta M}$-RK5-8 mutants may be processed by NHEJ resulting in detrimental telomere fusions. This fusion phenotype leads to the induction of cellular senescence, which is consistent with the phenotype of TRF2$^{\Delta B\Delta M}$ (van Steensel et al, 1998). My results also demonstrate that it is the loss of the Myb domain which acts as the driving force for the formation of telomere fusions. In conclusion, I have shown that more than one arginine residues in the basic domain of TRF2 is likely required for proper functioning of the human TRF2 protein *in vivo*. Perhaps these arginine residues in the basic domain are modified by methylation and regulate the protein-protein interactions of TRF2.

5.1 Arginines in the Basic Domain of TRF2 are Essential for Maintaining Telomere Integrity

To study the arginine residues in the basic domain of TRF2, eight out of the nine arginine residues were mutated. Overexpression of TRF2 carrying eight arginine mutations in the basic domain and in the presence or absence of the Myb domain leads to detrimental phenotypes in both HT1080 and BJ/hTERT cells. These phenotypes observed based on proliferation assays, anaphase bridge counting, metaphase spreads, senescence assays and telomere blotting supports the hypothesis that the positive charge in the basic domain of TRF2 alone is not sufficient to maintain its function. Thus, the phenotypes observed in this study are due to the loss of arginine residues and not due to the loss of the positive charge of the basic domain.

TRF2 mutants containing four amino acid substitutions from arginines to lysines in the basic domain were also examined. Although mutating four arginine residues did not always show as severe phenotype as mutating eight arginine residues in the basic domain of TRF2, these mutants still support the hypothesis that possibly all eight arginines or a stretch of arginine residues are necessary to maintain the protective function of TRF2. The TRF2 mutants were analyzed in both a tumor cell line and an immortalized human primary cell line to demonstrate that the phenotypes are reproducible and are not cell line-specific. However, the BJ/hTERT cell line proved to be a more sensitive functional assay system to investigate the differences between the vector control and the RK, RK1-4 and RK5-8 mutants.

Overexpression of TRF2 mutants carrying amino acid changes from arginines to lysines in the basic domain and in the presence or absence of the Myb domain in HT1080 and BJ/hTERT cells leads to decreased proliferation as compared to the vector. In both HT1080 and BJ/hTERT cells, TRF2-RK proliferated similarly to $TRF2^{\Delta B}$ and $TRF2^{\Delta M}$-RK had a proliferation rate that resembled $TRF2^{\Delta B\Delta M}$ in BJ/hTERT cells. These results corroborate the ability of the TRF2-RK and $TRF2^{\Delta M}$-RK mutants to recapitulate the $TRF2^{\Delta B}$ and $TRF2^{\Delta B\Delta M}$ decreased proliferation phenotypes. Additionally although the proliferation rates of TRF2-RK1-4 and TRF2-RK5-8 were not as low compared to TRF2-RK, a significant decrease in the proliferation potential was observed as compared to the vector in HT1080 and BJ/hTERT cells. These results reiterate the importance of the arginine residues in the basic domain of TRF2.

I further observed a senescence phenotype in both HT1080 and BJ/hTERT cells when the various TRF2 mutants were overexpressed. In both HT1080 and BJ/hTERT cells, all of the TRF2 mutants showed a similar number of senescent cells. A large amount of senescent cells were observed in TRF2-RK and $TRF2^{\Delta M}$-RK, which was close to the number of senescent cells in $TRF2^{\Delta B}$ and $TRF2^{\Delta B\Delta M}$ respectively. Taken together, my results indicate that the arginine residues in the basic domain of TRF2 are essential to maintain telomere integrity.

Furthermore, the results from my experiments may suggest that one or more arginines in the basic domain of TRF2 may act as a possible methylation sites. Currently, it is not known whether the function of the basic domain of TRF2 is regulated by post-translational modifications. The basic domain of TRF2 has many glycines and arginines,

and reflects a semi-conserved glycine and arginine rich (GAR) domain (Palm & de Lange, 2008). This GAR domain acts as a preferred substrate for protein arginine methyltransferases (PRMTs), which methylate arginine residues (McBride & Silver, 2001). TRF2 may be a substrate of PRMTs and its function and its interactions with DNA damage sensing and DNA repair enzymes may be regulated via methylation.

5.2 Overexpression of TRF2 Mutants Carrying Amino Acid Substitutions from Arginines to Lysines in the Basic Domain Results in Telomere Doublets

It has been shown that overexpression of $TRF2^{\Delta B}$ leads to rapid telomere deletion (Wang et al, 2004). Consistent with the previous findings, I have shown that $TRF2^{\Delta B}$ overexpression results in an increase in sister telomere loss and terminal deletions in BJ/hTERT metaphase cells. However, such an increase in sister telomere loss and terminal deletions are not observed in BJ/hTERT metaphase cells overexpressing TRF2-RK, TRF2-RK1-4 and TRF2RK-5-8. Instead, I detect an elevation in the formation of telomere doublets. Although telomere doublets have been reported previously, it is unclear how telomere doublets are generated but it may involve a recombination based mechanism (Ariyoshi et al, 2007, Michishita et al, 2008, Pennarun et al, 2008, Philippe et al, 1999, Undarmaa et al, 2004, van Overbeek & de Lange, 2006).

Telomere doublets has been observed in WS cells and Apollo knockdown cells (Ariyoshi et al, 2007, van Overbeek & de Lange, 2006). As mentioned earlier, WRN is mutated in WS and interacts with TRF2 through its basic domain (Li et al, 2008, Machwe et al, 2004, Opresko et al, 2002). It has been suggested that WRN is required for efficient replication of the G-rich telomeric DNA and helps in resolving the D-loop telomere

structure *in vitro* (Crabbe et al, 2004, Mohaghegh et al, 2001, Opresko et al, 2003, Opresko et al, 2004). WS cells have been observed to contain extra telomere signals also known as telomere doublets (Ariyoshi et al, 2007). Cells lacking WRN also have an increase in sister telomere loss and it is thought that this excessive telomere loss leads to the activation of DNA damage signalling (Chin et al, 1999, Crabbe et al, 2004, d'Adda di Fagagna et al, 2003, Herbig et al, 2004). Apollo is a 3' exonuclease and interacts with TRF2 through its homodimerization domain (Lenain et al, 2006, van Overbeek & de Lange, 2006). It is suggested that Apollo interacts with TRF2 to protect telomeric DNA during or after DNA replication (van Overbeek & de Lange, 2006). Apollo may additionally play a role in the resection of the 5'C-rich strand of telomeric DNA during replication (Lenain et al, 2006, van Overbeek & de Lange, 2006). Knockdown of Apollo in cells results in an increase of telomere doublets but no other telomere aberrations (van Overbeek & de Lange, 2006). This phenotype is consistent with the phenotype I observed when TRF2 mutants containing amino acid changes from arginines to lysines in the basic domain were expressed in BJ/hTERT cells. Although it is not known what mechanisms are responsible for the formation of the telomere doublets, it would be informative to investigate whether TRF2 containing the amino acid changes from arginines to lysines in the basic domain are still able to maintain protein-protein interactions with WRN and Apollo. The differences in the telomere loss phenotype observed in $TRF2^{\Delta B}$ as compared the TRF2 mutants may be explained by the inability of $TRF2^{\Delta B}$ to maintain communication and interactions with other proteins. However, the TRF2 mutants only

containing amino acid substitutions in the basic domain may still have the ability to communicate and interact with other TRF2 interacting proteins.

As well, the results from Southern blotting analysis were consistent with the data obtained from FISH performed on the TRF2 mutants. Analysis of the telomere blot indicates that there is no significant increase in telomere degradation in the TRF2-RK, TRF2-RK1-4 or TRF2-RK5-8 samples in BJ/hTERT cells. The telomere length in these TRF2 mutants closely resembles wild type TRF2 as opposed to $TRF2^{\Delta B}$, which shows strong evidence of telomere deletion. These data suggests that a different mechanism other than telomere deletion may be involved in the decreased proliferation and senescence phenotypes observed in the TRF2-RK, TRF2-RK1-4 and TRF2-RK5-8 BJ/hTERT cell lines. The senescence phenotype observed when these TRF2 mutants are overexpressed in BJ/hTERT cells may be due to the formation of telomere doublets. Furthermore, these results suggest that the amino acid substitutions introduced into the basic domain of TRF2 are not completely disrupting the protein folding of the protein. When the basic domain contained only the amino acid changes from arginines to lysines telomere doublets occurred but in the complete loss of the basic domain telomere loss was observed.

5.3 Amino Acid Changes from Arginines to Lysines in the Basic Domain of TRF2 in Combination with the Deletion of the Myb Domain Leads to Telomere Fusions

In HT1080 cells, expression of $TRF2^{\Delta M}$-RK, $TRF2^{\Delta M}$-RA, $TRF2^{\Delta M}$-RK1-4 and $TRF2^{\Delta M}$-RK5-8 all result in a high number of anaphase bridges as compared the vector, consistent with the previously published phenotype of $TRF2^{\Delta B\Delta M}$ (van Steensel et al,

1998). Overexpression of TRF2-RK, TRF2-RA, TRF2-RK1-4 and TRF2-RK5-8 in HT1080 cells did not induce a significant amount of anaphase bridges as compared to vector, in agreement with the published phenotype of $TRF2^{\Delta B}$ (Wang et al, 2004). Lagging chromosomes were additionally scored in HT1080 cells. The number of lagging chromosomes remained relatively unchanged, which further suggests that the fusion events are due to the amino acid changes from arginines to lysines in the basic domain of TRF2 in combination with the deletion of the Myb domain.

Furthermore, chromosome fusions were scored in BJ/hTERT metaphase cells overexpressing TRF2 mutants containing amino acid substitutions from arginines to lysines in the basic domain in combination with the deletion of the Myb domain. The metaphase FISH results indicate a significant increase in telomere fusion events in $TRF2^{\Delta M}$-RK, $TRF2^{\Delta M}$-RK1-4 and $TRF2^{\Delta M}$-RK5-8 mutants as compared to the vector and wild type TRF2. In addition, the percentage of metaphase cells containing more than one fusion event in the cell lines $TRF2^{\Delta M}$-RK, $TRF2^{\Delta M}$-RK1-4 and $TRF2^{\Delta M}$-RK5-8 were also significantly different from the vector. Although $TRF2^{\Delta M}$ did contain a number of fusion events, the number of fusions per chromatid end and the fraction of metaphase cells with more than one fusion event was lower and significantly different from $TRF2^{\Delta M}$-RK, $TRF2^{\Delta M}$-RK1-4 and $TRF2^{\Delta M}$-RK5-8. These results suggest that the fusion events observed were occurring due to both the loss of the Myb domain and a compromised basic domain.

Furthermore, expression of TRF2 mutants lacking the Myb domain and carrying arginine to lysine amino acid changes in the basic domain show evidence of the loss of

the 3' overhangs and the presence of high molecular weight telomere fusions on native and denatured telomere blots respectively. My results obtained from analysis of chromosomes in anaphase and metaphase as well as performing telomere blots suggest that the decreased proliferation rate and senescence phenotypes observed in TRF2$^{\Delta M}$-RK, TRF2$^{\Delta M}$-RK1-4 and TRF2$^{\Delta M}$-RK5-8 cells is due to the formation of telomere fusions. Interestingly, when TRF2 lacking the Myb domain is expressed in cells, TRF2 cannot bind and protect the telomeres. This telomere deprotection results in the loss of the 3'G-rich overhangs, leading to the formation of fusion events.

Additionally, although TRF2$^{\Delta M}$ was used as a control for these experiments, my overall results provide an analysis of the TRF2$^{\Delta M}$ deletion mutant as well. Currently there has only been one recent publication on the phenotype of TRF2$^{\Delta M}$ expression *in vivo* (Konishi & de Lange, 2008). Expression of TRF2$^{\Delta M}$ in BJ/hTERT cells did not demonstrate to have as severe detrimental phenotype as compared to the TRF2 mutants TRF2$^{\Delta M}$-RK, TRF2$^{\Delta M}$-RK1-4 and TRF2$^{\Delta M}$-RK5-8 upon examination of the proliferation assay, senescence assay, telomere blotting and analysis of anaphase and metaphase chromosomes.

5.4 Perspectives

For the future, one may investigate further into the mechanisms responsible for the formation of telomere doublets. Specifically, it will be informative to determine whether the telomere doublet phenotype is an intermediate recombination event acting through the same pathway as the telomere loss phenotype, as observed in TRF2$^{\Delta B}$. Based on my results, it is likely that the function of the basic domain of TRF2 is to prevent the

formation of telomere doublets and telomere loss by suppressing recombination events at telomeres. However, further investigation will be needed to investigate the DNA recombination and repair proteins required for the formation of telomere doublets. Also, as mentioned above one can examine whether the various TRF2 mutants maintain protein-protein interactions with WRN and Apollo. Overall, results from these experiments will allow researchers to gain a better understanding of the protective function of the basic domain of TRF2 and recombination events at telomeres.

Furthermore, one area of future research would be to determine if one arginine residue is more crucial than another arginine residue in the basic domain of TRF2. Point mutations can be introduced into each one of the arginine residues in the basic domain to reveal whether one arginine residue is indispensable to the function of TRF2. In general, it will be very informative to link the key arginine residues in the basic domain of TRF2 to a protein arginine methyltransferase. Ultimately, the results of my project combined with others will hopefully shed new light on the overall regulation of the protective function of TRF2.

Bibliography

Abraham RT (2001) Cell cycle checkpoint signaling through the ATM and ATR kinases. Genes Dev 15: 2177-2196

Ariyoshi K, Suzuki K, Goto M, Watanabe M, & Kodama S (2007) Increased chromosome instability and accumulation of DNA double-strand breaks in Werner syndrome cells. J Radiat Res (Tokyo) 48: 219-231

Bae NS & Baumann P (2007) A RAP1/TRF2 complex inhibits nonhomologous end-joining at human telomeric DNA ends. Mol Cell 26: 323-334

Bailey SM, Cornforth MN, Kurimasa A, Chen DJ, & Goodwin EH (2001) Strand-specific postreplicative processing of mammalian telomeres. Science 293: 2462-2465

Baird DM & Farr CJ (2006) The organization and function of chromosomes. EMBO Rep 7: 372-376

Bakkenist CJ & Kastan MB (2003) DNA damage activates ATM through intermolecular autophosphorylation and dimer dissociation. Nature 421: 499-506

Banin S, Moyal L, Shieh S, Taya Y, Anderson CW, Chessa L, Smorodinsky NI, Prives C, Reiss Y, Shiloh Y, & Ziv Y (1998) Enhanced phosphorylation of p53 by ATM in response to DNA damage. Science 281: 1674-1677

Bao S, Tibbetts RS, Brumbaugh KM, Fang Y, Richardson DA, Ali A, Chen SM, Abraham RT, & Wang XF (2001) ATR/ATM-mediated phosphorylation of human Rad17 is required for genotoxic stress responses. Nature 411: 969-974

Bartek J & Lukas J (2001) Mammalian G1- and S-phase checkpoints in response to DNA damage. Curr Opin Cell Biol 13: 738-747

Baumann P & Cech TR (2001) Pot1, the putative telomere end-binding protein in fission yeast and humans. Science 292: 1171-1175

Berdal KG, Johansen RF, & Seeberg E (1998) Release of normal bases from intact DNA by a native DNA repair enzyme. EMBO J 17: 363-367

Bianchi A, Stansel RM, Fairall L, Griffith JD, Rhodes D, & de Lange T (1999) TRF1 binds a bipartite telomeric site with extreme spatial flexibility. EMBO J 18: 5735-5744

Bilaud T, Brun C, Ancelin K, Koering CE, Laroche T, & Gilson E (1997) Telomeric localization of TRF2, a novel human telobox protein. Nat Genet 17: 236-239

Bilaud T, Koering CE, Binet-Brasselet E, Ancelin K, Pollice A, Gasser SM, & Gilson E (1996) The telobox, a Myb-related telomeric DNA binding motif found in proteins from yeast, plants and human. Nucleic Acids Res 24: 1294-1303

Blackburn EH (2001) Switching and signaling at the telomere. Cell 106: 661-673

Blackburn EH, Greider CW, Henderson E, Lee MS, Shampay J, & Shippen-Lentz D (1989) Recognition and elongation of telomeres by telomerase. Genome 31: 553-560

Blanco R, Munoz P, Flores JM, Klatt P, & Blasco MA (2007) Telomerase abrogation dramatically accelerates TRF2-induced epithelial carcinogenesis. Genes Dev 21: 206-220

Bohr VA, Smith CA, Okumoto DS, & Hanawalt PC (1985) DNA repair in an active gene: removal of pyrimidine dimers from the DHFR gene of CHO cells is much more efficient than in the genome overall. Cell 40: 359-369

Bradshaw PS, Stavropoulos DJ, & Meyn MS (2005) Human telomeric protein TRF2 associates with genomic double-strand breaks as an early response to DNA damage. Nat Genet 37: 193-197

Broccoli D, Smogorzewska A, Chong L, & de Lange T (1997) Human telomeres contain two distinct Myb-related proteins, TRF1 and TRF2. Nat Genet 17: 231-235

Canman CE, Lim DS, Cimprich KA, Taya Y, Tamai K, Sakaguchi K, Appella E, Kastan MB, & Siliciano JD (1998) Activation of the ATM kinase by ionizing radiation and phosphorylation of p53. Science 281: 1677-1679

Celli GB & de Lange T (2005) DNA processing is not required for ATM-mediated telomere damage response after TRF2 deletion. Nat Cell Biol 7: 712-718

Chang S, Multani AS, Cabrera NG, Naylor ML, Laud P, Lombard D, Pathak S, Guarente L, & DePinho RA (2004) Essential role of limiting telomeres in the pathogenesis of Werner syndrome. Nat Genet 36: 877-882

Chin L, Artandi SE, Shen Q, Tam A, Lee SL, Gottlieb GJ, Greider CW, & DePinho RA (1999) P53 Deficiency Rescues the Adverse Effects of Telomere Loss and Cooperates with Telomere Dysfunction to Accelerate Carcinogenesis. Cell 97: 527-538

Chong L, van Steensel B, Broccoli D, Erdjument-Bromage H, Hanish J, Tempst P, & de Lange T (1995) A human telomeric protein. Science 270: 1663-1667

Cimprich KA, Shin TB, Keith CT, & Schreiber SL (1996) cDNA cloning and gene mapping of a candidate human cell cycle checkpoint protein. Proc Natl Acad Sci U S A 93: 2850-2855

Counter CM, Meyerson M, Eaton EN, Ellisen LW, Caddle SD, Haber DA, & Weinberg RA (1998) Telomerase activity is restored in human cells by ectopic expression of hTERT (hEST2), the catalytic subunit of telomerase. Oncogene 16: 1217-1222

Court R, Chapman L, Fairall L, & Rhodes D (2005) How the human telomeric proteins TRF1 and TRF2 recognize telomeric DNA: a view from high-resolution crystal structures. EMBO Rep 6: 39-45

Crabbe L, Jauch A, Naeger CM, Holtgreve-Grez H, & Karlseder J (2007) Telomere dysfunction as a cause of genomic instability in Werner syndrome. Proc Natl Acad Sci U S A 104: 2205-2210

Crabbe L & Karlseder J (2005) In the end, it's all structure. Curr Mol Med 5: 135-143

Crabbe L, Verdun RE, Haggblom CI, & Karlseder J (2004) Defective telomere lagging strand synthesis in cells lacking WRN helicase activity. Science 306: 1951-1953

d'Adda di Fagagna F, Reaper PM, Clay-Farrace L, Fiegler H, Carr P, Von Zglinicki T, Saretzki G, Carter NP, & Jackson SP (2003) A DNA damage checkpoint response in telomere-initiated senescence. Nature 426: 194-198

de Gruijl FR, van Kranen HJ, & Mullenders LH (2001) UV-induced DNA damage, repair, mutations and oncogenic pathways in skin cancer. J Photochem Photobiol B 63: 19-27

de Laat WL, Appeldoorn E, Jaspers NG, & Hoeijmakers JH (1998) DNA structural elements required for ERCC1-XPF endonuclease activity. J Biol Chem 273: 7835-7842

de Laat WL, Jaspers NG, & Hoeijmakers JH (1999) Molecular mechanism of nucleotide excision repair. Genes Dev 13: 768-785

de Lange T (2005) Shelterin: the protein complex that shapes and safeguards human telomeres. Genes Dev 19: 2100-2110

de Lange T (2002) Protection of mammalian telomeres. Oncogene 21: 532-540

de Lange T & Petrini JH (2000) A new connection at human telomeres: association of the Mre11 complex with TRF2. Cold Spring Harb Symp Quant Biol 65: 265-273

de Lange T, Shiue L, Myers RM, Cox DR, Naylor SL, Killery AM, & Varmus HE (1990) Structure and variability of human chromosome ends. Mol Cell Biol 10: 518-527

Denchi EL & de Lange T (2007) Protection of telomeres through independent control of ATM and ATR by TRF2 and POT1. Nature 448: 1068-1071

Dimri GPm Lee X, Basile G, Acosta M, Scott G, Roskelley C, Medrano EE, Linskens M, Rubelj I, Pereira-Smith O (1995) A biomarker that identifies senescent human cells in culture and in aging skin in vivo. Proc Natl Acad Sci USA 92: 9363-9367

el-Deiry WS, Tokino T, Velculescu VE, Levy DB, Parsons R, Trent JM, Lin D, Mercer WE, Kinzler KW, & Vogelstein B (1993) WAF1, a potential mediator of p53 tumor suppression. Cell 75: 817-825

Evans E, Moggs JG, Hwang JR, Egly JM, & Wood RD (1997) Mechanism of open complex and dual incision formation by human nucleotide excision repair factors. EMBO J 16: 6559-6573

Fairall L, Chapman L, Moss H, de Lange T, & Rhodes D (2001) Structure of the TRFH dimerization domain of the human telomeric proteins TRF1 and TRF2. Mol Cell 8: 351-361

Ford JM & Hanawalt PC (1997) Role of DNA excision repair gene defects in the etiology of cancer. Curr Top Microbiol Immunol 221: 47-70

Francia S, Weiss RS, Hande MP, Freire R, & d'Adda di Fagagna F (2006) Telomere and telomerase modulation by the mammalian Rad9/Rad1/Hus1 DNA-damage-checkpoint complex. Curr Biol 16: 1551-1558

Friedberg EC (1996) Relationships between DNA repair and transcription. Annu Rev Biochem 65: 15-42

Greider CW & Blackburn EH (1985) Identification of a specific telomere terminal transferase activity in Tetrahymena extracts. Cell 43: 405-413

Griffith JD, Comeau L, Rosenfield S, Stansel RM, Bianchi A, Moss H, & de Lange T (1999) Mammalian telomeres end in a large duplex loop. Cell 97: 503-514

Hahn WC (2005) Telomere and telomerase dynamics in human cells. Curr Mol Med 5: 227-231

Hainaut P & Hollstein M (2000) P53 and Human Cancer: the First Ten Thousand Mutations. Adv Cancer Res 77: 81-137

Hanaoka S, Nagadoi A, & Nishimura Y (2005) Comparison between TRF2 and TRF1 of their telomeric DNA-bound structures and DNA-binding activities. Protein Sci 14: 119-130

Hanawalt PC (2002) Subpathways of nucleotide excision repair and their regulation. Oncogene 21: 8949-8956

Harley CB, Futcher AB, & Greider CW (1990) Telomeres shorten during ageing of human fibroblasts. Nature 345: 458-460

Hayflick L & Moorehead PS (1961) The serial cultivation of human diploid cell strains. Exp Cell Res 25: 585-621

Herbig U, Jobling WA, Chen BP, Chen DJ, & Sedivy JM (2004) Telomere shortening triggers senescence of human cells through a pathway involving ATM, p53, and p21(CIP1), but not p16(INK4a). Mol Cell 14: 501-513

Hezel AF, Bardeesy N, & Maser RS (2005) Telomere induced senescence: end game signaling. Curr Mol Med 5: 145-152

Hirao A, Kong YY, Matsuoka S, Wakeham A, Ruland J, Yoshida H, Liu D, Elledge SJ, & Mak TW (2000) DNA damage-induced activation of p53 by the checkpoint kinase Chk2. Science 287: 1824-1827

Hoeijmakers JH (2001) Genome maintenance mechanisms for preventing cancer. Nature 411: 366-374

Hollstein M, Sidransky D, Vogelstein B, & Harris CC (1991) P53 Mutations in Human Cancers. Science 253: 49-53

Houghtaling BR, Cuttonaro L, Chang W, & Smith S (2004) A dynamic molecular link between the telomere length regulator TRF1 and the chromosome end protector TRF2. Curr Biol 14: 1621-1631

Houtgraaf JH, Versmissen J, & van der Giessen WJ (2006) A concise review of DNA damage checkpoints and repair in mammalian cells. Cardiovasc Revasc Med 7: 165-172

Hsu HL, Gilley D, Blackburn EH, & Chen DJ (1999) Ku is associated with the telomere in mammals. Proc Natl Acad Sci U S A 96: 12454-12458

Hsu HL, Gilley D, Galande SA, Hande MP, Allen B, Kim SH, Li GC, Campisi J, Kohwi-Shigematsu T, & Chen DJ (2000) Ku acts in a unique way at the mammalian telomere to prevent end joining. Genes Dev 14: 2807-2812

Huffman KE, Levene SD, Tesmer VM, Shay JW, & Wright WE (2000) Telomere shortening is proportional to the size of the G-rich telomeric 3'-overhang. J Biol Chem 275: 19719-19722

Hwang BJ, Ford JM, Hanawalt PC, & Chu G (1999) Expression of the p48 xeroderma pigmentosum gene is p53-dependent and is involved in global genomic repair. Proc Natl Acad Sci U S A 96: 424-428

Karlseder J, Broccoli D, Dai Y, Hardy S, & de Lange T (1999) p53- and ATM-dependent apoptosis induced by telomeres lacking TRF2. Science 283: 1321-1325

Karlseder J, Hoke K, Mirzoeva OK, Bakkenist C, Kastan MB, Petrini JH, & de Lange T (2004) The telomeric protein TRF2 binds the ATM kinase and can inhibit the ATM-dependent DNA damage response. PLoS Biol 2: E240

Karlseder J, Smogorzewska A, & de Lange T (2002) Senescence induced by altered telomere state, not telomere loss. Science 295: 2446-2449

Kim SH, Kaminker P, & Campisi J (1999) TIN2, a new regulator of telomere length in human cells. Nat Genet 23: 405-412

Kipling D & Cooke HJ (1990) Hypervariable ultra-long telomeres in mice. Nature 347: 400-402

Klapper W, Krams M, Qian W, Janssen D, & Parwaresch R (2003) Telomerase activity in B-cell non-Hodgkin lymphomas is regulated by hTERT transcription and correlated with telomere-binding protein expression but uncoupled from proliferation. Br J Cancer 89: 713-719

Konishi A & de Lange T (2008) Cell cycle control of telomere protection and NHEJ revealed by a ts mutation in the DNA-binding domain of TRF2. Genes Dev 22: 1221-1230

Lakin ND, Hann BC, & Jackson SP (1999) The ataxia-telangiectasia related protein ATR mediates DNA-dependent phosphorylation of p53. Oncogene 18: 3989-3995

Lee JH & Paull TT (2005) ATM activation by DNA double-strand breaks through the Mre11-Rad50-Nbs1 complex. Science 308: 551-554

Lejnine S, Makarov VL, & Langmore JP (1995) Conserved nucleoprotein structure at the ends of vertebrate and invertebrate chromosomes. Proc Natl Acad Sci U S A 92: 2393-2397

Lenain C, Bauwens S, Amiard S, Brunori M, Giraud-Panis MJ, & Gilson E (2006) The Apollo 5' exonuclease functions together with TRF2 to protect telomeres from DNA repair. Curr Biol 16: 1303-1310

Li B, Jog SP, Reddy S, & Comai L (2008) WRN controls formation of extrachromosomal telomeric circles and is required for TRF2DeltaB-mediated telomere shortening. Mol Cell Biol 28: 1892-1904

Li B, Oestreich S, & de Lange T (2000) Identification of human Rap1: implications for telomere evolution. Cell 101: 471-483

Lindsey-Boltz LA, Bermudez VP, Hurwitz J, & Sancar A (2001) Purification and characterization of human DNA damage checkpoint Rad complexes. Proc Natl Acad Sci U S A 98: 11236-11241

Lingner J, Hughes TR, Shevchenko A, Mann M, Lundblad V, & Cech TR (1997) Reverse transcriptase motifs in the catalytic subunit of telomerase. Science 276: 561-567

Liu D, O'Connor MS, Qin J, & Songyang Z (2004) Telosome, a mammalian telomere-associated complex formed by multiple telomeric proteins. J Biol Chem 279: 51338-51342

Loayza D & De Lange T (2003) POT1 as a terminal transducer of TRF1 telomere length control. Nature 423: 1013-1018

Longhese MP (2008) DNA damage response at functional and dysfunctional telomeres. Genes Dev 22: 125-140

Longhese MP, Foiani M, Muzi-Falconi M, Lucchini G, & Plevani P (1998) DNA damage checkpoint in budding yeast. EMBO J 17: 5525-5528

Machwe A, Xiao L, & Orren DK (2004) TRF2 recruits the Werner syndrome (WRN) exonuclease for processing of telomeric DNA. Oncogene 23: 149-156

Makarov VL, Hirose Y, & Langmore JP (1997) Long G tails at both ends of human chromosomes suggest a C strand degradation mechanism for telomere shortening. Cell 88: 657-666

Matsuoka S, Rotman G, Ogawa A, Shiloh Y, Tamai K, & Elledge SJ (2000) Ataxia telangiectasia-mutated phosphorylates Chk2 in vivo and in vitro. Proc Natl Acad Sci U S A 97: 10389-10394

McBride AE & Silver PA (2001) State of the arg: protein methylation at arginine comes of age. Cell 106: 5-8

McElligott R & Wellinger RJ (1997) The terminal DNA structure of mammalian chromosomes. EMBO J 16: 3705-3714

McGowan CH (2002) Checking in on Cds1 (Chk2): A checkpoint kinase and tumor suppressor. Bioessays 24: 502-511

Mellon I, Spivak G, & Hanawalt PC (1987) Selective removal of transcription-blocking DNA damage from the transcribed strand of the mammalian DHFR gene. Cell 51: 241-249

Melo J & Toczyski D (2002) A unified view of the DNA-damage checkpoint. Curr Opin Cell Biol 14: 237-245

Michishita E, McCord RA, Berber E, Kioi M, Padilla-Nash H, Damian M, Cheung P, Kusumoto R, Kawahara TL, Barrett JC, Chang HY, Bohr VA, Ried T, Gozani O, & Chua KF (2008) SIRT6 is a histone H3 lysine 9 deacetylase that modulates telomeric chromatin. Nature 452: 492-496

Miyachi K, Fujita M, Tanaka N, Sasaki K, & Sunagawa M (2002) Correlation between telomerase activity and telomeric-repeat binding factors in gastric cancer. J Exp Clin Cancer Res 21: 269-275

Mohaghegh P, Karow JK, Brosh Jr RM,Jr, Bohr VA, & Hickson ID (2001) The Bloom's and Werner's syndrome proteins are DNA structure-specific helicases. Nucleic Acids Res 29: 2843-2849

Moyzis RK, Buckingham JM, Cram LS, Dani M, Deaven LL, Jones MD, Meyne J, Ratliff RL, & Wu JR (1988) A highly conserved repetitive DNA sequence, (TTAGGG)n, present at the telomeres of human chromosomes. Proc Natl Acad Sci U S A 85: 6622-6626

Mu D, Hsu DS, & Sancar A (1996) Reaction mechanism of human DNA repair excision nuclease. J Biol Chem 271: 8285-8294

Mu D, Park CH, Matsunaga T, Hsu DS, Reardon JT, & Sancar A (1995) Reconstitution of human DNA repair excision nuclease in a highly defined system. J Biol Chem 270: 2415-2418

Munoz P, Blanco R, Flores JM, & Blasco MA (2005) XPF nuclease-dependent telomere loss and increased DNA damage in mice overexpressing TRF2 result in premature aging and cancer. Nat Genet 37: 1063-1071

Nakanishi K, Kawai T, Kumaki F, Hiroi S, Mukai M, Ikeda E, Koering CE, & Gilson E (2003) Expression of mRNAs for telomeric repeat binding factor (TRF)-1 and TRF2 in atypical adenomatous hyperplasia and adenocarcinoma of the lung. Clin Cancer Res 9: 1105-1111

Nijjar T, Bassett E, Garbe J, Takenaka Y, Stampfer MR, Gilley D, & Yaswen P (2005) Accumulation and altered localization of telomere-associated protein TRF2 in immortally transformed and tumor-derived human breast cells. Oncogene 24: 3369-3376

Nishikawa T, Nagadoi A, Yoshimura S, Aimoto S, & Nishimura Y (1998) Solution structure of the DNA-binding domain of human telomeric protein, hTRF1. Structure 6: 1057-1065

Nugent CI & Lundblad V (1998) The telomerase reverse transcriptase: components and regulation. Genes Dev 12: 1073-1085

Olovnikov AM (1996) Telomeres, telomerase, and aging: origin of the theory. Exp Gerontol 31: 443-448

Olovnikov AM (1973) A theory of marginotomy. The incomplete copying of template margin in enzymic synthesis of polynucleotides and biological significance of the phenomenon. J Theor Biol 41: 181-190

Opitz OG (2005) Telomeres, telomerase and malignant transformation. Curr Mol Med 5: 219-226

Opresko PL, Cheng WH, von Kobbe C, Harrigan JA, & Bohr VA (2003) Werner syndrome and the function of the Werner protein; what they can teach us about the molecular aging process. Carcinogenesis 24: 791-802

Opresko PL, Otterlei M, Graakjaer J, Bruheim P, Dawut L, Kolvraa S, May A, Seidman MM, & Bohr VA (2004) The Werner syndrome helicase and exonuclease cooperate to resolve telomeric D loops in a manner regulated by TRF1 and TRF2. Mol Cell 14: 763-774

Opresko PL, von Kobbe C, Laine JP, Harrigan J, Hickson ID, & Bohr VA (2002) Telomere-binding protein TRF2 binds to and stimulates the Werner and Bloom syndrome helicases. J Biol Chem 277: 41110-41119

Ouellette MM, McDaniel LD, Wright WE, Shay JW, & Schultz RA (2000) The establishment of telomerase-immortalized cell lines representing human chromosome instability syndromes. Hum Mol Genet 9: 403-411

Palm W & de Lange T (2008) How Shelterin Protects Mammalian Telomeres. Annu Rev Genet

Paull TT & Lee JH (2005) The Mre11/Rad50/Nbs1 complex and its role as a DNA double-strand break sensor for ATM. Cell Cycle 4: 737-740

Paulovich AG, Armour CD, & Hartwell LH (1998) The Saccharomyces cerevisiae RAD9, RAD17, RAD24 and MEC3 genes are required for tolerating irreparable, ultraviolet-induced DNA damage. Genetics 150: 75-93

Pennarun G, Granotier C, Hoffschir F, Mandine E, Biard D, Gauthier LR, & Boussin FD (2008) Role of ATM in the telomere response to the G-quadruplex ligand 360A. Nucleic Acids Res 36: 1741-1754

Petit C & Sancar A (1999) Nucleotide excision repair: from E. coli to man. Biochimie 81: 15-25

Philippe C, Coullin P, & Bernheim A (1999) Double telomeric signals on single chromatids revealed by FISH and PRINS. Ann Genet 42: 202-209

Prives C & Hall PA (1999) The p53 pathway. J Pathol 187: 112-126

Ravanat JL, Douki T, & Cadet J (2001) Direct and indirect effects of UV radiation on DNA and its components. J Photochem Photobiol B 63: 88-102

Rhind N & Russell P (2000) Chk1 and Cds1: linchpins of the DNA damage and replication checkpoint pathways. J Cell Sci 113 (Pt 22): 3889-3896

Saldivar JS, Wu X, Follen M, & Gershenson D (2007) Nucleotide excision repair pathway review I: implications in ovarian cancer and platinum sensitivity. Gynecol Oncol 107: S56-71

Shay JW & Bacchetti S (1997) A survey of telomerase activity in human cancer. Eur J Cancer 33: 787-791

Smogorzewska A, Karlseder J, Holtgreve-Grez H, Jauch A, & de Lange T (2002) DNA ligase IV-dependent NHEJ of deprotected mammalian telomeres in G1 and G2. Curr Biol 12: 1635-1644

Smogorzewska A & de Lange T (2002) Different telomere damage signaling pathways in human and mouse cells. EMBO J 21: 4338-4348

Smogorzewska A, van Steensel B, Bianchi A, Oelmann S, Schaefer MR, Schnapp G, & de Lange T (2000) Control of human telomere length by TRF1 and TRF2. Mol Cell Biol 20: 1659-1668

Song K, Jung D, Jung Y, Lee SG, & Lee I (2000) Interaction of human Ku70 with TRF2. FEBS Lett 481: 81-85

Stansel RM, de Lange T, & Griffith JD (2001) T-loop assembly in vitro involves binding of TRF2 near the 3' telomeric overhang. EMBO J 20: 5532-5540

Stavropoulos DJ, Bradshaw PS, Li X, Pasic I, Truong K, Ikura M, Ungrin M, & Meyn MS (2002) The Bloom syndrome helicase BLM interacts with TRF2 in ALT cells and promotes telomeric DNA synthesis. Hum Mol Genet 11: 3135-3144

Sugasawa K, Ng JM, Masutani C, Iwai S, van der Spek PJ, Eker AP, Hanaoka F, Bootsma D, & Hoeijmakers JH (1998) Xeroderma pigmentosum group C protein complex is the initiator of global genome nucleotide excision repair. Mol Cell 2: 223-232

Suzuki N, Shimamoto A, Imamura O, Kuromitsu J, Kitao S, Goto M, & Furuichi Y (1997) DNA helicase activity in Werner's syndrome gene product synthesized in a baculovirus system. Nucleic Acids Res 25: 2973-2978

Takai H, Smogorzewska A, & de Lange T (2003) DNA damage foci at dysfunctional telomeres. Curr Biol 13: 1549-1556

Tarsounas M, Munoz P, Claas A, Smiraldo PG, Pittman DL, Blasco MA, & West SC (2004) Telomere maintenance requires the RAD51D recombination/repair protein. Cell 117: 337-347

Tyrrell RM (1994) The molecular and cellular pathology of solar ultraviolet radiation. Mol Aspects Med 15: 1-77

Undarmaa B, Kodama S, Suzuki K, Niwa O, & Watanabe M (2004) X-ray-induced telomeric instability in Atm-deficient mouse cells. Biochem Biophys Res Commun 315: 51-58

van Overbeek M & de Lange T (2006) Apollo, an Artemis-related nuclease, interacts with TRF2 and protects human telomeres in S phase. Curr Biol 16: 1295-1302

van Steensel B & de Lange T (1997) Control of telomere length by the human telomeric protein TRF1. Nature 385: 740-743

van Steensel B, Smogorzewska A, & de Lange T (1998) TRF2 protects human telomeres from end-to-end fusions. Cell 92: 401-413

Vaziri H & Benchimol S (1998) Reconstitution of telomerase activity in normal human cells leads to elongation of telomeres and extended replicative life span. Curr Biol 8: 279-282

Venema J, Mullenders LH, Natarajan AT, van Zeeland AA, & Mayne LV (1990) The genetic defect in Cockayne syndrome is associated with a defect in repair of UV-induced DNA damage in transcriptionally active DNA. Proc Natl Acad Sci U S A 87: 4707-4711

Venema J, van Hoffen A, Karcagi V, Natarajan AT, van Zeeland AA, & Mullenders LH (1991) Xeroderma pigmentosum complementation group C cells remove pyrimidine dimers selectively from the transcribed strand of active genes. Mol Cell Biol 11: 4128-4134

Verdun RE, Crabbe L, Haggblom C, & Karlseder J (2005) Functional human telomeres are recognized as DNA damage in G2 of the cell cycle. Mol Cell 20: 551-561

Verdun RE & Karlseder J (2006) The DNA damage machinery and homologous recombination pathway act consecutively to protect human telomeres. Cell 127: 709-720

Vousden KH & Lu X (2002) Live or let die: the cell's response to p53. Nat Rev Cancer 2: 594-604

Wang RC, Smogorzewska A, & de Lange T (2004) Homologous recombination generates T-loop-sized deletions at human telomeres. Cell 119: 355-368

Watson JD (1972) Origin of concatemeric T7 DNA. Nat New Biol 239: 197-201

Watt PM, Hickson ID, Borts RH, & Louis EJ (1996) SGS1, a homologue of the Bloom's and Werner's syndrome genes, is required for maintenance of genome stability in Saccharomyces cerevisiae. Genetics 144: 935-945

Winkler GS, Sugasawa K, Eker AP, de Laat WL, & Hoeijmakers JH (2001) Novel functional interactions between nucleotide excision DNA repair proteins influencing the enzymatic activities of TFIIH, XPG, and ERCC1-XPF. Biochemistry 40: 160-165

Wood RD (1997) Nucleotide excision repair in mammalian cells. J Biol Chem 272: 23465-23468

Wright WE, Tesmer VM, Huffman KE, Levene SD, & Shay JW (1997) Normal human chromosomes have long G-rich telomeric overhangs at one end. Genes Dev 11: 2801-2809

Wyllie FS, Jones CJ, Skinner JW, Haughton MF, Wallis C, Wynford-Thomas D, Faragher RG, & Kipling D (2000) Telomerase prevents the accelerated cell ageing of Werner syndrome fibroblasts. Nat Genet 24: 16-17

Xin H, Liu D, Wan M, Safari A, Kim H, Sun W, O'Connor MS, & Songyang Z (2007) TPP1 is a homologue of ciliate TEBP-beta and interacts with POT1 to recruit telomerase. Nature 445: 559-562

Ye JZ & de Lange T (2004) TIN2 is a tankyrase 1 PARP modulator in the TRF1 telomere length control complex. Nat Genet 36: 618-623

Ye JZ, Hockemeyer D, Krutchinsky AN, Loayza D, Hooper SM, Chait BT, & de Lange T (2004) POT1-interacting protein PIP1: a telomere length regulator that recruits POT1 to the TIN2/TRF1 complex. Genes Dev 18: 1649-1654

Yu CE, Oshima J, Fu YH, Wijsman EM, Hisama F, Alisch R, Matthews S, Nakura J, Miki T, Ouais S, Martin GM, Mulligan J, & Schellenberg GD (1996) Positional cloning of the Werner's syndrome gene. Science 272: 258-262

Zhao H & Piwnica-Worms H (2001) ATR-mediated checkpoint pathways regulate phosphorylation and activation of human Chk1. Mol Cell Biol 21: 4129-4139

Zhong Z, Shiue L, Kaplan S, & de Lange T (1992) A mammalian factor that binds telomeric TTAGGG repeats in vitro. Mol Cell Biol 12: 4834-4843

Zhou BB & Bartek J (2004) Targeting the checkpoint kinases: chemosensitization versus chemoprotection. Nat Rev Cancer 4: 216-225

Zhu XD, Kuster B, Mann M, Petrini JH, & de Lange T (2000) Cell-cycle-regulated association of RAD50/MRE11/NBS1 with TRF2 and human telomeres. Nat Genet 25: 347-352

Zhu XD, Niedernhofer L, Kuster B, Mann M, Hoeijmakers JH, & de Lange T (2003) ERCC1/XPF removes the 3' overhang from uncapped telomeres and represses formation of telomeric DNA-containing double minute chromosomes. Mol Cell 12: 1489-1498